CENTER FOR
TRANSPORTATION
STUDIES

UNIVERSITY OF MINNESOTA

CORROSION OF COATED AND UNCOATED REINFORCING STEEL IN CONCRETE

Thomas E. Lorentz,
Catherine W. French and
Roberto T. Leon
Civil and Mineral Engineering

Sponsored by:
Center for Transportation Studies

Structural Engineering Report No. 92-03

Corrosion of Coated and Uncoated Reinforcing Steel in Concrete

Prepared by

Thomas E. Lorentz
Catherine W. French
Roberto T. Leon

Final Report Prepared for

UNIVERSITY OF MINNESOTA
CENTER OF TRANSPORTATION STUDIES
and
NATIONAL SCIENCE FOUNDATION
Research Grant No. BCE-8451536

May 1992

Abstract

An experimental program designed to investigate the effects of various material properties on the corrosion of reinforcing steel in concrete was conducted at the University of Minnesota. The test specimens were constructed to promote macrocell corrosion. A total of 96 prism and cracked slab specimens were subjected to an accelerated corrosion process for periods ranging from 35 to 48 weeks. The impact of the following variables on the corrosion of reinforcing steel in concrete was monitored in this program:

1. Water/cementitious ratio.
2. Addition of condensed silica fume.
3. Percentage of entrained air in the concrete.
4. Type of reinforcing steel and coating.
5. Cracked concrete.

The corrosion current, specimen resistance, driving potential, and Cu-$CuSO_4$ half-cell potential were monitored regularly to follow the corrosion process. The most significant variables determined in the University of Minnesota experimental program were the concentration levels (7.5% vs. 10%) of condensed silica fume (CSF), the significance of cracked concrete on the corrosion of reinforcing steel, and the lack of any notable corrosion resulting in concrete specimens containing bars with significantly damaged epoxy-coatings, despite high levels of chloride contamination.

Acknowledgement

The corrosion investigation was conducted in the structural engineering laboratory in the Department of Civil and Mineral Engineering at the University of Minnesota, under funds from the Center for Transportation Studies at the University of Minnesota and NSF Grant No. BCS-8451536. The donation of material and use of equipment from Simcote, Inc., St. Paul, Minnesota is acknowledged and appreciated. In addition, gratitude is expressed for the contributions provided by North Star Steel, Minnesota Rebar and Florida Wire and Cable Company.

Table of Contents

Page Number

Abstract i

Acknowledgements ii

List of Tables vi

List of Figures vii

1.0 Introduction 1

1.1. Statement of Problem Scope 1

1.2. Statement of Intent of Research 3

1.3. Organization of Thesis 4

2.0 Principles of Corrosion 6

2.1. Corrosion as an Electrochemical Process 6

2.2. Components of an Electrochemical Cell 6

2.3. Metallic Corrosion 9

3.0 Corrosion of Steel in Concrete 17

3.1. Types of Corrosion Cells 19
3.1.1. General Corrosion 21
3.1.2. Pitting Corrosion 23
3.1.3. Galvanic Corrosion 24
3.1.4. Differential Concentration Cells 24
3.1.5. Stray Current 26
3.1.6. Hydrogen Embrittlement 27

3.2. Factors Affecting the Corrosion of Reinforcing Steel in Concrete 27
3.2.1. Factors Effecting the Concrete Environment 28
3.2.1.1. Permeability 28
3.2.1.2. Role of Water 31
3.2.1.3. Role of Oxygen 34
3.2.1.4. Concrete Materials/Components 35
3.2.2. Physical Parameters 36

3.2.3.	Other Considerations in Concrete Quality	37
3.3.	Aggressive Environments	37
3.3.1.	Chloride Contamination	37
3.3.2.	Carbonation	40
4.0	Study of Current Literature	42
4.1.	Corrosion Test Measurement Methods	43
4.1.1.	Polarization Methods	43
4.1.2.	Potential Measurements	47
4.1.3.	Other Corrosion Monitoring Methods	51
4.2.	Simulated Pore Solution Tests	52
4.3.	Concrete Specimen Tests	59
5.0	Experimental Procedure	79
5.1.	Initial Tests on Proposed Acrylic Coating	79
5.2.	Experimental Variables	82
5.3.	Specimen Preparation	90
5.3.1.	Experimental Corrosive Environment	100
5.4.	Experimental Measurement Techniques	101
5.5.	Monitoring Cycle	109
5.6.	Additional Test Specimens	110
6.0	Results and Discussion	112
6.1.	Presentation of Results	112
6.1.1.	Comparison of Behavior of Specimens within a Variable Goup	113
6.1.1.1.	Specimens Exhibiting Atypical Behavior	114
6.2.	Concrete Material Effects	120
6.2.1.	Air Entrainment	121
6.2.2.	Condensed Silica Fume	122
6.2.2.1.	pH Measurements of CSF Concrete	132
6.2.3.	Effect of Reinforcing Steel Coatings	135
6.2.3.1.	Coated vs. Uncoated Bars	135
6.2.3.2.	Epoxy vs. Epoxy Grit Bars	136
6.2.3.3.	Effects of Damaged Epoxy Coating	141
6.3.	Cracked vs. Uncracked Specimen Behavior	144

6.4. Physical Investigations 147
6.4.1. Chloride Ion Concentration Results 147
6.4.2. Reinforcing Steel Visual Inspections 155
6.4.2.1. Visual Inspection of Uncoated Reinforcement 156
6.4.2.2. Visual Inspection of Epoxy-Coated Reinforcement 164
6.5. Comparison of Cu-$CuSO_4$ Half-Cell Potential with Measured Current 167
7.0 Conclusions and Recommendations 171
References 178
Appendix A 186
Appendix B 197

List of Tables

Table		Page
3.1	Galvanic Series of Metals and Alloys	25
3.2	Maximum Chloride Ion Concentration for Corrosion Protection	39
4.1	Interpretation of $Cu/CuSO_4$ Half Cell Readings	50
4.2	Chloride Ion Threshold Concentrations From Test Slabs	61
4.3	Chloride Ion Concentrations After 830 Daily Saltings	62
5.1	Corrosion Project Variable Listing	83
5.2	Concrete Mix Proportions	87
5.3	Type I Portland Cement Chemical Composition	88
5.4	Holiday and Scratch Survey - Epoxy Bars	91
5.5	Holiday and Scratch Survey - Epoxy Grit Bars	92
5.6	Measured Concrete Data	98
6.1	Concrete Powder pH Results	134
6.2	Acid Soluble Chloride Content Results	150
6.3	Water Soluble Chloride Content Results	151
6.4	Acid vs. Water Soluble Chloride Content Results	152

List of Figures

Figure		Page
2.1	Daniell Cell	7
2.2	Pourbaix Diagram for Iron and Water	11
2.3	Typical Behavior of a Metal	15
3.1	Macrocell Corrosion	20
3.2	Microcell Corrosion	22
4.1	Polarization Curve - Tafel Extrapolation	46
4.2	Polarization Curve - Linear Polarization	48
5.1	Experimental Variables	84
5.2	Specimen Identification Code	85
5.3	Holiday and Scratch Survey - Epoxy Bars	91
5.4	Holiday and Scratch Survey - Epoxy Grit Bars	92
5.5	Specimen Plan Views	94
5.6	Specimen Front Elevation	96
5.7	Instant Off Voltage Measurement	105
6.1	Current/Resistance History, Group IA355+.BLK	115
6.2	Current/Resistance History, Group IA405+.BLK	116
6.3	Current/Resistance History, Group IB358-.BLK	117
6.4	Current/Resistance History, Group IC355+.BLK	118
6.5	Current/Resistance History, Group IA405-.EPO	119

6.6 Current/Resistance History, Epoxy Bars - Air 123
6.7 Current/Resistance History, Black Bars - Air 124
6.8 Current/Resistance History, Damaged Epoxy - Air 125
6.9 Current/Resistance History, Black Bars - CSF 127
6.10 Resistance Measurements, Range of Values 128
6.11 Current/Resistance History, Black Bars - CSF 129
6.12 Current/Resistance History, Black Bars - CSF 130
6.13 Current/Resistance History, Black Bars - CSF 131
6.14 Concrete Powder pH Results 134
6.15 Current/Resistance History, Mix IA355+ 137
6.16 Current/Resistance History, Mix IB355+ 138
6.17 Current/Resistance History, Mix IC355+ 139
6.18 Current/Resistance History, Mix IA405- 140
6.19 Current/Resistance History, Mix IB358+ 142
6.20 Current History, Mix XA358- 145
6.21 Current History, Mix IA355- 146
6.22 Sample Locations for Chloride Ion Tests 148
6.23 Visual Comparison Black Bars - Significant Corrosion 160
6.24 Visual Comparison Black Bars - Insignificant Corrosion 163
6.25 Visual Comparison Epoxy Bars 165
6.26 Current vs. Half Cell Potential 168

Chapter 1.0 Introduction

1.1. Statement of Problem Scope

The corrosion of reinforcing and prestressing steel in concrete structures is a problem that has severe economic as well as human consequences. The durability of reinforced concrete structures may be severely compromised when the structure is subjected to a combination of corrosion inducing elements such as chlorides and water.

Two studies which focused on bridges and parking ramps (common reinforced concrete structures routinely affected by corrosion damage) illustrate the extent of the economic impact. In 1983, the U.S. Federal Highway Administration (FHWA) estimated a total cost (to the year 1996) of 2.6 billion dollars to restore only bridges on the interstate highway system damaged from corrosion of reinforcement [7].

In 1991, a seven year survey on the repair history of a group of 49 Canadian parking structures was published [58]. The repairs resulted from concrete durability problems, specifically corrosion induced damage such as cracking and spalling. This study reported that the average cost of repairing a sampled corrosion damaged parking ramp was approximately $474,000 per ramp. Based on the sizes of the sampled garages, this figure represents a repair cost of approximately $270 per square foot of surface. The average yearly expenditures of the 49 surveyed ramps for repairs over the seven year study was approximately $33,000/ramp.

While the costs reported above are significant, the structures considered represent only a very small portion of the total number of reinforced concrete structures that are subject to corrosion damage. The approximately 30,000 bridges on the interstate highway system considered in the FHWA study quoted earlier represent only 5% of the total number of bridges (with spans $\geq$ 20 feet) in the United States [59].

While the Canadian parking ramp research previously quoted gives an indication of the cost of corrosion repair for typical parking structures, these figures are not readily extended to estimate the total yearly expenditure for parking structures in the United States. This is primarily due to the fact that the total number of reinforced concrete parking structures in the United States has not been tabulated at this date. However, the Parking Market Research Company of McLean, Virginia, estimates that the total annual cost of parking ramp repair in the United States for 1989 was between $450 and $700 million, based on actual construction projects reported [62].

Damage to reinforced concrete structures from reinforcing steel corrosion is not limited to bridges and parking structures. These examples are used to illustrate the magnitude of the economic impact that corrosion has on only a portion of the structures exposed to the phenomenon.

One of the primary goals of any structural engineer must be to create structures which are safe for occupants and the surrounding public under reasonable service conditions. Corrosion damage in reinforced and

prestressed concrete structures can occur to the extent that the structure may fail, in some cases this failure could be a catastrophic collapse without warning. Evidence to this possibility is given by a 1984 Minneapolis parking garage collapse and the much discussed Berlin Congress Hall collapse in 1981. Even if one could neglect the economic impact of this problem, the human consequences of corrosion damage make it imperative that the engineering community develop and implement materials and design methods which can be used to eliminate or significantly retard the corrosion of reinforcing steel in concrete.

1.2. Statement of Intent of Research

The research described by the author into the phenomenon of the corrosion of reinforcing steel in concrete was undertaken at the Department of Civil and Mineral Engineering at the University of Minnesota. The goal of this study was to develop an experimental program which would explore the effects of concrete and reinforcing steel material properties on the corrosion of coated and uncoated steel in concrete.

There has been a wide variety of research into the corrosion of reinforcing steel in concrete, and although a great deal of progress has been made in the past 20 years, the problem is not yet solved. The interaction between the complicated nature of the corrosion process, and the tremendous variations possible in reinforced concrete materials and mixtures requires additional study by experts in several disciplines.

Reinforcing steel corrosion can and has been studied from a number of viewpoints; electrochemists, metallurgists, and engineers are a few of the professionals interested in this problem. This experimental program was designed to examine the corrosion process from the structural engineering perspective, to determine material properties that the design community can specify which will have the greatest effect on the prevention of reinforcing steel corrosion.

This study focused on investigation the impact of the following variables on the corrosion of reinforcing steel in concrete:

1. Water/cementitious ratio.
2. Addition of condensed silica fume.
3. Percentage of entrained air in the concrete.
4. Type of reinforcing steel.
5. Type of reinforcing steel coating.
6. Cracked concrete.

A detailed description of these variables is included in Section 5.2.

The experimental program consisted of 96 reinforced concrete specimens that were subject to an accelerated corrosive environment for time periods ranging from 35 to 48 weeks. The 96 specimens included 32 combinations of the experimental variables with 3 identical specimens for each variable combination.

1.3. Organization of Thesis

Beginning with Chapter 2.0, an elementary explanation of the general principles of corrosion is presented. Chapter 3.0 focuses on the particular

phenomenon of corrosion of reinforcing steel in concrete. The types of corrosion cells and the factors affecting the corrosion process in concrete are discussed in detail.

An overview of some of the previous research into the corrosion of reinforcing steel in concrete is presented in Chapter 4.0. The development of the experimental program at the University of Minnesota was influenced by portions of several of the studies described in this section. Applicable parts of past research that inspired either test methodology or physical models used int the reported program are referenced where appropriate.

The experimental procedures, including a description and rationale of the test assumptions and variables, specimen preparation, and measurement techniques used are described in Chapter 5.0. Chapter 6.0 contains the results of this research. Experimental results are presented in both tabular and graphic formats. Comparisons are made with respect to other published results where appropriate. Chapter 7.0 concludes with a summary of significant results, observations and recommendations for further study.

Chapter 2.0 Principles of Corrosion

Corrosion can be defined as the deterioration or destruction of a material as a result of exposure to its environment [44]. Metallic corrosion has been compared to extractive metallurgy in reverse, because the tendency of refined metals is to revert back to their native form, often oxides, sulfides or chlorides. The process of refining natural ore requires the input of a tremendous amount of energy. Through the corrosion process, the metal is transformed back to a lower energy state.

2.1. Corrosion as an Electrochemical Process

Metallic corrosion is an electrochemical process. In order to understand the principles of corrosion, it is necessary to understand the electrochemical mechanism that drives the phenomenon. Fontana describes any reaction that can be divided into two (or more) partial reactions of oxidation and reduction as electrochemical [44].

2.2 Components of an Electrochemical Cell

A common example of an electrochemical reaction is illustrated by a Daniell cell (Figure 2.1). In this cell, a zinc (Zn) rod is immersed in a weak sulfuric acid solution (H_2SO_4), together with a copper (Cu) rod in a copper sulfate solution ($CuSO_4$). The two solutions are separated by a porous barrier which allows ions to pass, but prevents the solutions from mixing. In the reaction that occurs, metallic zinc (Zn^{2+}) is lost to the sulfuric acid solution and the zinc rod becomes negatively charged. When the rods are connected

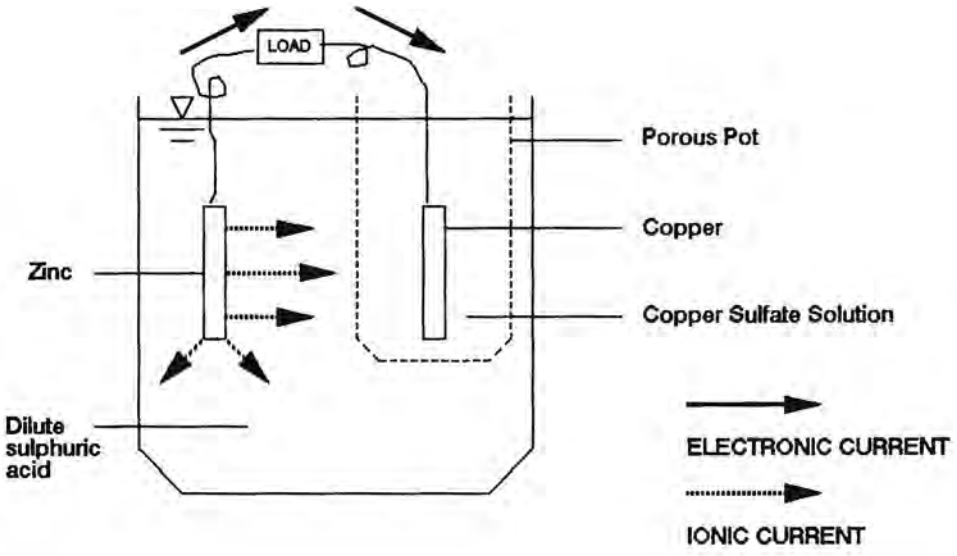

The Daniell Cell

Figure 2.1

electrically (i.e. with a conductive wire), the excess electrons on the zinc rod travel across the wire to the copper rod. When the copper sulfate solution is exposed to the excess electrons, a metal ion reduction occurs, and copper ions are deposited on the copper rod. Since the sulfate ions do not participate in this reaction, the partial reactions could be viewed as:

$$Zn \rightarrow Zn^{2+} + 2e \quad \text{Anodic reaction} \qquad (2.1)$$

$$Cu^{2+} + 2e \rightarrow Cu \quad \text{Cathodic reaction} \qquad (2.2)$$

The net result of the Daniell Cell is loss of metallic zinc from the zinc rod and accumulation of copper sponge on the copper rod. The aqueous solutions in the Daniell Cell are called the electrolytes, and the two metal rods are considered electrodes.

An oxidation reaction (anodic) can be described as one in which there is an increase in valence or a production of electrons. A reduction in valence or consumption of electrons indicates a reduction reaction (cathodic). In the Daniell cell, the zinc electrode is termed the anode and the copper electrode is called the cathode. Since both the anodic and cathodic reactions are partial reactions, they must both occur at the same time and at the same rate, which leads to one of the primary laws of metallic corrosion: *during metallic corrosion, the rate of oxidation must equal the rate of reduction* [44].

The anodic reaction in almost all corrosion processes can be generalized as the oxidation of a metal to its ion. The cathodic reaction in metallic corrosion could be one of, or a combination of, several reactions. In addition

to the metal deposition illustrated by the Daniell Cell, the most common cathodic reactions are hydrogen evolution, oxygen reduction, and metal ion reduction. All of the cathodic reactions consume electrons.

The electrochemical corrosion process involves the passage of ions from an anode to a cathode through an electrolyte. In order for an electrolyte to exist, a certain level of moisture is required. Therefore, in order for the electrochemical process to occur, water must be present. This fact is of particular note when considering to incorporate corrosion engineering practices into reinforced or prestressed concrete design. The reinforcing steel in RC members not subject to external sources of moisture are not likely to experience significant corrosion problems.

2.3. Metallic Corrosion

The phenomenon of metallic corrosion is a process that can only be formally described using theories of electrochemical thermodynamics. The theories of chemistry and classical thermodynamics alone are insufficient to describe or predict the complex reactions that occur in metallic corrosion.

Using these theories, Marcel Pourbaix devised a graphical representation of a given metal/electrolyte system that establishes equilibrium conditions for the system in terms of electrochemical potential and pH. These Pourbaix diagrams may be used in predicting the spontaneous direction of a reaction, estimating the composition of corrosion products, and predicting environmental conditions that would restrict corrosion activity [44,56].

Figure 2.2 illustrates a typical Pourbaix diagram for iron and water.

Pourbaix, or potential-pH diagrams are limited in the fact that although they illustrate the equilibrium conditions for a given metal and electrolyte system, they give no indication of the rate of the illustrated reaction. Potential-pH diagrams also do not represent equilibrium conditions when contaminants (i.e. chlorides or other substances) are present in the electrolyte [50].

The rate of any electrochemical reaction can be limited by either physical or chemical factors. According to Fontana, "the electrochemical reaction is said to be polarized (or retarded) by these environmental factors" [44]. There are two types of polarization: activation and concentration. Both types of polarization could affect the reaction rate for the same corrosion cell, however, they would typically occur at different stages in the corrosion process.

Activation polarization is caused by an impediment to the reaction at the electrode-electrolyte interface. As an example, the anodic reaction for the corrosion of iron in water which is exposed to the atmosphere is as follows:

$$Fe \rightarrow Fe^{++} + 2e^{-} \qquad (2.3)$$

At the anode, the iron ions go into solution, and as a result the anode is left with an excess of electrons. The electrons remain in the metal, and may travel to an adjacent or separate location (the cathode), depending on the type of corrosion cell. In order to maintain equilibrium, an equivalent quantity

Pourbaix Diagram for Iron and Water at 25° C.

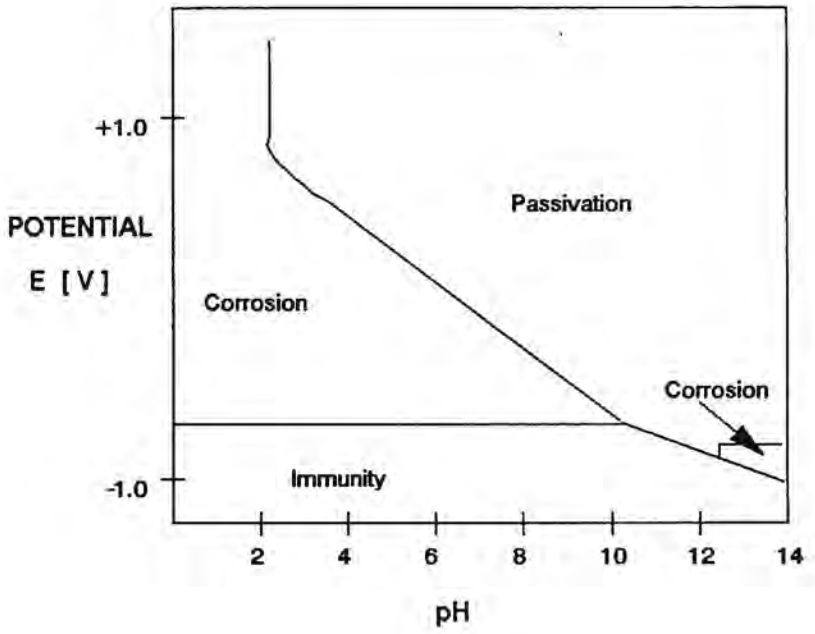

Figure 2.2

of hydrogen (H^+) is adsorbed or attached to the cathodic surface. The result is a thin film of hydrogen around the surface of the cathode. When the cathodic surface is completely covered with the hydrogen film, there is a resulting charge equilibrium within the corrosion cell which retards the corrosion process until the hydrogen film is destroyed by a reduction reaction. The rate of corrosion is controlled by the slowest of these steps occurring at the electrode-electrolyte interface, therefore it is considered activation polarization. Activation polarization often controls the corrosion reaction at the early stages on the process.

Concentration polarization occurs when the reaction is controlled by a deviation of electrode concentration on the electrode surface relative to that of the electrolyte. In concentration polarization, the reduction rate is controlled by the process occurring in the electrolyte [57]. Continuing with the example of the corrosion of iron in oxygenated water, the hydrogen film surrounding the cathodic area of the electrode is generally reduced or destroyed by one of the following reactions:

$$O_2 + 2H_2O + 4e^- \rightarrow 4OH^- \qquad (2.4)$$

$$2H^+ + 2e^- \rightarrow H_2 \uparrow \qquad (2.5)$$

Reaction (2.5) is a more active reaction and is likely to occur in limited cases, especially in the presence of an acidic environment. The explanation for this is based on the thermodynamic principles of free energy. Acidic solutions

have a higher free energy and would tend to support the more active reaction [44].

Reaction (2.4) is the more common cathodic reaction occuring in basic or neutral environments. In this reaction, dissolved oxygen in the electrolyte diffuses to the surface of the electrode where it is reduced by the electrons from the anodic reaction. This cathodic reaction is dependent on the presence of dissolved oxygen next to the electrode. The rate of this reaction is controlled by a process which occurs in the electrolyte, instead of at the surface of the electrode. If the corrosion process is slowed due to the diffusion rate of oxygen in the electrolyte, the reaction is considered controlled by concentration polarization.

The corrosion of reinforcing steel in concrete can be described on a simplified level by the reactions (2.3) and (2.4), shown for the corrosion of iron in an aerated solution [7,40,41,42]. In Chapter 3.0, the discussion of these reactions will be expanded.

The distinction between the two types of polarization is very important. Knowledge of which type of polarization is controlling a given cathodic reaction allows one to determine the effects of changing environmental variables on the corrosion rate. For instance, if the cathodic reaction is controlled by activation polarization, changing the diffusion rate in the electrolyte will have no effect on the rate of the reaction [44]. It is important to note that the corrosion of reinforcing steel in concrete is usually controlled

by concentration polarization of the cathodic reaction (2.3).

During the process of corrosion, many engineering metals such as iron, chromium, nickel, titanium and their alloys, reflect the property of passivity. Passivity, as simply described by Fontana, is "a loss of chemical reactivity under certain environmental conditions" [44]. Pourbaix diagrams can provide information which may illustrate the types of environments which may promote this passive state. Specifically for the iron-water system, we note that regions of high pH provide an environment that is generally free from corrosion. The importance of this fact on the corrosion of reinforcing steels in concrete will be addressed in Chapter 3.0.

Faraday conducted experiments on the phenomena of passivity in the 1840's. His original hypothesis, that a thin film generated on the surface of the metal prevented corrosion, has been substantiated, although the nature of the passive film still remains unknown [44]. The behavior of a typical metal exhibiting passive tendencies can be illustrated by Figure 2.3 which shows a plot of the electrode potential vs. corrosion rate. The same "S"-shaped curve would result if we replaced electrode potential with increasing oxidizing power of the solution [44].

Figure 2.3 illustrates the decrease in corrosion activity which accompanies the transition between active and passive states. Current electrochemical theory concludes that this decrease in corrosion current density is a result of the formation of the passive film. Because the reduction

Typical Behavior of a Metal Exhibiting Passive Tendencies

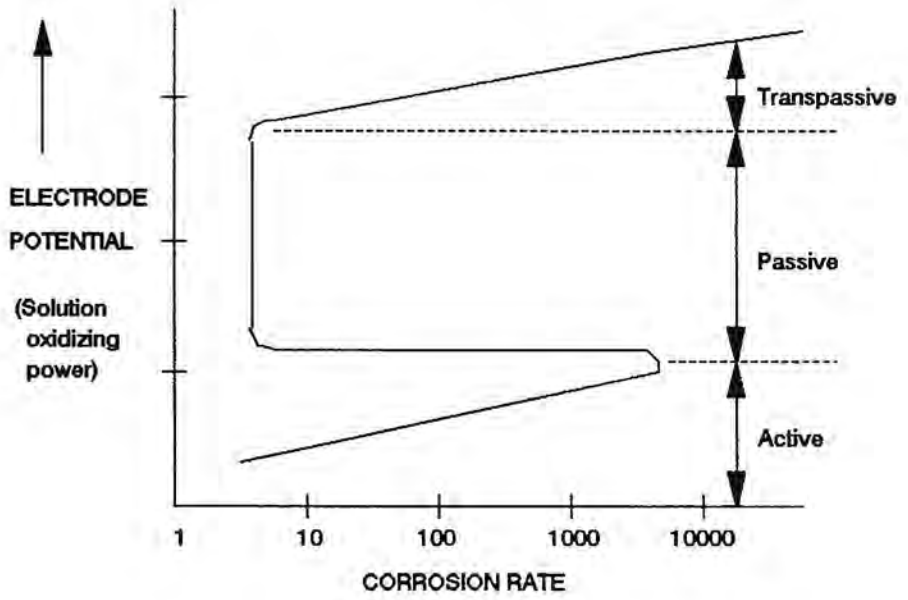

Figure 2.3

in the rate of reaction is a result of conditions at the electrode-electrolyte interface, this is an example of activation polarization. The destruction of this film is illustrated at the transition zone between the passive and transpassive zones. At these very high potentials the corrosion current density, and therefore the metallic dissolution rate, increases again.

Chapter 3.0 Corrosion of Steel in Concrete

Concrete surrounds reinforcing steel with an alkaline environment that will protect the steel from corrosion unless there is an intrusion which changes the normally passive state. While there has been some discussion of the exact nature of the cause of the passivation, there is evidence in support of the theory that this passive state is caused by the formation of an insoluble oxide film over the surface of the reinforcing steel [42,44,50,56].

Iron or steel in a highly alkaline environment has been shown to form a film of γFe_2O_3 (gamma ferric oxide) if oxygen is available [56]. The pH of uncontaminated concrete is normally between 13.5 -13.8 [8], and if the concrete is exposed to air, oxygen is almost always present due to the porosity of the concrete matrix. This combination can create an ideal environment for formation of the passive layer on the reinforcement, which explains why in many applications, the reinforcing steel in concrete is virtually corrosion resistant. That is, until the passivation state is destroyed by either mechanical or chemical intervention.

The actual chemical reactions which occur during the corrosion of reinforcing steel in concrete are extremely complex, and vary in many cases due to differences in the composition of the concrete matrix and varying concentrations of extraneous substances such as chlorides. However, the simplified model of the corrosion of iron in the presence of water and oxygen initially described in Section 2.3. by reactions (2.3) and (2.4), give an

elementary view of the corrosion reaction.

Stated here again, these reactions are:

$$Fe \rightarrow Fe^{++} + 2e^{-} \quad (2.3)$$

$$O_2 + 2H_2O + 4e^{-} \rightarrow 4OH^{-} \quad (2.4)$$

These partial reactions can be added to obtain the overall reaction:

$$2Fe + 2H_2O + O_2 \rightarrow 2Fe^{++} + 4OH^{-} \rightarrow 2Fe(OH)_2 \quad (3.1)$$

The ferrous hydroxide which results from this reaction is somewhat unstable in the presence of oxygen. Given sufficient oxygen, this corrosion product will be oxidized to the ferric salt, $Fe(OH)_3$, which is the common red rust.

$$2Fe(OH)_2 + \tfrac{1}{2}O_2 + H_2O \rightarrow 2Fe(OH)_3 \quad (3.2)$$

In uncracked concrete, the corrosion products from reinforcing steel will tend to remain in the ferrous state (e.g. ferrous hydroxide). As soon as the concrete is cracked, the increase in available oxygen from the atmosphere could convert the ferrous hydroxide to the ferric state, which causes the familiar red-brown stains. However, predicting the actual reaction products produced by the corrosion process of reinforcing steel in concrete is very difficult. Depending on the pH, the chemical content and the oxygen concentration of the concrete environment, and the metallurgic composition of the reinforcing steel, the hydrated oxide products from reactions (3.1) and (3.2) could possibly convert to magnetite (Fe_3O_4), hematite (Fe_2O_3), or goethite (FeOOH) [55].

3.1. Types of Corrosion Cells

Corrosion cells may be defined in terms of relative size as either microcells, or macrocells. Macrocell corrosion, refers to forms of corrosion in which the anodic and cathodic elements of the cell are either separate, discrete elements, or relatively large portions of one element become distinctly anodic or cathodic. An example of macrocell corrosion would result from an electrical connection (typically provided by wire ties, chairs or expansion joints) between negative and positive moment steel in a reinforced concrete (RC) member. The two layers of steel could be subjected to differential environmental conditions (eg. oxygen availability or chloride concentration) which would cause a potential difference between the two layers of steel. Given the proper conditions, a corrosion cell would initiate, with the anodic and cathodic elements being distinct reinforcement layers. Figure 3.1 illustrates a macrocell model for reinforced concrete.

Microcell corrosion includes forms of corrosion which occur over limited, very localized areas. Microcell corrosion occurs when the anodes and cathodes are formed alternately in very close proximity to each other on the same reinforcement bar. The development of electrochemical potential differences along the same bar will initiate microcell corrosion. These potential differences can be caused by a number of heterogeneities in the reinforcing steel environment or in the bar itself. Examples of these causes may be variation in metallurgical composition and residual stresses in the

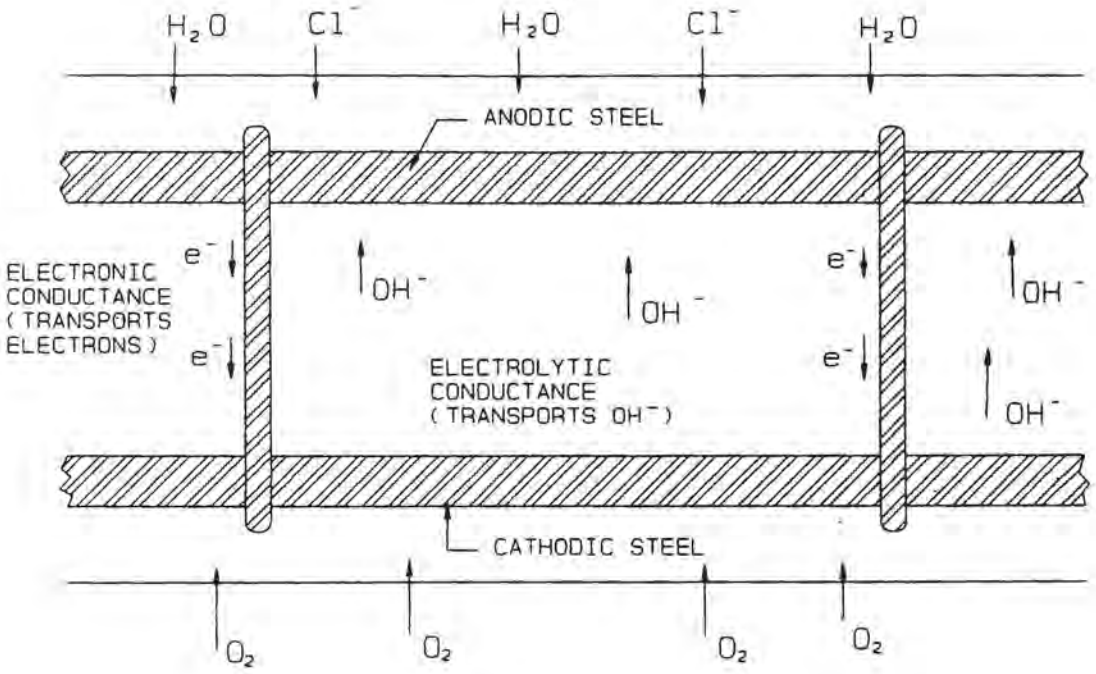

Macrocell Corrosion Illustration

Figure 3.1

steel, differential levels of oxygen, moisture content, chloride, and pH, in the concrete. A result of microcell activity, pitting corrosion, is a potentially catastrophic deterioration mechanism due to the concentrated loss of material at one section. Figure 3.2 illustrates a microcell corrosion model for reinforcing steel in concrete.

For the purpose of this paper, we will restrict the discussion of the forms of corrosion to those types most likely to occur in connection with reinforcing steel in concrete. These include: uniform or general corrosion, pitting corrosion, galvanic corrosion, differential concentration cells, stray current and hydrogen embrittlement. Although hydrogen embrittlement is not a specific form of corrosion, it is included in this discussion because it often occurs as a direct result of corrosion. It is important to note that while it is convenient to discuss these forms of corrosion as independent phenomenon, all are interrelated to an extent.

3.1.1. General Corrosion

General corrosion is characterized by a uniform corrosive attack occurring over an entire metal surface or a large area. In this type of corrosion the anodic and cathodic sites are adjacent to one another, resulting in uniform corrosion of the metal. General corrosion of steel in concrete is normally a result of either: 1) carbonation reducing the pH of the concrete over a large area of steel, or 2) introduction of a sufficiently large concentration of chloride. In either case, the net result is the general

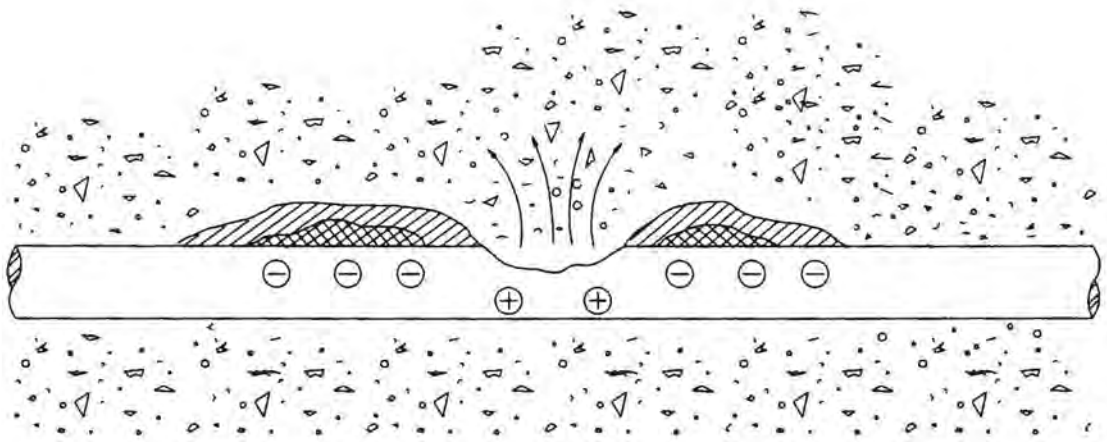

Microcell Corrosion Illustration - Pitting Corrosion

Figure 3.2

breakdown and destruction of the passive film surrounding the steel.

Uniform corrosion of reinforcing steel in concrete usually results in cracking and spalling of the concrete because the corrosion products increase the volume of the original bar, creating very large stresses in the concrete [7]. The resulting concrete deterioration can lead to loss of mechanical bond to the reinforcement (loss of strength), disruption in service (potholes), and aesthetic concerns. The metallic loss occuring on the reinforcing steel as a result of the corrosion process can also lead to a loss of cross-sectional steel area, resulting in increased stresses and potential failure.

3.1.2. Pitting Corrosion

Pitting corrosion is a very specific localized phenomenon in which anodic and cathodic sites are located adjacent to one another on a single electrode. No definitive theory on the initiation of pitting corrosion is agreed upon [42,44,50], however it is very likely that the destruction of the passivity of a specific site is a necessary factor.

Pitting corrosion is a microcell process which is actually self-perpetuating. As metal is dissolved at the anodic site, a pit is formed. The conditions inside the pit become increasingly acidic and more metal is dissolved. At the same time, the area surrounding the pit sustains the oxygen reducing cathodic reaction. Because the concentration of the solution inside the pit contains virtually no oxygen, no oxygen reduction occurs in the pit. The net result is that the surrounding area is cathodically protected from

further corrosion.

3.1.3. Galvanic Corrosion

Galvanic corrosion is a result of electrical contact between two dissimilar metals. Galvanic corrosion is usually a macrocell corrosion process. The rate and degree of corrosion are not only a function of the relative sizes of the two electrodes and the conductivity of the electrolyte environment, but primarily dependent on the electrical potential that can be developed between the two metals. This potential difference can be illustrated with the aid of a galvanic series, which is a list of metals and alloys arranged according to their relative potentials in a given environment (see Table 3.1). Table 3.1 is based on potential measurements and galvanic corrosion tests conducted by the International Nickel Company. The greater the potential difference between two metals, the larger the corrosion rate. In concrete construction, care must be exercised in locating any dissimilar metal items such as hangers or ducting which may contact the reinforcing steel network.

3.1.4. Differential Concentration Cells

These corrosion cells may occur because of different concentrations of either soluble ions or oxygen. In areas where metals may pass through zones having different concentrations of soluble ions, the potential differences that occur as a result of these differential concentrations may be great enough to cause corrosion. This is precisely the situation which occurs in bridge or parking ramp decks where chlorides from road salt migrate down into the

Galvanic Series of Metals and Alloys in Seawater at 25° C.

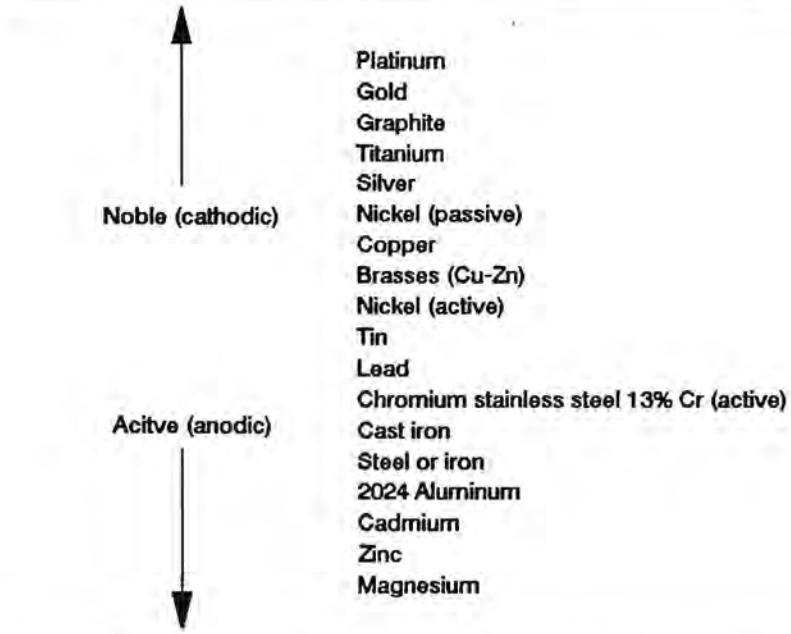

Table 3.1

concrete forming concentration gradients within the deck. This condition is very likely to result in the formation of a corrosion macrocell between electrically connected layers of reinforcing steels in the deck or supporting RC members. Corrosion cells occurring as a result of differential pH cells have also been established [18].

Differential oxygen concentration zones may also initiate a corrosion cell. While the complete absence of oxygen will effectively block the corrosion process, conditions which would increase the availability of oxygen to support the cathodic reaction, while decreasing the supply of oxygen at the anode could be the catalyst to a corrosion reaction. Differential oxygen zones are readily found in concrete construction. Because the oxygen level in concrete depends on porosity, the oxygen level at a given reinforcing steel location is a function of depth. Construction practices such as patching may cause oxygen concentration variations if the porosity of the patch concrete varies significantly from the surrounding concrete.

3.1.5. Stray Current

In some reinforced concrete structures, there is the possibility of alternating or direct current being picked up by the reinforcing steel system. The source could be lightning conductors, generators, improperly grounded cathodic protection systems, power transmission lines, or a wide variety of other transmitters [7,8,50]. Stray current impressed upon reinforced concrete structures may cause parts of the reinforcing system to become anodic to

others and initiate or greatly accelerate the corrosion process.

3.1.6. Hydrogen embrittlement

Hydrogen embrittlement is caused when atomic hydrogen penetrates into the steel lattice itself, resulting in steel which is embrittled and subject to cracking at much lower tensile stresses than expected. While hydrogen embrittlement is not a form of corrosion, the atomic hydrogen produced by the corrosion of steel in concrete may be the cause of subsequent hydrogen embrittlement of the reinforcing steel or prestressing strand. Low-alloyed, high-strength steels commonly used in prestressing strand are particularly subject to hydrogen induced cracking [57].

Hydrogen embrittlement is particularly dangerous in prestressed concrete structures due to the continuous stress state in the steel strands. Given the correct conditions, the prestressing strands would be subject to a combination of section loss by corrosion activity and hydrogen embrittlement by adsorption of atomic hydrogen, which could lead to a sudden failure of the reinforcement. The catastrophic failure of the Berlin Congress Hall in 1981 is a widely used example of hydrogen embrittlement caused by the corrosion of prestressing cables in concrete [7].

3.2. Factors Affecting the Corrosion of Reinforcing Steel in Concrete

The initiation of an electrochemical corrosion cell in concrete is dependent on the concrete quality, the moisture level present, the availability of oxygen, and exposure to an aggressive agent which will affect the stability

of the passive state [7,8,39].

The primary aggressive agent in phenomenon of reinforcing steel corrosion in concrete is the chloride ion. The chloride ion can be introduced to the concrete matrix from either contaminated mix materials or admixtures, or external sources such as deicing salts or exposure to marine environments. As the chlorides reach the layer of the reinforcing steel, the passive layer is gradually destroyed and corrosion may occur.

When concrete is exposed to external sources of chloride contamination, the rate of migration or diffusion into the hardened concrete will play a significant factor in the initiation of corrosive activity. In the case of chloride contaminated mix materials, the depassivation of the reinforcing steel would begin immediately upon casting, the corrosion rate itself would be controlled by other factors such as amounts of water and oxygen present.

3.2.1. Factors Effecting the Concrete Environment

Variations in concrete quality can be caused by the mix design, the quality of the aggregates and materials, placing and finishing techniques, and curing conditions. Concrete consists of a mix of cement, aggregates, water and admixtures, each with a wide range of compositions and effects on the corrosion resistance of the final composite.

3.2.1.1. Permeability

In discussing the permeability of concrete and its impact on the corrosion of reinforcing steel one must consider the effects of water, oxygen,

and the chloride ion on the concrete matrix. Each of these individual agents are needed to develop the general corrosion process in concrete. The water is needed for an electrolyte to facilitate the flow of ions between the electrodes, the oxygen is needed to maintain the cathodic reaction, and the chloride ion is needed to initiate the corrosion process. Each of these, water, oxygen, and chloride ion, must diffuse through the concrete to the steel. Neglecting both cracking and aggregate defects, the overall permeability of the concrete is determined by the permeability of the cement paste, which is a direct function of the water/cement (w/c) ratio [7,23].

Fluid flow through cement paste can be described by D'Arcy's law for flow through a porous medium:

$$v = K_p \frac{h}{x} \tag{3.1}$$

Where: v = Flow rate
K_p = Permeability coefficient
h = Hydraulic head
x = Thickness of specimen

Mindness and Young discuss the permeability coefficient, K_p, of cement paste as a function of both w/c ratio and age [23]. As the hydration in concrete continues, the capillary network becomes increasingly blocked by the formation of calcium silicate hydrate (CSH) and K_p becomes increasingly

smaller.

The permeability of concrete is also directly affected by pore size and distribution. Pores present in concrete cover a wide range of sizes. Gel pores have diameters of approximately 2.5 nanometers (10^{-9} meters) and are formed as a result of hydration of the cement, while capillary pores have diameters ranging from 10 to 10,000 nanometers and are the remains of water filled space in the cement matrix [29]. Increasingly larger pores, having diameters up to 0.2 millimeters, are formed from air voids.

There is a marked difference between pore size and pore distribution of normal portland cements and those cements containing pozzolans or blast furnace slag [26]. Condensed silica fume (a microsilica which contains a silica content of 85 percent or greater) is an extremely fine particle sized pozzolanic admixture which has been shown to result in concrete pores much smaller than those of regular concrete [28,29]. This is due primarily to the strong pozzolanic reaction in which the silica reacts with the calcium hydroxide produced by the hydration of cement to form additional calcium silicate hydrate (CSH) which blocks interconnected capillary pores in the concrete. The ultra-fine nature of condensed silica fume (0.1-0.2 μm) also allows the microsilica to fill voids between the cement paste and aggregate, further decreasing porosity.

Perraton, Aitcin and Vezina have studied the water, air and chloride permeability of silica fume and non-silica fume concretes [32]. Their research

has shown that the decrease in the water permeability of non-pozzolanic concretes with w/c ratios of 0.50 or less, compared with CSF concretes with comparable w/c ratios is negligible. Basically, at this level of water/cementitious ratio, concrete can be considered impervious to water, regardless of the level of condensed silica fume contained. However, the level of chloride ion permeability drastically decreases in concretes containing CSF.

The AASHTO T277-831 test for determination of chloride ion permeability of concrete is based on the measurement of current passed through a specific concrete sample when one end is immersed in a sodium chloride solution and a constant potential difference is maintained across the sample for a period of six hours [58]. The AASHTO test relates chloride permeability to the total value of charge passed (in coulombs). Perraton, et al., reported that concretes containing no CSF had values of charge passed (in coulombs) 4 times greater than concretes containing 5% CSF by weight of cement. Further, concretes containing 7.5% CSF by weight of cement were found to have negligible chloride permeability, similar to that of polymer impregnated concrete. Beyond the level of 7.5% CSF, the Perraton, et. al. test showed "no significant decrease in chloride ion permeability" [32].

3.2.1.2. Role of Water

Research in reinforced and prestressed concrete corrosion has targeted proper mix design as essential to developing the corrosion resistance for any

concrete structural element [3]. One of the primary variables to be considered in mix design is the water/cementitious (w/c) ratio. Other factors include the presence of fly ash, blast furnace slag, and admixtures.

There is strong evidence [17,10,12,14] that increased w/c ratios result in increasingly rapid corrosive deterioration of reinforcing steel over samples with lower w/c ratios in similar conditions. The most probable explanation for this trend is the increased permeability of the higher w/c ratio concrete.

Pfeifer, Landgren and Zoob [15] have reported an 80% reduction in long-term chloride permeability to a 1" depth in normal concrete when reducing w/c ratios from 0.51 to 0.40. A reduction of 95% is reported when the w/c ratio was further reduced to 0.28.

Current trends in concrete mix design for bridge decks and other uses exposed to chloride contamination are to limit w/c ratios to 0.35 or less [16]. Experiments represented in the literature surveyed have used w/c ratios in the range of 0.30 to 0.72 for normal and non-pozzolanic concretes. Concretes containing condensed silica fume (CSF) have been tested with water to cementitious ratios ranging from 0.18 to 0.50. Note that condensed silica fume is a cementitious material, and the quantity of CSF must be considered in calculating the w/c ratio.

While the quantity of water initially present in the concrete mix has been shown to have an impact on the corrosion resistance of reinforcing steel in concrete, the presence or absence of external moisture is also a critical

component; where external moisture is defined as the moisture to which the concrete is exposed under service conditions.

Water serves a two-fold purpose in the corrosion of steel in concrete. As shown in Chapter 3.0, the controlling cathodic reaction for corrosion of steel in concrete (reaction (2.4)) requires the presence of water. In order to have an electrochemical cell in concrete, water is required for both the cathodic reaction, and also to carry ions between the electrodes in the electrolyte.

Because the corrosion rate of the anode and cathode must be the same, the absence of water or oxygen at the cathode will effectively stop the corrosion process. But because both oxygen and water can exist in the gaseous form, and the concrete in its entirety is somewhat permeable, the cathodic reaction will likely occur unless the concrete or rebar is covered with an impermeable (e.g. epoxy) coating.

The primary importance of water in controlling the corrosion rate of steel is its effect on the resistivity value of concrete. Resistivity, ρ, is related to resistance but is a characteristic of a material rather than of a particular specimen. Resistivity is a microscopic quantity which has values at every point in a body, while resistance is a macroscopic quantity which applies over an entire body or extended region. The two measurements can be defined by the following relationship:

$$R=\rho\frac{l}{A} \qquad (3.2)$$

Where: R = Resistance (ohms)
ρ = Resistivity (ohm·cm)
l = Length (cm)
A = Cross-sectional area (cm^2)

The comparative electrolytic characteristics of different concretes can be discussed using resistivity measurements. An accepted method of determining an approximate value for the resistivity of concrete is by the four electrode "Wenner method" of measuring soil resistivity [42,50]. These measurements are only approximate, due primarily to the non-homogeneous nature of concrete, but also the effects of humidity and the possible presence of stray electrical fields.

Saturated concrete provides an electrolytic medium in which the flow of electrons from the anode to the cathode can take place. Dry concrete has a resistivity of approximately 1 X 10^9 ohm-cm, and saturated concrete has a resistivity of roughly 1 X 10^4 ohm-cm [48]. The extremely high resistivity of the dry concrete effectively breaks the electrochemical connection. It is important to note that concrete containing condensed silica fume also exhibits a markedly increased resistivity (2 to 4 times that of concrete without CSF), which may lead to a lower corrosion rate [28].

3.2.1.3. Role of Oxygen

The electrochemical description of the corrosion process has shown

that oxygen plays an essential role in controlling the rate of the cathodic reaction. There is a potential for a lack of oxygen to ultimately control the corrosion rate. In most above-ground structures, oxygen is not the controlling factor, due to a ready supply of atmospheric oxygen. However, in underwater structures, the availability of oxygen can definitely have a limiting effect on the rate of corrosion.

3.2.1.4. Concrete Materials/Components

The type of cement used can also have a significant role in the durability of the concrete structure. There is wide agreement [8,24,40] that the composition of the cement, specifically the quantity of tricalcium aluminate (C_3A) present, can increase the resistance of the concrete to attack by aggressive agents. Tricalcium aluminate has been shown to react with the presence of chloride ions and complex these ions out of solution. Cements with higher percentages of C_3A have the potential to bind more chlorides [7,42]. However, there is evidence that tricalcium aluminate may only have a significant impact on chlorides that are initially present in the mix [25]. The ability of C_3A to bind chlorides introduced to the hardened concrete is less evident.

Aggregates and admixtures can affect the durability of the concrete mix by introducing chloride directly into the mix. In this case the reinforcement is subjected to an aggressive agent prior to any service exposure, and the corrosion rate could be greatly accelerated. Aggregates

may have deleterious substances, such as chlorides or sulfates, coating the particles or within the interior pore systems. These substances may originate from source deposits or from stockpile contamination [3].

Admixtures such as calcium chloride have been widely used for many years as set accelerators. However, the effect of accelerated rebar corrosion due to these chemicals has been clearly documented, and ACI 212.1R has set recommended limits on their use [46,47]. Several agencies in Europe have already banned the use of calcium chloride in reinforced concrete [3]. There are a number of non-chloride accelerating agents, such as calcium nitrate, available as substitutes for the chloride-based accelerators.

3.2.2. Physical Parameters

Concrete cover is a common variable that has great impact on reinforcing steel corrosion test results. It is also possibly the single most important factor that the reinforced concrete designer can influence with regard to durable concrete structures. It has been shown that the permeability of gases and liquids in concrete is dependent on travel distance (Eq. 3.1). Because the breakdown of the passive concrete environment is dependent on the infiltration of various components to the level of the reinforcing steel, the concrete cover will directly affect the time needed to breakdown the passivity.

The designer of concrete structures exposed to corrosion inducing conditions should note that an average standard deviation of concrete cover

discovered by the State of New York and the FHWA is ± 10 mm (± 3/8 in.). Therefore, to obtain a minimum cover 90% of the time, the plan cover must be specified 13 to 16 mm (1/2 to 5/8 in.) greater than the minimum cover desired [3].

3.2.3. Other Considerations in Concrete Quality

Quality workmanship is necessary in mixing, placing and curing of durable concrete. A corrosion resistant mix design may not perform as expected unless quality controlled mixing is assured. Variations in the homogeneity of the concrete can be introduced by consolidation techniques in placement. Improper curing techniques can result in avoidable shrinkage cracks which allow aggressive corrosion agents direct access to the reinforcing steel. All of these areas of concrete construction are crucial to the expected corrosion resistant performance of a reinforced or prestressed concrete structure.

3.3. Aggressive environments

Two of the most common aggressive agents encountered by concrete structures are CO_2, (induced by carbonation) and the chloride ion. Studies have found that the chloride ion, which is present in road salts and seawater, is the primary cause for the accelerated corrosion and resulting deterioration of concrete structures [8,40].

3.3.1. Chloride Contamination

Based largely on studies sponsored by the Federal Highway

Administration in the early 1970's [10,11,12], the American Concrete Institute (ACI) Committee 201 provided the first set of limits on chlorides in concrete (ACI 201.2R-77) [43]. These limits are based on water soluble chloride ion concentrations prior to service exposure (chlorides present in aggregates, mix water, and admixtures). ACI 318-83, **Building Code Requirements for Reinforced Concrete,** set guidelines for the maximum concentrations of chloride present in concrete based on application, slightly revising the initial water soluble limits, and better defining the service categories. In 1985, ACI 222R-85 recommended the maximum acid-soluble chloride content, measured by ASTM test method C 114, as 800 ppm and 2000 ppm chloride (by weight of cement) for prestressed and reinforced concrete, respectively. The current ACI building code (ACI 318-89) guidelines for chloride concentrations are listed in Table 3.2. These limits are based on water-soluble chlorides and are given in percent by mass of cement.

When chloride ions are introduced into the concrete matrix, some of the chlorides are chemically bound into the hydrated cement. Chemically bound chlorides are not available to react with the concrete pore water solution and destroy the passivity of the environment. This is the rationale behind the ACI listing limits of chloride concentration in terms of water-soluble chlorides. The binding capacity of any given concrete mix is largely determined by the type and composition of the cement used.

Maximum Chloride Ion Concentration for Corrosion Protection
From ACI 318-89
Building Code Requirements for Reinforced Concrete

Type of Member	Maximum water-soluble chloride ion in concrete Percent by mass of cement
Prestressed concrete	0.06
Reinforced concrete exposed to chloride in service	0.15
Reinforced concrete that will be dry or protected from moisture in service	1.00
Other reinforced concrete construction	0.30

Table 3.2

3.3.2. Carbonation

Carbonation is described as the reaction of acids in the environment with the cementitious products in concrete which reduces the pH of the concrete. These environmental acids are primarily the CO_2 (carbon dioxide) in the atmosphere and the SO_3 (sulphates) in rain. Of these two sources, the atmospheric CO_2 has a more significant effect [42]. The carbon dioxide reacts with hydroxides in the concrete matrix, forming carbonates and water. This reaction lowers the concrete pore solution pH to < 9.0 [42,49]. When the depth of carbonation reaches the reinforcing steel, the lower pH significantly reduces or destroys the passive environment surrounding the reinforcement and given adequate amounts of oxygen and water, the steel may corrode.

Given the chemistry and thermodynamics involved in the carbonation process, theoretically all concrete should completely carbonate to a pH below 9 [49] for the ideal equilibrium condition. However, this ideal equilibrium model does not consider the rate at which equilibrium will be reached. Due to physical barriers, equilibrium may never be reached. Because of the drastically different rates of diffusion of CO_2 in water and air (water $\approx 10^4$ times lower than air) the moisture content of the concrete pores has a large effect on the rate of carbonation. Water filled pores will drastically reduce the rate of carbonation. If some of the concrete pores are partly filled with water (most cases), carbonation will proceed only to the depth which the pores

have dried out.

In Europe, carbonation has been considered an important factor in the corrosion damage of many building components. However, to date, little attention has been paid to the long term effects of carbonation in North American concrete structures [48]. Field studies on a range of Canadian building components such as balconies, cast-in-place shear walls, and pre-cast cladding have indicated that a small proportion of buildings will probably experience corrosion damage from carbonation within their service life [48].

While the process of carbonation is of significant interest in the general discussion of durable concrete structures, the primary concern over carbonation effects should be focused on structures that are not subject to other corrosion initiating agents, such as chlorides. The rate at which these structures would be exposed to corrosion due to the carbonation process is far slower than the rate of depassivation due to the ingress of chlorides.

Chapter 4.0 Study of Current Literature

In surveying a number of published reports dealing with the corrosion of steel reinforcement in concrete, differences in concrete quality, exposure to corrosion initiators (e.g. chlorides), sample geometry, experimental environment, length of test, and monitoring methods were encountered.

The primary corrosion initiator used in almost all of the experiments reviewed was a sodium chloride (NaCl) sodium chloride solution to simulate the chloride ion present in the deicing salts used on pavement and bridge decks in northern climates. However, several tests have used calcium chloride ($CaCl_2$) to determine the increase in corrosive activity due to the use of this compound as a set accelerating admixture [46,47]. Dehghanian and Locke have reported a significant increase in corrosion current rate of steel in concrete mixed with Cl_2 over concrete mixed with NaCl. The explanation of this behavior is as yet undefined. However, the diffusivity of chloride ions in cement paste has differed depending on the type of cation associated with the chloride ion [8].

Exposure to the chloride ion (Cl^-) can be introduced into the experimental concrete environment by either direct addition to the concrete components during the mix, external applications such as ponding or spraying, or a combination of the two methods. In tests which accelerated rather than realistic chloride exposure rates were recorded, the practice of "seeding" the concrete with an initial chloride content of between 1 and 2

pounds of chloride ion per cubic yard of concrete was typical. A value of approximately 1.5 pounds of Cl^- per cubic yard of concrete is considered to be a threshold for the breakdown of the initially passive steel environment.

There are two basic experimental techniques employed in the study of corrosion of reinforcing steel in concrete. One method is to simulate the concrete environment with a chemical solution. The other method is to monitor the corrosion of the reinforcement placed in actual concrete samples.

4.1. Corrosion Test Measurement Methods

There are a number of corrosion measurement methods currently used to study the corrosion of reinforcing steel in concrete. Some of these methods are limited to laboratory research projects, but others can and have been used in actual field tests of RC structures. Corrosion monitoring methods also can be divided into qualitative and quantitative methods. Some methods can be used to estimate the amount of corrosion for a quantitative analysis, while other methods are limited to detecting the (probable) presence of corrosion, or relative strength of the corrosion cell.

4.1.1. Polarization Methods

Two common techniques for corrosion rate measurements, Tafel extrapolation and linear polarization, are based on the recording of polarization curves, determined by either potentiostatic, potentiodynamic, or galvanostatic techniques. The RILEM report "Corrosion of Steel in Concrete" describes polarization as follows: "The change in potential of a corrosion

system due to the change in intensity of the current passing through the system is known as polarization" [42]. The plot of the variation in potential vs. the variation in current is defined as the polarization curve. Given proper instrumentation, and experienced interpretation, these techniques may be used to determine the actual corrosion rate, or instanteous corrosion intensity of a given corrosion cell. They may also give information about the morphology of the corrosion cell, i.e. pitting corrosion, or general corrosion.

Typically for these measurements, a three electrode system is used to monitor the potential curves of the corrosion cell or specimen. The three electrode system consists of a reference, counter and working electrode. The working electrode is actually part of the corrosion cell that is under investigation. In the monitoring of corrosion of reinforcing steel in concrete, the working electrode would be a section of the steel reinforcement. The counter electrode sometimes called the auxiliary electrode, is associated with the corrosion current. And the reference electrode monitors the change in potential of the working electrode. Typically, the reference electrode is a standard half cell, such as a copper-copper sulfate half cell.

In potentiostatic tests, the corrosion cell is subjected to small stepwise perturbations of voltage and the resulting changes in current are measured. In potentiodynamic tests, the corrosion cell is subjected to a continuous increase in potential with the resulting changes in current being measured. In both cases, the change in potential must be applied slowly to obtain

reproducible results. In galvanostatic tests, a stepwise increase in current is applied through the counter electrode, and the resulting changes in potential of the working electrode are measured. In the monitoring of corrosion cells in concrete, the test equipment must internally compensate for the ohmic drop between electrodes (due to the relatively high resistivity of concrete) for accurate measurements, or the ohmic drop needs to be calculated by separate experiments.

One method in which the polarization curves may be used to calculate the corrosion current is by Tafel extrapolation, sometimes referred to as the "intersection method". Figure 4.1 shows a simplified plot of anodic and cathodic polarization curves of a typical corrosion cell. If the potential of the working electrode is plotted against the log of the corrosion current, at relatively high values of current, both the anodic and cathodic polarization curves behave as linear functions. These linear segments of the polarization curve are referred to as the "Tafel regions". As shown in Figure 4.1, the intersection of the Tafel slopes can be used to calculate the instantaneous corrosion intensity, i_{corr} [44,57]. As an example, for an iron and water system (one metal specimen), the intersection of the Tafel slopes occurs where the rate of hydrogen evolution is equivalent to the rate of metallic dissolution.

One of the most widely used methods of laboratory corrosion measurements is the linear polarization (polarization resistance) method. Linear polarization corrosion measurement theory is based on the observation

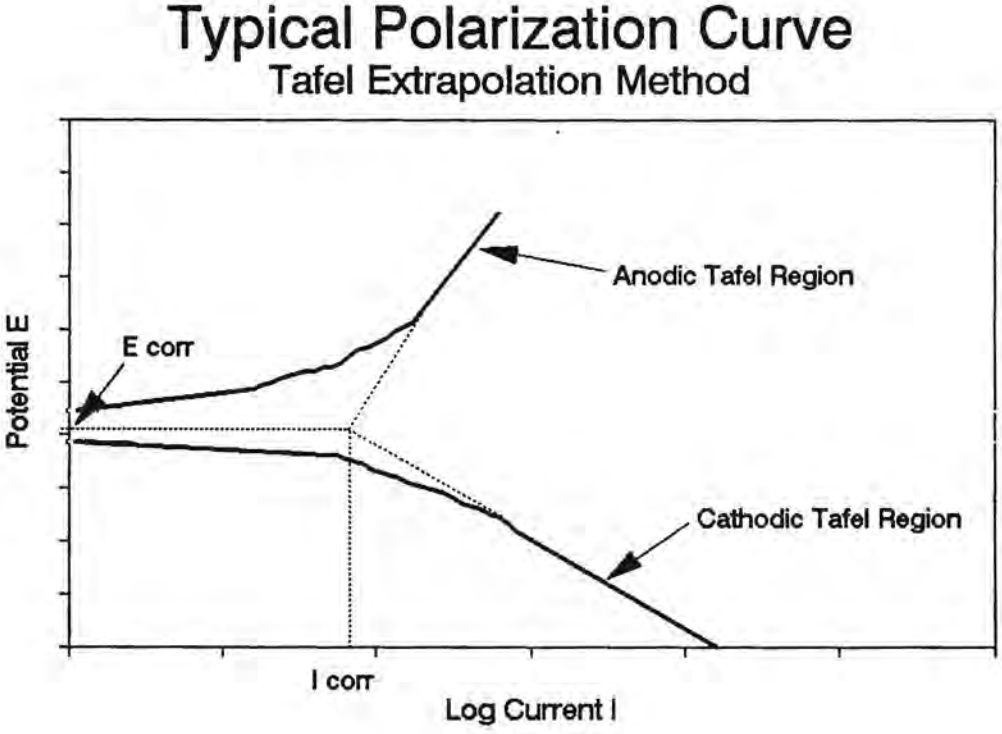
Typical Polarization Curve
Tafel Extrapolation Method
Anodic Tafel Region
E corr
Potential E
Cathodic Tafel Region
I corr
Log Current I

Figure 4.1

that applied current density is a linear function of electrode potential for a small region around the corrosion potential (see Figure 4.2). This is based on the Stern-Geary equation characterization of the polarization curve, given in the following equation:

$$\frac{\Delta E}{\Delta i_{app}} = \frac{\beta_a \beta_c}{2.3(i_{corr})(\beta_a + \beta_c)} \qquad (4.1)$$

Where: $\Delta E/\Delta i_{app}$ = Slope of Polarization Curve at E_{corr}
β_a = Anodic Tafel Slope
β_c = Cathodic Tafel Slope
i_{corr} = corrosion current [amperes]

The values β_a and β_c refer to the Tafel slopes of the anodic and cathodic reactions respectively, these values can be approximated for the steel/concrete system. By determining the slope of the linear portion of the polarization curve ($\Delta E/\Delta i_{app}$), one can determine the corrosion rate of the system by expressing the i_{corr} value in terms of current density (current/electrode surface area) [45]. Linear polarization measurements have been shown to return very good results on systems in which macrocell corrosion is not taking place [7]. In macrocell corrosion systems the steel is polarized away from its normal free-corrosion potential, and the results have been less reliable.

4.1.2. Potential Measurements

ASTM has standardized a useful technique to detect the probable

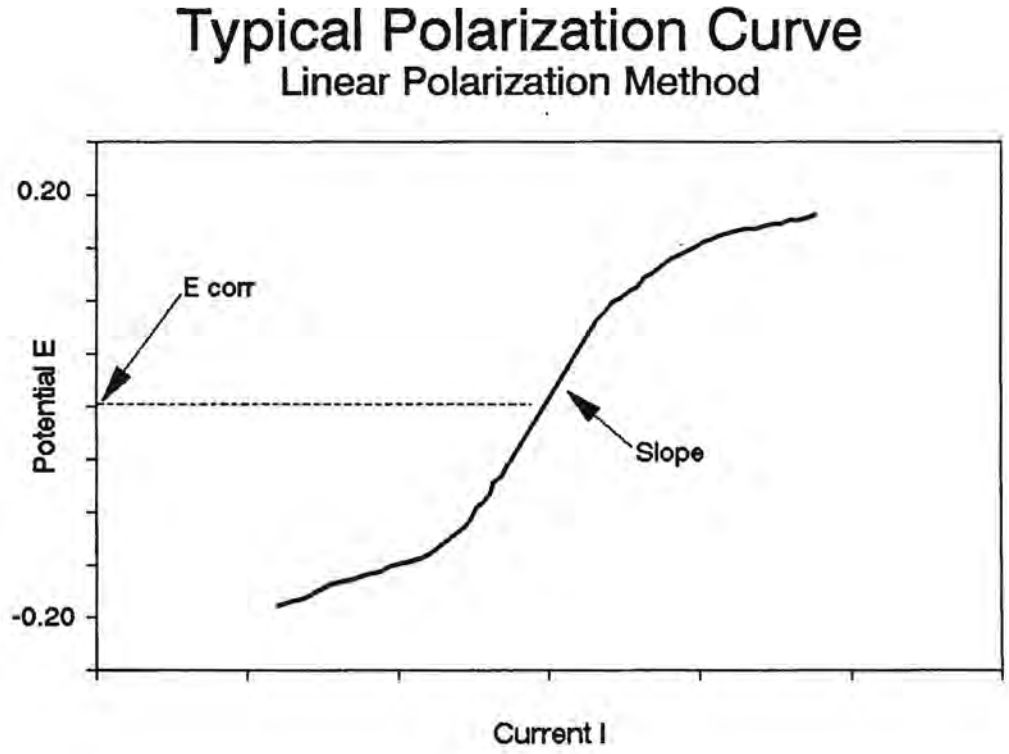
Typical Polarization Curve
Linear Polarization Method
0.20
-0.20
Potential E
E corr
Slope
Current I

Figure 4.2

presence of corrosion activity of reinforcing steel in concrete by the method of potential measurements [51]. In this method, the potential difference between the reinforcing steel under consideration and a standardized half cell is measured with a voltmeter. Based on a large amount of experience with corrosion of steel in concrete, ASTM has determined the probability of corrosion for a given system based on the potential measurements (see Table 4.1). It should be emphasized that the potential measurement technique does not have the ability to determine the corrosion rate, rather it indicates the probable presence of a corrosion cell.

In this measurement method, the most commonly used reference cells are copper-copper sulfate, silver-silver chloride, and saturated calomel. Laboratory studies have found that the silver-silver chloride or saturated calomel reference electrodes are both stable and accurate. However, for field testing of actual structures, the durable and relatively inexpensive copper-copper sulfate half cell is primarily used.

In taking a field survey, a grid is typically marked on the surface of the structure, with the potential reading taken at the grid points. The concrete surface at the grid point locations should be cleaned to remove any coatings or dirt build-up. A portion of the concrete cover is removed, exposing a small section of reinforcing steel which would provide electrical continuity for the area of concrete to be mapped. These locations should be determined from the reinforcement plans, if possible. The steel is cleaned and a good electrical

Interpretation of Cu/$CuSO_4$ Half Cell Readings

As Per ASTM C-876 [51]

Half Cell Reading [Volts]	Interpretation
> -0.20	90% probability of no corrosion activity
-0.20 to -0.35	uncertain
< -0.35	90% probability of corrosion activity

Table 4.1

connection is established by a set screw or clip. A wire from this connection would run to one of the portable voltmeter inputs. Another wire would run from the portable voltmeter to the half-cell probe. The probe is moved between grid points assigned to the current reinforcement connection, and the potential readings are recorded. After the potential data is recorded, a potential map can be produced from grid locations and potential readings. This map is not unlike a topographic map, but instead of showing equal elevations, shows lines of equal potential. This map gives the engineer a reference guide for locating regions undergoing corrosion activity.

4.1.3. Other Corrosion Monitoring Methods

Other electrochemical methods of corrosion monitoring which have been used with less frequency in the study of corrosion of reinforcing steel in concrete are AC impedance techniques, and electrochemical noise techniques. These methods are limited in that they require extensive instrumentation and the analysis of the results is complex. These techniques are currently used in a limited number of theoretical laboratory studies [42,50].

Early experimental work on the corrosion of reinforcing steel in concrete relied on visual examination of specimens as an indication of significant corrosion activity. The visual examination of concrete may indicate the presence of corrosion, but is not always a reliable indication. For field investigations, delamination, and rust staining of a concrete surface are

two possible indications that reinforcing steel corrosion is occurring. Unfortunately, when these symptoms are observable at the concrete surface, significant damage to the structure may have already occured.

4.2. Simulated Pore Solution Tests

Simulated concrete pore solutions have been used in studying the chloride threshold for corrosion of steel in concrete, and the effect of differential pH, surface condition, salt concentration and aeration cells in concrete. The most common simulated pore solutions are sodium hydroxide (NaOH), potassium hydroxide (KOH), and calcium hydroxide ($Ca(OH)_2$). Simulated solutions having a representative pH of approximately 12-13 have been used to represent the initial uncontaminated concrete environment. Slater points out that the pH of a saturated calcium hydroxide solution (pH 12.6) would be lower than that actually observed from porewater which has been extracted from hardened portland cement concrete (pH 13-14) [7]. It has been shown that a reduction in the pH of the concrete environment will accelerate the breakdown of the initial passive state of the reinforcing steel. Therefore, pore solution tests occuring in lower pH environments may give conservative results compared to normal concrete, or may more accurately desecribe the behavior of concretes which have lower pH values (such as those containing CSF).

Gouda and Mourad have performed extensive studies on the corrosion of steel reinforcement in simulated concrete environments [18,19,20,21].

They studied the impact of four differential environmental effects: pH, oxygen level (aeration), salt concentration, and steel surface conditions on the corrosion of reinforcing steel.

All of the Gouda and Mourad tests were performed using glass electrolytic cells having two compartments. The compartments were connected electrically by a sintered glass disc having a resistance of almost zero. Each system contained two small pieces of reinforcing steel rods (one piece of steel in each compartment) measuring roughly 2 inches in length and machined to a 0.2 inch diameter, giving a constant exposed area of 1.25 $in.^2$. The steel was connected to a saturated calomel electrode in order to measure the system potentials.

The experimental system contained 375 ml of electrolyte. The test solution for the pH, aeration, and surface condition experiments was NaOH in varying concentrations. The differential salt concentration experiment used sodium chloride solutions as an electrolyte. All test solutions were prepared from reagent grade chemicals in distilled water and were renewed every 2 hours. The pH of each cell compartment was monitored using a Model 25-China pH meter with a sensitivity of $\pm$ 0.1 pH.

In each of the studies done by Gouda and Mourad, the experimental equipment, methods and procedures were identical. Each study considered the addition of chloride ion to the sample cell, as well as the effect of varying values of solution pH. The performance of the corrosion cells was monitored

by potential/time measurements of both separate and coupled electrodes, galvanic current/time measurements of coupled electrodes, and by the experimental determination of the potential vs. current relationships (Evans diagrams). All studies were carried out a minimum of two times at a constant 25 °C.

Their work has shown galvanic corrosion cells present in the corrosion of steel reinforcement in concrete can be caused by zones of differential pH, salt concentration, steel surface conditions and aeration cells. Some of these conditions could be considered potentially probable in almost all structural concrete exposed to the environment, and all four of these differential conditions could be present simultaneously in many RC structures. Their work illustrates the possibility of corrosion of reinforcing steel in concrete is not necessarily limited to structures exposed to deicing salts or ocean environments.

Wheat and Eliezer attempted to identify a chloride concentration threshold value in the corrosion of steel in concrete using both simulated pore solutions and cast concrete cylinders [4]. Both systems used No. 3, Grade 60 bars in an "as received" condition.

The simulated pore solution used in this study was 0.6 M KOH + 0.2 M NaOH + 0.027 M $Ca(OH)_2$. The 3 in. and 6 in. pieces of reinforcing steel were placed in 1 or 2 liter containers of the solution, respectively. The systems remained undisturbed for 28 days to simulate a typical 28 day curing

period for reinforced concrete before potentiodynamic curves were recorded. The potentiodynamic curves were made under both natural and added oxygen-aerated conditions for comparison. Sodium chloride was added at a rate of 10 g/day. Potentials were monitored daily and potentiodynamic polarization scans were made with a Princeton Applied Research (PAR) 350-1 Corrosion Measurement System. This test continued for approximately 4 weeks after the 28 day curing period.

The Wheat and Eliezer test assumed that all bars shared the same environment with respect to pH, oxygen, and chloride exposure. Given the information regarding the conditions of the experiment, this assumption appears valid within reasonable limits. Yet they were unable to identify a specific chloride level associated with the initiation of corrosion. Their test results reported that between two specimens registering almost identical significant corrosion potential values, chloride concentration values differed by as much as a factor of three.

Wheat and Eliezer suggested the reason for lack of a unique value of chloride ion concentration to trigger corrosion was the inhomogeneous surface conditions of each bar. Other explanations for the inconsistent relationship could be small variations in oxygen content, pH and chloride concentration within the assumed constant environment of each system. This test illustrates the complexity of quantifying threshold values for corrosion initiation in reinforced steel in concrete. Nonhomogeneous

conditions abound in the concrete environment, and certain conditions can have either a magnifying or limiting effect on the corrosion process. While both the ACI and the FHWA have set limiting values for concentrations of chloride present in concrete [8,38], these values are not given as absolute indicators for the presence or absence of steel corrosion in concrete.

Hinatsu, Gradon and Foulkes attempted to develop a standard procedure for measuring the electrochemical behavior of iron in concrete using both in situ, and simulated pore solutions [17]. This study is important in that it directly compares the electrochemical activity of iron in cement mortar with iron in a simulated pore solution.

The electrochemical cell used in this study was a "three electrode" design. The working electrodes were constructed from 0.01 inch diameter, 99.999% iron wire. The exposed length of each electrode was approximately 0.40 in., with a nominal exposed surface area of about 0.013 in^2. The Pyrex glass cell held four platinum wire counter electrodes in glass compartments placed in an equidistant array around the center working electrode. The cell held approximately 200 ml of electrolyte. A Luggin capillary maintained electrical contact with a saturated calomel reference electrode. All tests were conducted at 25 ± 0.2 °C.

The mortar coated working electrodes were cast using portland cement paste (meeting CSA standard CAN 3-A5-M83) in a 0.50 cm diameter plastic form (1.5 cm length). The cast cylinders were cured in 100% relative

humidity.

Varying concentrations of NaOH and KOH solutions were used as electrolytes for the simulated pore condition tests. These solutions allowed the pH of the iron environment to range from 12.9 to 13.6. The mortar covered specimens used a saturated $Ca(OH)_2$ solution (pH = 12.4) as an electrolyte. All solutions were prepared from analytical grade chemicals and de-ionized water.

This study compared the effects of varying w/c ratio from 0.30 to 0.60 with a constant curing time of 5 days, and a varying curing time from 1 to 50 days with a constant w/c ratio of 0.45. The effects of 1 M sodium chloride applied externally, (into the $Ca(OH)_2$ electrolyte) versus 1 M sodium chloride applied internally (replacing water in the cement mix) were recorded for the mortar covered electrodes.

Hinatsu, et al. chose to monitor the cyclic voltammetry of the electrodes as the technique to describe the electrochemical behavior of steel in cement. The combination of the thin cement cover and small electrode area used in this study provided an iR drop value low enough to be measured by a Princeton Applied Research (PAR) model 273 potentiostat. Voltammograms plotting current density vs. potential (V vs. saturated calomel electrode) were used to graphically compare the corrosion activity for a given system.

From their results, Hinatsu, et al., acknowledge that the general

corrosion mechanism in cement mortar is similar to that in simulated pore solutions. However, their findings indicate that significant enhancement (three to fourfold) of the passivation of iron occurs in portland cement, as compared to iron in sodium hydroxide (NaOH) or potassium hydroxide (KOH) solution. This enhancement of the passivation process was attributed to the presence of calcium hydroxide ($Ca(OH)_2$) in concrete. Monteiro, et al., describe a lime rich layer, visible under scanning electron microscope, which surrounds the steel over most of its surface [35]. This lime layer enhances the passivity of the steel in the concrete environment. In discussing their results, Hinatsu, et al., strongly recommend that additional tests on the behavior of reinforcing steel in concrete be conducted using in-situ conditions, rather than simulated pore solutions. This recommendation was due to the magnitude of the passivation effects exhibited by the in-situ specimens over the specimens tested in a simulated pore solution.

While reinforcing steel corrosion tests in simple alkaline solutions cannot exactly duplicate the complex environment actually present in concrete, these simulated solution tests can still be a valid method of illustrating the basic electrochemical corrosion reaction. The simulated environment studies enable researchers to carefully monitor conditions such as pH and chloride levels with precision not usually available to in-situ tests. The test environmental conditions can also be easily altered, and the effect on corrosion studied.

4.3. Concrete Specimen Tests

There are several experiments which effectively monitored the corrosion of reinforcing steel in actual concrete samples and are often cited in the literature. Pfeifer, Landgren and Zoob's study [15] is impressive in size, scope and clarity of presentation. K.C. Clear, et al., have completed time-to-corrosion studies on concrete slabs for the Federal Highway Administration (FHWA) that address a wide range of corrosion factors [10,11,12,13,14]. The five volumes of "Time-To-Corrosion of Reinforcing Steel in Concrete Slabs" that present their findings span nine years of work (1973-1982), and are frequently referenced in papers discussing corrosion of reinforcing steel in concrete.

Both the Pfiefer, Landgren and Zoob study [15], and the studies by Clear et. al. [10,11,12,13,14] used test procedures based on the assumption that a primary cause of reinforcement corrosion is the presence of macroscopic galvanic cells in the concrete.

In 1972, the FWHA began a sponsored study performed by Clear, et. al. [10,11,12], in which 124 reinforced concrete slabs (4 ft. by 5 ft. by 6 in.) were subjected to daily salt applications over an extended period of time in outdoor conditions. Volume One of this study concerns the effects of mix design and construction parameters on the corrosion resistance of reinforced concrete [10]. Volume Two reports the electrical potential and chloride intrusion data of the concrete specimens after 330 daily salt applications

[11]. In Volume Three of this study, the performance results after 830 daily salt applications are summarized [12]. The performance of the slabs was determined using results of electrical half-cell potential monitoring (copper-copper sulfate, CSE), visual inspections, and chloride analysis.

As a result of their initial work [10], Clear, Hay, and Lewis, obtained values for an average threshold concentration of chloride at which corrosion was initiated in concrete reinforcement. The threshold values expressed as parts per million based on concrete weight are listed in Table 4.2. The threshold values from Table 4.2 could also be expressed as parts per million based on weight of cement. Expressed in this convention, their results indicate a mean threshold value of 2000 ppm Cl^- by weight of cement.

Extensive tests (over 1200 samples) on the chloride content versus slab depth gave Clear, et al., not only the ability to relate chloride concentration with time-to-corrosion of reinforcing steel, but the results of these studies also found concrete w/c ratio and depth of clear cover as having major influence on the time to corrosion [12]. The results of chloride penetration and concentration for variable w/c ratios from Clear's study are given in Table 4.3.

Volume Three of the FHWA study by Clear also addresses the relationship between daily salting of test slabs to the frequency of field salting of actual structures [12]. A quantitative relationship between simulated test and actual field performance is necessary if one is to extend information

Chloride Ion Threshold Concentrations From Test Slabs

Reference [12]

Cement Factor [94# bags/cu yd]	Cement Content [lbs/cu yd]	Corrosion Threshold [lbs/cu yd]	Corrosion Threshold [ppm]
6.00	564.0	1.13	289
6.75	634.5	1.27	324
7.00	658.0	1.32	337
8.00	752.0	1.50	383
8.75	822.5	1.65	421

ppm: Parts per million by weight of concrete
(This conversion is based on a concrete unit weight of 3915 lbs/cu yd.)

Table 4.2

Chloride Ion Concentrations After 830 Daily Saltings Mean Values [ppm]

Reference [12]

Sample Group	W/C Ratio	Sample Location Depth, inches				
		0.28	1.00	2.00	3.00	4.00
1	0.40	5108	404	BL	BL	BL
2	0.50	5644	2912	450	140	BL
3	0.60	7126	3499	983	197	135

ppm: Parts per million by weight of concrete
(This conversion is based on a concrete unit weight of 3915 lbs/

BL: Baseline value
Chloride values which were less than 102 ppm were considered to be baseline values (i.e. chlorides originally present in materials)

Table 4.3

gained from simulated tests to expected performance of existing and proposed structures.

In order to relate the effects of daily salting on specimens with real-time seasonal saltings, twenty-eight - 2 ft. x 2.5 ft. x 6 inch concrete slabs were fabricated using the same mix design and fabrication procedures as the standard time-to-corrosion test slabs. After 330 daily saltings, these slabs were found to exhibit similar chloride profiles as the larger standard slabs, so results could be translated to the larger slabs. The small slabs were introduced to different three types of chloride exposure: a) standard test daily ponding with 3% NaCl solution; b) salting with rock salt (NaCl) only when snow or ice is on the slab with no dams to retain melted solution on the slabs (8 saltings in 1974-75 winter season); c) ponding with 3% NaCl solution twice per week from December 1, 1974, to February 28, 1975, i.e., 26 saltings per season.

The results of this correlation experiment show that based on average corrosion threshold depths, one time-to-corrosion salting for this study was equivalent to roughly between 0.70 and 0.82 field saltings. If one estimates a typical number of saltings per season in a northern climate (Minneapolis, Minnesota) to be 25, then 830 time-to-corrosion salt applications would be equivalent to approximately 23 service years. This assumes all other exposure conditions to be the same for both sample and service structure, and neglects the effects of cyclic loading and cracking on the actual

structure. Cyclic loading and the typical service cracks which would be present on an actual structure would accelerate the migration of chlorides to the level of the reinforcing steel at concentrated locations.

Vermani, Clear and Pasko monitored the corrosion performance of epoxy-coated reinforcing steel, and a calcium nitrite admixture to protect black reinforcing steel in concrete in an experimental study for the Federal Highway Administration [14]. Both systems were compared to uncoated steel in concrete without admixtures. Results of this test were based on thirty-one relatively large slabs monitored over a two year test period (1980-82).

Test specimens were cast in 2 ft. x 5 ft. x 6 in. slabs containing two mats of steel reinforcement. The top mat consisted of four 51 inch long bars with two 18 inch long cross bars directly below. The bottom mat of steel consisted of seven 51 inch long bars with four 18 inch long cross bars beneath them. All epoxy-coated bars were #6 bars, uncoated #4, #5, and #6 steel bars were used. A clear cover of 3/4 inch over the top mat of steel was provided in all specimens. The distance between the longer bars in the top and bottom mats was 2-3/8 inches. Test slabs were cast with thr following reinforcing steel configurations: a) epoxy-coated bars in the top mat, uncoated bars in the bottom mat; b) epoxy-coated bars in both mats; c) uncoated bars in both mats. The concrete for all specimens had a w/c ratio of 0.53. The concrete was mixed and placed in two lifts. The lower lift in

each specimen was chloride free. The upper lifts of all samples contained a specified amount of sodium chloride dissolved in the concrete mix water. After consistent curing procedures were complete, the slabs were mounted on 3 ft. posts at the FWHA outdoor exposure site and monitoring began. The combination of relatively permeable concrete (w/c = 0.53), high chloride concentrations at the top steel level, a large bottom (cathodic) steel to top (anodic) steel area ratio, and a small separation distance between the steel layers contributed to an accelerated corrosion environment.

The large difference in chloride concentrations between the top and bottom steel levels creates a potential difference between the two steel levels, which drives the corrosion cell. A large cathode connected to a small anode creates an "area" effect which accelerates the corrosion process. Because the overall reaction of corroding reinforcing steel is usually controlled, or limited, by the reduction reaction occuring at the cathode, a larger cathodic area is able to increase the limiting reaction and therefore accelerate the total reaction rate. The small separation distance between the steel layers reduces the internal resistance of the corrosion cell, and therefore aids the corrosion reaction.

The results of the Virmani, Clear and Pasko study indicated that epoxy-coated reinforcing steel provided a very effective corrosion prevention system, by increasing the electrical resistance between the macrocell anode and cathode (i.e. top and bottom mat of reinforcing steel). It was concluded

in the report that if an uncoated reinforcing steel bar is assigned an arbitrary life of one year in chloride contaminated concrete, epoxy-coated reinforcing steel bars would require 46 years exposure in the same environment for the corrosion cell to consume an equivalent amount of iron [14].

Virmani, et al., also concluded that the use of calcuim nitrite admixtures were effective in reducing the corrosion of uncoated reinforcing steel in chloride contaminated concrete. If uncoated reinforcing steel in nitrite-free concrete is assigned an arbitrary life of one year, "it would require between 5 and 29 years for the same rebar in concrete containing 2.75 percent calcium nitrite solids by weight of cement and chlorides in the range of 22.6 to 8.4 lbs Cl^-/yd^3 to undergo equal iron consumption" [14].

In 1987, Pfeifer, Landgren and Zoob authored their test for the FHWA [15]. The purpose of this test was to monitor and compare the effectiveness of several currently available corrosion protection systems for reinforced and prestressed concrete. The initial portion of this study consisted of testing 124 prisms in a pilot program. After the 44 week pilot study, systems showing the most promising corrosion protection were incorporated into 19 full-size specimens, tested over a period of 370 days.

The pilot prisms were 12 inches square with variable depths of 7, 8 and 9 inches, corresponding to top mat clear covers of 1, 2, and 3 inches respectively. The steel reinforcement in each prism was distributed into a top mat of 2-#4 reinforcing bars and a bottom mat of 4-#4 bars. The bottom mat

of reinforcement was placed with one inch of clear cover in all test configurations, in order to provide equal access of oxygen to the bottom steel. A 4 inch thickness of concrete was maintained between the steel mats in all specimens. In addition to variable depth of clear cover, Pfeifer et al. configured systems with variable water/cement ratios of 0.32, 0.40 and 0.50, variable cement factors (94 lb. bags/cu. yd.) of 4.60, 6.08, and 7.47, the use of coated, uncoated and galvanized reinforcing steels, the addition of calcium nitrite admixture, and the application of penetrating silane and methacrylate coating systems, into 58 total combinations.

The specimen design and test details used in this study allowed for accelerated corrosion to take place due to the following specifics. The test prisms were subjected to moisture and chloride by ponding with a 15 percent sodium chloride solution (roughly 5 times the chloride level of seawater). The ponding cycle used in this study was 100 hours with ponded solution at 60 to 80 °F., followed by a fresh water rinse and 68 hours of drying at 100 °F. The alternating wetting and drying periods accelerated the migration of chlorides through the concrete. Elevated temperatures are known to accelerate corrosion reactions [44]. The experimental procedure introduced an electrochemical potential difference between the two mats of reinforcing steel as a result of differing chloride concentrations between the two levels of reinforcing steel. The concrete at the bottom layer of steel remained in a considerably lower chloride ion concentration environment relative to the top

mat, due to the greater distance required for the ions to permeate. In addition, this experiment took advantage of the previously described "area effect" for a macroscopic corrosion cell, by having twice the amount of cathodic steel (bottom mat) to anodic steel (top mat) area.

The corrosion monitoring variables and techniques used in the Pfeifer et al. [14] and the Virmani et al. [15] studies were essentially the same. The variables measured were as follows:

1. Corrosion current
2. Instant-off potential (Driving voltage)
3. Electrical resistance between the top and bottom mats
4. Half-cell electrical potentials between the top and bottom mats (vs. copper-copper sulfate electrode)

In both of these studies, galvanic current was assumed to occur when the top steel became "anodic" and the bottom steel became "cathodic" due to a change in the electrochemical potentials of the surroundings of the two layers of steel. This difference in electrochemical potentials could be traced to differences in oxygen content, pH, and moisture content, but was primarily due to the differential concentration of chloride ions surrounding the two layers of steel. By electrically connecting the top and bottom mats of reinforcing steel with an external circuit and monitoring the current flow, the authors were able to determine the rate of corrosion by applying Faraday's law.

$$M = \frac{I_{corr_T} tW}{FV} \qquad (4.2)$$

Where:
- M = corrosion loss (g/cm^2)
- I_{corrT} = total current involved in the process (amp.-hour)
- t = time (hours)
- W = molecular weight (grams)
- V = valence
- F = 96500 coulombs

The corrosion current could be related to the amount of metal lost to corrosion by the fact that each 1.0 amp-hour of current consumes 1.04 grams of iron.

The "instant-off" potential was taken to determine the electromotive force driving the corrosion cell. Both the Pfeifer et al. and the Virmani et al. investigations defined this reading as the voltage difference between the two mats of steel taken immediately after openning the circuit between the two. The instantaneous reading is necessary due to the fact that the individual layers of steel will begin to polarize away from each other after the electrical connection between the two layers is opened.

The impedance (resistance), in ohms, of the electrical path between the two mats of steel was determined in both studies using an AC electrical resistance monitor. This measurement, together with the current and the driving voltage readings were related by the Ohm's law equation:

$$V = IR \qquad (4.3)$$

Where: V = Instantaneous driving voltage (volts)
I = Corrosion current (amperes)
R = Resistance (ohms)

Both studies also included the measurement of the electrical potential between the top mats of reinforcing steel and copper-copper sulfate (Cu-$CuSO_4$) half-cells placed at various locations on the top surface of the concrete specimens. Half-cell measurements allow for benchmark comparisons as to the relative potential difference between any given electrode (anode or cathode), and a standardized electrode (the half-cell). Based on work done by Stratfull and others at Caltrans, [7] this nondestructive test is now recognized as a method to indicate probable zones of corrosion activity, and is described by ASTM C 876 [51] (see Section 4.1.2).

The Pfeifer, Landgren and Zoob study used a linear regression analysis to determine a relationship between their experimentally determined corrosion current and potential readings. Based on 209 half-cell potential readings from 52 concrete specimens, the following relationship was derived:

$$I = -774.2P - 184.2 \qquad (4.4)$$

Where: I = corrosion current (microamperes)
P = Cu-$CuSO_4$ half-cell potential (volts)

Based on this analysis, the Pfeifer, et al., study determined that

corrosion could occur at half-cell potential readings between -0.20 and -0.25 volts. The ASTM C 876 test specifications list that readings between -0.20 and -0.35 volts are in the "uncertain" range, while readings < -0.35 volts have a 90% probability of corrosion activity occuring [51].

After 44 weeks of testing, the Pfeifer, Landgren and Zoob study had 22 specimens that developed significant corrosion activity, while 102 specimens did not. The results clearly indicated that the depth of clear cover over the reinforcement was a significant corrosion inhibitor. In no cases, did any specimen with a clear cover greater than 2 inches exhibit any corrosion activity. Within the specimen groups having 1 inch of clear cover, there was no consistent effect of variable w/c ratio.

A 1986 corrosion study was undertaken by Hope and Ip at Queen's University, Kingston, Ontario, Canada, on concrete slabs exposed to both laboratory and outdoor conditions [27]. The purpose of this test was to address the effects of chloride in concrete containing admixed chloride and chloride-bearing aggregates. The authors were primarily interested in the measurement of microcell corrosion of the steel.

Hope and Ip cast sixty 2.5 x 12 x 16 in. (64 x 300 x 400 mm) slabs, in ten sets of six. The slabs were cast with three 0.51 in. (13 mm) diameter mild steel electrodes for corrosion monitoring - two working electrodes and one reference electrode. Differential levels of calcium chloride dihydrate, from 0 to 2 percent by mass of cement, were admixed into eight of the sets. Two

sets of slabs contained chloride-bearing aggregates, 0.136 and 0.197 percent chloride-ion content respectively, in bound form. CSA, Type 10, normal portland cement was used in all slabs. The water/cement ratio was 0.45, aggregate/cement ratio 4.45, air content of 6 percent, and slump 3 ± 1 in. (75 ± 25 mm).

Half of the slabs were stored outdoors, the remainder in the laboratory. The laboratory slabs were subjected to alternate wet and dry cycles of 3 and 11 days. The wet cycle was accomplished by soaking in aerated water; the dry cycle was completed in laboratory air. After 310 days, two slabs from each set were cycled with a 14 day oven drying period at 100 °C, a 14 day wet soaking period, and a 14 day air drying period. Corrosion measurements were typically made every three and 14 days on the indoor slabs, and every month on the outdoor slabs. The primary corrosion monitoring system used by Hope and Ip was the linear polarization technique.

Based on the results of their experimental program, Hope and Ip concluded that the chloride threshold limit to initiate corrosion of reinforcing steel in concrete was between 2000 and 4000 ppm calcium chloride dihydrate by mass of cement, depending on the test method. These results correlated well with the work discussed earlier, performed by Clear et al. [12], which indicated a mean threshold value of 2000 ppm Cl^- for corrosion initiation.

Coggins and French studied the chloride ion concentrations found in

three prestressed girders and the deck of a twenty year old bridge removed from service over Interstate 694 in Minneapolis, Minnesota [33]. Samples were taken at various depths from 20 locations on each of two girders, 7 locations on another girder, and 5 locations on the original bridge deck. The samples were analyzed by the "Berman method" for determining total chloride content.

Their findings indicated that chloride ion concentrations present in prestressed bridge girders at depths of less than 1-1/2 inches varied greatly due to the degree of exposure associated with the location of the samples. The total chloride concentration values at depths of 1-1/2 inches or less ranged from 1180 to 40 ppm by weight of concrete.

The actual maximum chloride ion values recorded at depths of 1-1/2 inches or greater were not found to be significantly higher than 250 ppm by weight of concrete. Coggins and French found no evidence of corrosion of the prestressing strands in the bridge girders, except for the end faces where the epoxy coating had been chipped. Rust stains on the concrete were present at this location, however no spalling was evident.

Samples taken from the original bridge deck contained a much greater concentration of chloride ion. This result is expected due to the direct application and ponding of deicing salts upon the deck. The top steel layer in the deck was located at a depth of 1-1/2 inches. At this depth, the reported chloride ion concentrations ranged from 1110 to 1940 ppm by

weight of concrete. Coggins and French estimated a 20% cement factor, which translates into chloride concentrations present at the level of steel from 5550 to 9700 ppm by weight of cement. Despite the fact that average chloride concentration values at this depth were found to be twice the FHWA replacement level of 3000 ppm by weight of cement [8], the deck investigated showed no significant deterioration due to corrosion effects.

It is significant, that even with the gross simplifications described in the 1972 Clear and Hay study [12], the results from that investigation show a loose correlation with actual samples from structures that were in-service. The 20-year old bridge deck analyzed by Coggins and French contained an average value of 1900 ppm chloride by weight of concrete at the one inch depth [33]. Based on typical concrete construction practices in the late 1960's, one could estimate the w/c ratio of the bridge deck to be between 0.40 and 0.50. The chloride concentration at a one inch depth of a concrete slab from the Clear and Hay study after 830 saltings (roughly 23 service years) for w/c ratio of 0.50 was 2912 ppm, and for w/c ratio of 0.40 was 404 ppm, chlorides by weight of concrete (see Table 4.2). This comparison, while not conclusive, tends to confirm that the time-to-corrosion values used to relate the experimental method used in the FHWA studies to actual field saltings were not unrealistic.

Jang and Iwasaki examined the corrosion of reinforcing steel in concrete from a metallurgic viewpoint, i.e. how the composition of the rebars

affects the corrosion process, and the impact of the corrosion phenomenon on the microstructure of reinforcing steel [55]. Reinforcing steel was tested in both a simulated pore solutions and actual concrete blocks. The goal of their study was to develop a simple galvanic current measurement method of corrosion monitoring, and to study the effect of chloride concentration, welding and bending on the corrosion or reinforcing steel in concrete.

Corroded rebar samples taken from an in-situ bridge deck and tunnel pavement in St. Paul and Minneapolis, Minnesota were also analyzed. The concrete containing the reinforcing steel samples had been subjected to years of applied road salts based on common service conditions for a northern snow belt state. The concrete surrounding the field samples was reported to contain 1100 ppm Cl^-. Assuming a 4000 lb./cu. yd. unit weight for the concrete, and a cement factor of 6, the result is equivalent to approximately 7800 ppm Cl^- by weight of cement. This value is roughly 2 to 3 times the value needed to initiate corrosion determined by Hope, Ip and Clear, as discussed earlier.

Jang and Iwasaki monitored the reactions of two electrically connected samples of reinforcing steel placed in environments having differing chloride concentrations and found that the behavior of the rebars was galvanic. The measurements were made with a Princeton EG&G Model 350-A corrosion measurement console. The rebar containing the higher salt concentration became the anode, while rebar in the chloride-free environment became the

cathode. The measurements taken between reinforcing steels in a simulated concrete solution corresponded well to those taken between field specimens of rebar embedded in concrete.

The results from the Jang and Iwasaki investigation support the macrocell model of reinforcing steel corrosion in concrete. From the simulated corrosion cell experiments, Jang and Iwasaki found that the galvanic currents between rebar specimens increased with increasing chloride concentration. A very significant result reported from this study was that the galvanic current measurements of welded and bent reinforcing steels were approximately two orders of magnitude higher than those of ordinary rebars.

Jang and Iwasaki explain that welding can lead to significant differences in the electrochemical properties between weld metal, heat-affected zone, and base metal. As a result, "the weld metal was more active than the base metal, and acted as an anode" [55]. The bent reinforcing steel experienced plastic deformations which formed areas of dislocations of the metal. Areas with a high density of dislocations are described as unstable thermodynamically and in a high energy state compared to areas without dislocations. The plastic deformation of the reinforcing steel leads to adjacent areas with significant differences electrochemical properties, thus resulting in higher corrosion rates than unbent reinforcing steel.

From microscopic study of corroded reinforcing steel, Jang and Iwasaki found that in addition to sites of plastic deformation and weld locations,

severe corrosion occurred near grid-intersections and material defects in the microstructure of the reinforcing steel. They also found that the corrosion of rebars initiated and propagated along rebar material grain boundaries. In short, impurities in the form of inclusions (e.g. sulfur), and dissimilar constituents (e.g. ferrite and pearlite) commonly found in the mild steel usually used as reinforcing steel can have a significant effect on the corrosion rate of steel in an aggressive environment.

The Jang and Iwasaki results lead to important considerations from the structural design perspective. The designer of RC structures should be cognoscente of the fact that welded reinforcing steel has a much higher potential to suffer corrosion than non-welded reinforcement. For the structures that are considered particularly susceptible to the threat of reinforcing steel corrosion, the designer may wish to consider options other than welding for reinforcing steel. Additionally important, although not always considered in RC design, is the quality of the reinforcing steel itself. Jang and Iwasaki have shown that reinforcing steel having a high percentage of impurities is susceptible to corrosion.

A great number of other excellent research projects have been done on the corrosion of reinforcing steel in concrete. The body of knowledge on reinforcing steel corrosion has grown dramatically in the past 20 years. And even though the phenomenon of corrosion of steel in concrete is extremely complex, advances in corrosion protection have been made. Corrosion

research has resulted in the improvement of materials (e.g. epoxy coated rebars, non-chloride based admixtures), corrosion prevention systems such as cathodic protection systems, and corrosion measurement methods.

As a result of corrosion research on reinforcing steel in concrete, new and more effective methods of field measurement studies have been developed. Current work in corrosion systems monitoring equipment has developed linear polarization (L.P.) test equipment suitable for field studies of structures [46]. These systems have several advantages over the previous standard field corrosion monitoring technique of half-cell potential mapping (ASTM C 876 - 87). The L.P. procedure is relatively rapid, the corrosion rate is actually calculated (rather than the probability of corrosion), and there is a growing world-wide database that can be used in interpreting the results.

As concrete technology continues to grow, and incorporate new materials and admixtures, the research into the corrosion of reinforcing steel in concrete must continue. Particular emphasis is now being placed on the effects of cracks, and concrete additives such as condensed silica fume [53, 63]. Continued research on other protective systems, such as concrete sealers and coatings, is ongoing [26].

Chapter 5.0 Experimental Procedure

As discussed in Chapter 4.0, previous research investigating the corrosion of reinforcing steel in concrete has considered the effects of coated and galvanized reinforcement, depth of clear cover over reinforcement, w/c ratio, cement content, corrosion inhibiting admixtures, and various types of concrete sealants or coatings. These research programs have clearly shown that reduced w/c ratios, epoxy coated reinforcing steel, and increased clear cover depth significantly reduce the incidence of reinforcing steel corrosion [10,11,12,13,14,15].

This study, conducted at the University of Minnesota, contributes additional information to the current state of knowledge on the corrosion effects of uncoated, coated, and damaged coated reinforcing steels in concrete, the effects of variable percentages of entrained air in concrete, and the effects of varying concentrations of condensed silica fume (CSF) added to the concrete as a pozzolan. In addition, the relative performance of cracked vs. uncracked concrete specimens, with regard to corrosion, was investigated.

5.1. Initial Tests on Proposed Acrylic Coating

One of the goals of this study was to compare the relative performance of various types of reinforcing steel coatings when subjected to an accelerated corrosion test in concrete. In addition to commercially available reinforcing steel coatings, one of the coatings studied was an acrylic coating

(SAS) that was not currently used as a reinforcing steel coating. The SAS coating had previously been marketed as a protective concrete coating or sealant, and as a corrosion protective coating for agricultural equipment. Promising advantages of the SAS coating were its ease of application (spray or dip) and the comparatively thin coating thickness, which might have significantly enhanced the bond characteristics of coated rebar.

To determine the suitability of the SAS coating for the protection of reinforcing steel in concrete, the coating was subjected to tests for nonmetallic coatings for concrete reinforcing bars (one physical, one electrochemical), as outlined by the National Bureau of Standards (NBS) [63]. One test was used to evaluate the abrasion resistance of the coating, and another test was used to determine the effects of electrochemical stresses on the coating.

The abrasion resistance testing of the acrylic coating was carried out by an independent testing laboratory (Twin City Testing), in accordance with ASTM D1044-56. The coating was applied to a standard steel plate, then subjected to rotations under an abrasion wheel with a 1000 gram load. According to the ASTM standard, weight loss of the coating should be determined after every 1000 cycles. The NBS document indicates that a costing that exhibits a weight loss > 100 mg. per 1000 cycles is indicative of poor abrasion resistance. None of the sample plates coated with the proposed acrylic coating completed 1000 test cycles before complete loss of

coating.

A second test indicating the effects of electrochemical stresses on the proposed acrylic coated reinforcing steels was performed using an applied voltage test. In this test, two identically coated, #4 reinforcing steel bar specimens were subjected to a potential difference of two volts while immersed in a saturated solution of calcium hydroxide containing 7% sodium chloride. The specimens were visually inspected for hydrogen gas formation at the cathodic bar, and the appearance of corrosion products on the anodic bar. In the NBS study results, a number of different epoxy-coated specimens underwent testing over an 80 hour period without showing signs of hydrogen gas evolution or corrosion products.

The applied voltage test performed in this study included reinforcing steel specimens having one, two, and three coats of the proposed acyrlic coating. The coatings were applied by immediate dipping of sandblasted clean reinforcing steel specimens into the acrylic coating. The bars were allowed to dry between coats. Additional specimens having commercially applied Scotchkote® 213 epoxy-coatings were subjected to the same applied voltage test.

In applied voltage tests on each of the proposed acrylic coated reinforcing steel samples, regardless of number of coatings, the acrylic coating visually dissolved almost immediately upon application of the potential difference between bars. In the test with the specimens having three coats

of the proposed acrylic coating, vigorous bubbling of hydrogen gas evolution occured at the cathodic bar, while the anodic bar was completely coated with rust after a period of two minutes. The single and double coated specimens exhibited similar behavior in shorter or equal time periods. After one hour of testing under the same conditions, the commercially applied epoxy-coated specimens showed no signs of corrosion activity or hydrogen gas evolution. The test was discontinued after one hour.

As a result of the failure of the SAS coating in both of the durability tests performed, the coating was eliminated as a potential variable in the experimental study.

5.2. Experimental Variables

The variables studied in this test included altering specimen geometry, CSF content, w/c ratio, nominal entrained air content, initial chloride content, reinforcing steel type and coating (epoxy, plain deformed, epoxy with grit, plain undeformed). Each of the variable sets was represented with three identical specimens. The variable sets are described in Table 5.1. A graphical illustration of the experimental variables is provided in Figure 5.1.

Specimen identification was maintained by two different inventory methods: 1) a symbolic alphanumeric notation was developed to identify different variable groups, 2) a unique three digit number was given to each specimen. The symbolic variable group notation is illustrated in Figure 5.2. The symbolic identification method allows one to identify all of the

Corrosion Project Variable Listing

Specimen number	Symbolic Identification	# Specimens	W/C ratio	Nominal Air %	Nominal CSF %	rebar type	seeded Cl	Geometry
128-130	IA355+.BLK	3	0.35	5	0.0	black	yes	prism
131-133	IA355+.EPG	3	0.35	5	0.0	ep. grit	yes	prism
125-127	IA355+.EPO	3	0.35	5	0.0	epoxy	yes	prism
134	IA355+.UND	1	0.35	5	0.0	undeformed	yes	prism
110-112	IA355-.BLK	3	0.35	5	0.0	black	no	prism
113-115	IA355-.EPO	3	0.35	5	0.0	epoxy	no	prism
116-118	IA405+.BLK	3	0.40	5	0.0	black	yes	prism
122-124	IA405+.EPG	3	0.40	5	0.0	ep. grit	yes	prism
119-121	IA405+.EPO	3	0.40	5	0.0	epoxy	yes	prism
100-102	IA405-.BLK	3	0.40	5	0.0	black	no	prism
135-137	IA405-.BLK	3	0.40	5	0.0	black	no	prism
106-108	IA405-.EPG	3	0.40	5	0.0	ep. grit	no	prism
103-105	IA405-.EPO	3	0.40	5	0.0	epoxy	no	prism
213-215	IB355+.BLK	1	0.35	5	7.5	black	yes	prism
210-212	IB355+.EPD	3	0.35	5	7.5	ep. damaged	yes	prism
207-209	IB355+.EPO	3	0.35	5	7.5	epoxy	yes	prism
204-206	IB355-.BLK	3	0.35	5	7.5	black	no	prism
216-218	IB358+.BLK	3	0.35	8	7.5	black	yes	prism
222-224	IB358+.EPD	3	0.35	8	7.5	ep. damaged	yes	prism
219-221	IB358+.EPO	3	0.35	8	7.5	epoxy	yes	prism
201-203	IB358-.BLK	3	0.35	8	7.5	black	no	prism
304-306	IC355+.BLK	3	0.35	5	10.0	black	yes	prism
307-309	IC355+.EPO	3	0.35	5	10.0	epoxy	yes	prism
301-303	IC355-.BLK	3	0.35	5	10.0	black	no	prism
313-315	IC358+.BLK	3	0.35	8	10.0	black	yes	prism
316-318	IC358+.EPO	3	0.35	8	10.0	epoxy	yes	prism
310-312	IC358-.BLK	3	0.35	8	10.0	black	no	prism
421-423	XA355-.BLK	3	0.35	5	0.0	black	no	slab
431-433	XA355-.EPO	3	0.35	5	0.0	epoxy	no	slab
401-403	XB358-.BLK	3	0.35	8	7.5	black	no	slab
410-412	XB358-.EPO	3	0.35	8	7.5	epoxy	no	slab
441-443	XC358-.BLK	3	0.35	8	10.0	black	no	slab
451-453	XC358-.EPO	3	0.35	8	10.0	epoxy	no	slab

Table 5.1

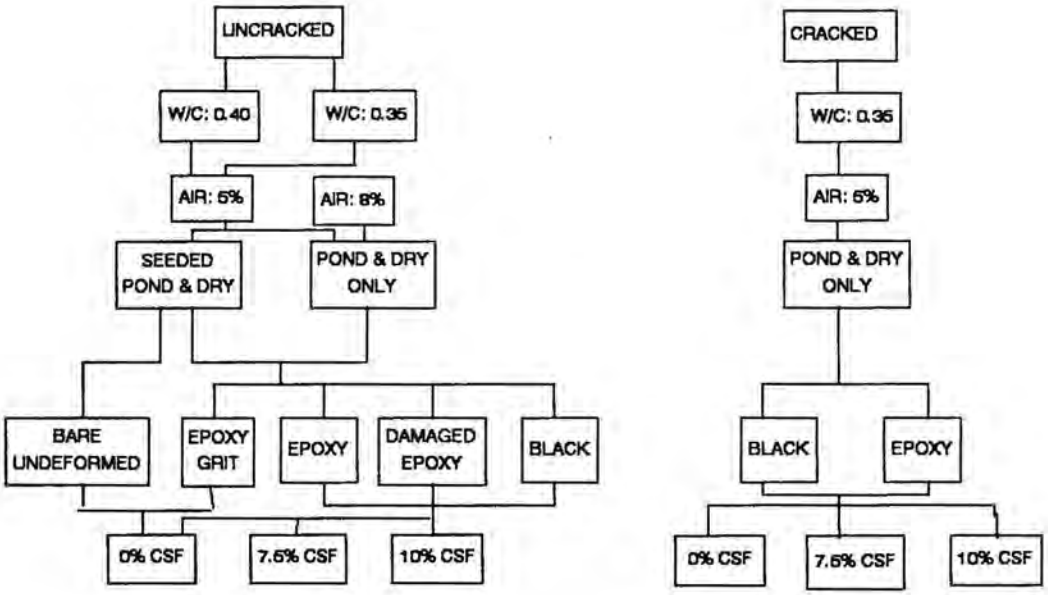

GRAPHIC REPRESENTATION OF EXPERIMENTAL VARIABLES

Figure 5.1

SPECIMEN IDENTIFICATION CODE

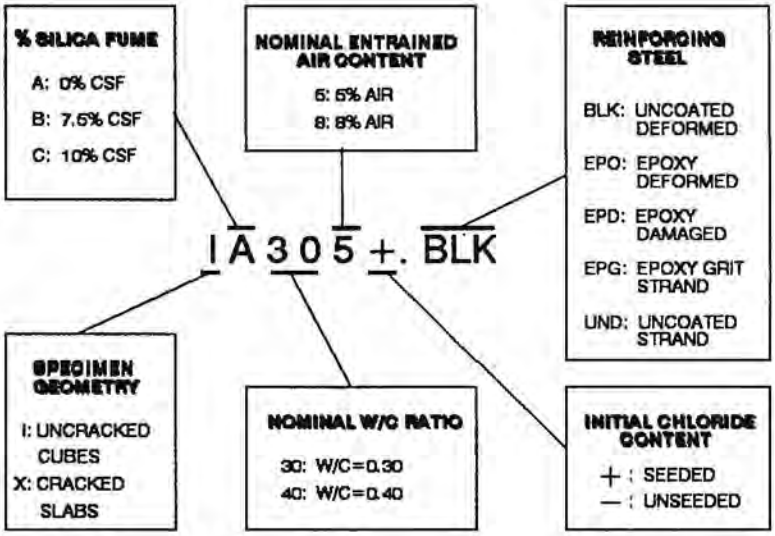

FIGURE 5.2

experimental variables present in any given group of specimens.

A total of six different concrete mix designs were studied. The mix designs are listed in Table 5.2. The coarse aggregate used for all specimens in this study was gravel with a nominal maximum size of 3/4 inch. The fine aggregates had a measured fineness modulus of 2.9. The total quantity of aggregates, and ratio of coarse to fine aggregates (1.25:1) was kept constant for all mix designs.

All mix designs used an ASTM Type I ordinary portland cement, of which the nominal chemical composition is listed in Table 5.3. All mix designs had a cement content of 610 lbs./cu. yard (276 kg.).

Condensed silica fume, when included in the mix design, was introduced to the mix in the form of a slurry (Force 10,000 manufactured by W.R. Grace & Co.). The three nominal percentages of silica fume included in this study were 0%, 7.5%, and 10%, by weight of cement. The silica fume slurry had a unit weight of 11.5 lbs/gallon. Each gallon of slurry mixture contained 5.5 lbs. of condensed silica fume, 5.6 lbs. of water, and 0.4 lbs. of a dispersing agent. The silica fume mix designs included the weight of the water in the slurry in the total water/cementitious ratio for the mix.

The reinforcement used in this study included both coated and uncoated bars. Coated bar types included as-received fusion bonded epoxy-coated rebars (Scotchkote® 213 epoxy coating) which met the ASTM A 775/A 775M - 89 standards, and epoxy grit coated undeformed wire

Concrete Mix Proportions

Mix Designator	Water [lbs]	Type I Cement [lbs]	F.A. (Sand) [lbs]	C.A. (Gravel) [lbs]	Silica Fume [lbs]	Air Admix. [ounces]	HRWRA Admix. [ounces]
IA355	214	610	1305	1625	0	18.3	42.9
IA405	244	610	1305	1625	0	15.6	42.9
IB355	183	610	1305	1625	46	18.3	42.9
IB358	183	610	1305	1625	46	24.3	42.9
IC355	173	610	1305	1625	61	18.3	42.9
IC358	173	610	1305	1625	61	24.3	42.9

All quantities given as per cubic yard concrete

Table 5.2

Type I Portland Cement
Chemical Composition
(nominal values)

Constituent	% By Weight
SiO2	21.20
Al2O3	4.90
Fe2O3	2.35
CaO	64.00
MgO	2.50
SO3	3.00
Free Lime	1.13
K2O	0.58
Na2O	0.43
Loss on ignition	0.97

Caculated Compound Composition

Constituent	% By Weight
Tricalcium Silicate (C3S)	53.90
Dicalcium Silicate (C2S)	20.30
Tricalcium Aluminate (C3A)	9.00
Tetracalcium Aluminoferrite (C4AF)	7.10

Table 5.3

(Armstrong C-701 epoxy coating), which met ASTM A 882 specifications. Specimens were also cast with intentionally damaged Scotchkote epoxy coating to simulate a potential service situation in which a portion of the coating is damaged and not repaired. The epoxy grit coated wire was used "as-received" from Florida Wire and Cable Company. The coated wire is commonly used as spiral confinement reinforcing in columns or deep piles.

The intentionally damaged rebar had the epoxy-coating removed at six approximately equally spaced locations along the 12 inch portion of each bar that was inside the concrete specimen. The coating was removed in approximately 1/4 inch square patches by a stationary grinding wheel.

The first type of reinforcing steel used was Grade 60 deformed steel bars which met ASTM A615 specifications. The uncoated bars and the Scotchkote epoxy-coated bars of this type were both rolled from the same heat of steel at North Star Steel Co., St. Paul, Minnesota. The second type of steel studied in this investigation was a smooth Grade 80 steel wire from Florida Wire and Cable. The study included a single specimen series with uncoated smooth wire which was the same base steel used in the epoxy grit coated reinforcment.

All of the coated reinforcement used in this study were subjected to a scratch and holiday detection survey. A holiday is defined to be the location of a small hole in the epoxy coating of a reinforcing bar. A holiday is small enough that it is not usually visible to the naked eye. Each bar used was

inspected by a hand-held holiday detection device, which located the coating blemishes electronically. The holidays and scratches were marked, recorded, and a statistical summary of the findings is listed in Tables 5.4 - 5.5, and illustrated in Figures 5.3 - 5.4.

ASTM D 3963M-87 requires that the coating on epoxy coated reinforcing bars be visually free from holes, voids and damaged areas. In addition, there should be, on average, no more than two holidays per linear foot. These specifications apply to the bars immediately after coating on the production line [64]. The specification allowance for damage due to shipment and handling requires any damaged areas larger than 1/4 by 1/4 inch to be repaired, with the total patched area on any bar not exceeding 5% of the total bar surface area. None of the coated bars that were used "as-received" in this study had areas of coating damage greater than 1/4 by 1/4 inch.

5.3. Specimen Preparation

Two sizes of concrete corrosion test specimens were constructed, small blocks (prisms) and larger slabs. The prism specimens (see Plate 1a) were cast in 12.5 by 12.5 by 7 inch (31.8 by 31.8 by 17.8 cm.) forms. The geometry of these specimens was similar to that of the specimens in the previously discussed research done by Pfeifer, Landgren and Zoob [15]. The slab specimens (see Plate 1b), designed to test the effect of cracks on the corrosion process, were 12 by 48 by 7 inches (30.5 by 121.9 by 17.8 cm.). Figure 5.5 illustrates the plan view of both prism and slab specimen

Holiday and Scratch Survey
Epoxy Coated Reinforcing Bars - As Received

Bar Diameter:	0.50"
Bar Length:	18"
Number of Bars:	110

SUMMARY DATA ALL BARS

Mean number of Scratches and Holidays per Bar**	8.95
Standard Deviation	6.49
Mean number of Scratches and Holidays per foot of length	7.16
Mean number of Scratches and Holidays per Sq. inch surface	0.38

** Holidays and scratches located within 1.5" from bar ends were not included in this survey.

TABLE 5.4

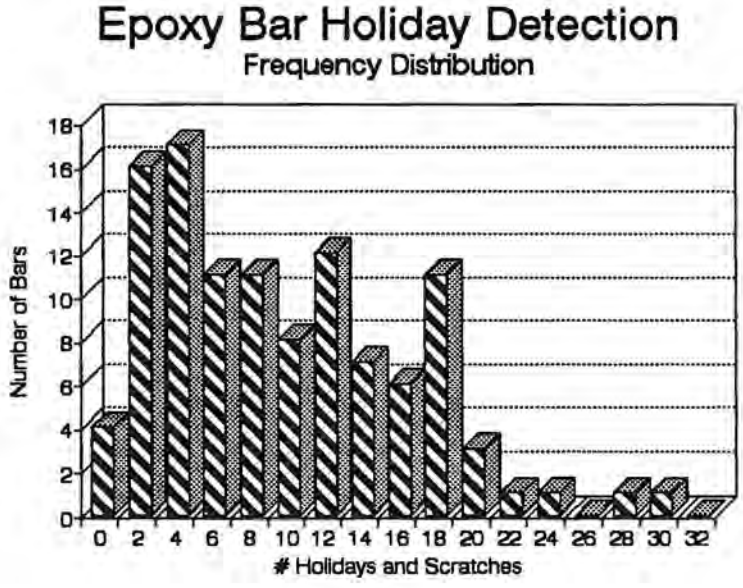

Figure 5.2

Holiday and Scratch Survey
Epoxy Grit Coated Reinforcing Bars - As Received

Bar Diameter:	0.50"
Bar Length:	18"
Number of Bars:	85

SUMMARY DATA ALL BARS

Mean number of Scratches and Holidays per Bar**	7.44
Standard Deviation	5.64
Mean number of Scratches and Holidays per foot of length	5.95
Mean number of Scratches and Holidays per Sq. inch surface	0.32

** Holidays and scratches located within 1.5" from bar ends were not included in this survey.

Table 5.5

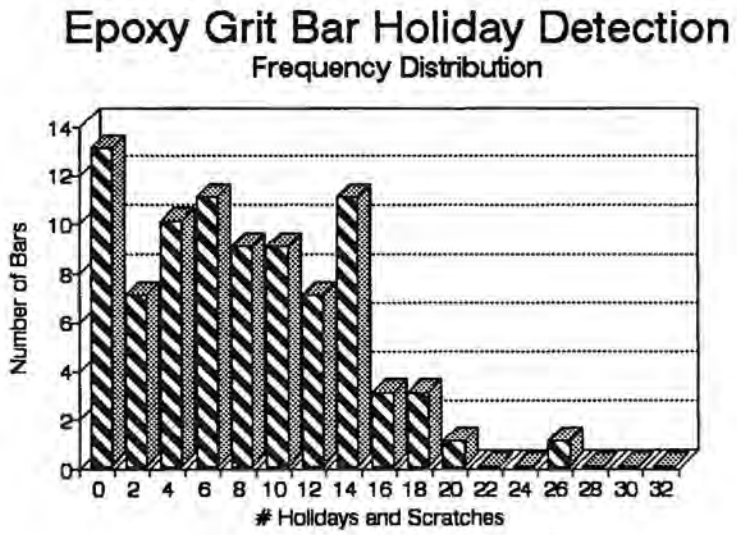

Figure 5.4

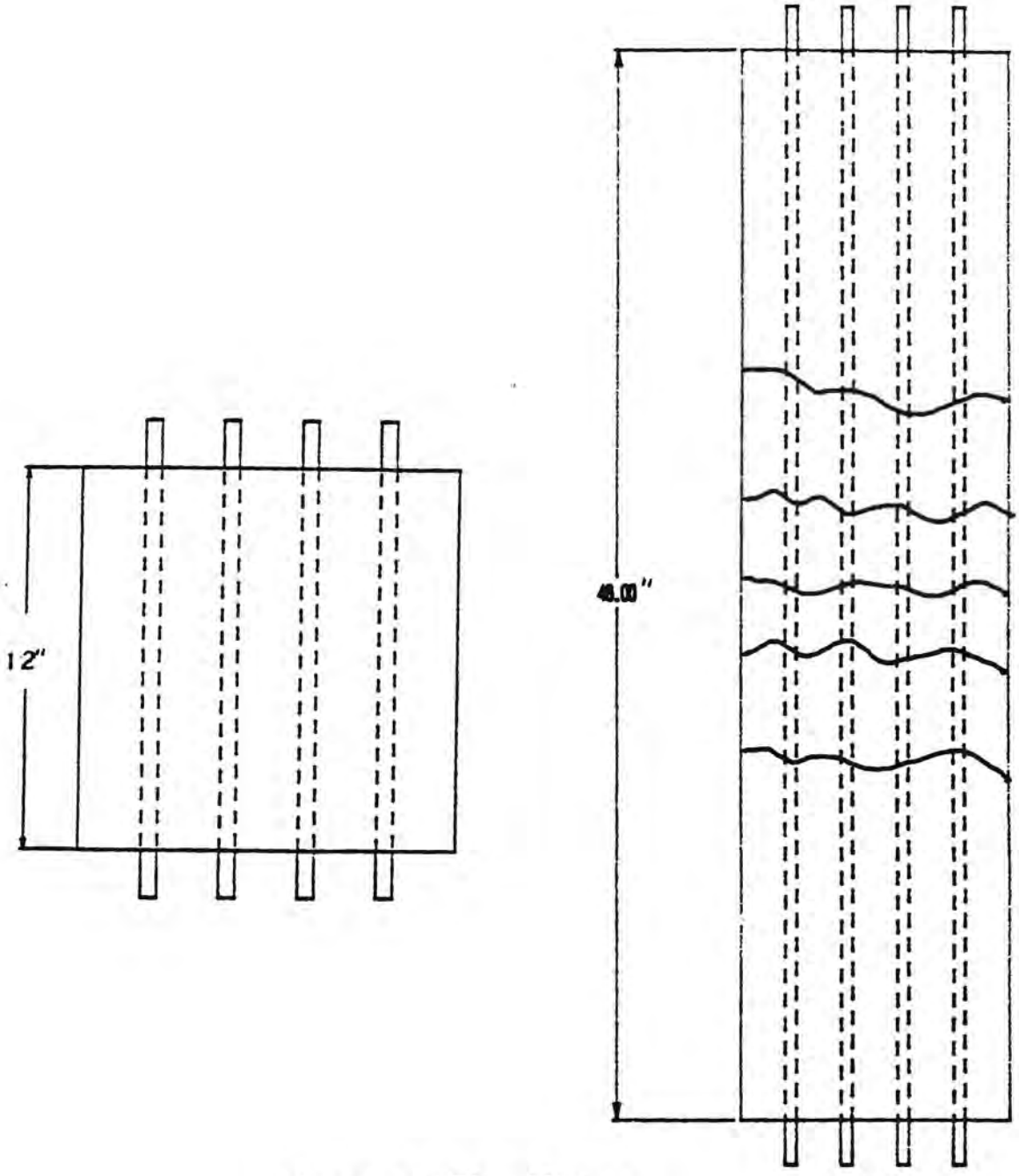

Specimen Plan Views

Figure 5.5

geometry. The front elevation views of both prism and slab specimens are identical (see Figure 5.6). All specimens contained two layers of reinforcing steel. Both the top and bottom layers of reinforcing steel had one inch of clear cover. For the top mat, 2-#4 bars were placed in a horizontal plane with 2.5 inches (6.4 cm.) between the bars. The bottom mat consisted of 4-#4 bars which were centered in a plane parallel to the top mat. All of the specimens were constructed with 4 inches (10.2 cm.) of concrete separating the top and bottom mats. The orientation of the reinforcing steel contained in the specimens used in this study was used in several other macrocell reinforcing steel corrosion studies [15,52].

All of the concrete used in the block specimens was mixed in the structural engineering laboratory at the University of Minnesota, using a 9 cubic foot rotary mixer. The concrete was mixed in relatively small batches (5 cubic feet), so that only a three specimen set having all the same variables was mixed at a time. Because they were not batched together, care was taken to assure continuity for specimens having the same mix design, but different bar types. In these cases, the specimens were all cast on the same day, using the same procedure.

The larger slab specimens were cast from ready-mixed concrete. In these cases, the specimens having the same mix design, but different bar types were all cast from the same concrete batch. The mix designs and materials used in both the block and slab specimens were consistent. The

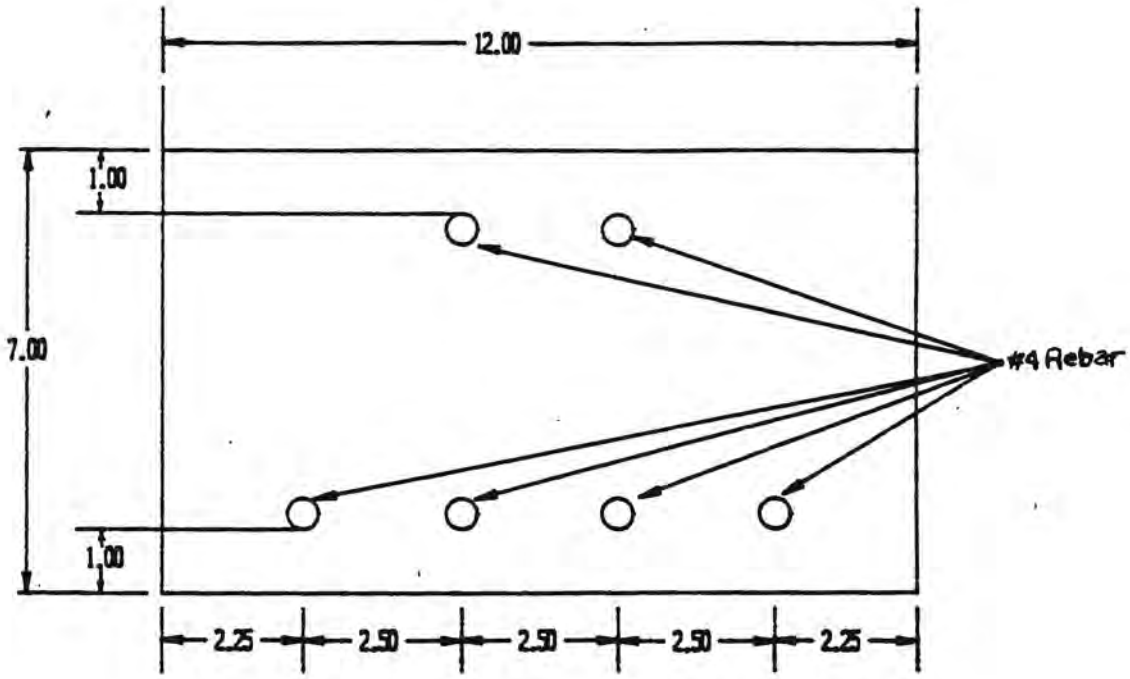

Specimen Front Elevation

Figure 5.6

cement, aggregate, and admixtures used in the block specimens were obtained from the ready-mix supplier.

During each concrete pour, at least three 6 inch diameter concrete cylinders were cast for compressive strength testing. Other quality control tests conducted included measuring the slump and entrained air content of the plastic concrete. Table 5.6 lists measured concrete data with respect to the individual variable groups.

The specimens were cast in reusable plywood forms. The forms were brushed with a commercial form oil prior to casting. After the specimens were cast, they were covered with polyethelene sheeting and kept moist for one week prior to stripping.

After curing, the rebars in each layer were electrically connected together. The top and bottom mats of each specimen were electrically connected with #16 AWS copper wire and nesting banana plugs. Each of the block specimens had a 1 inch concrete dike cast on the top to hold the ponded salt water. Some of these dikes were damaged when the forms were stripped, and in those cases, plexiglass strips were caulked around the top edge of the specimen. All the specimens had the sides covered with a methylmethacrylate concrete sealant. All of the exposed bars and connections were covered with a two part epoxy patching compound.

In order to study the effects of cracks on the corrosion process, the slab specimens had permanent cracks induced with a deflection controlled

Measured Concrete Data

Specimen Identification	W/C ratio	Nominal Air %	Measured Air %	Nominal CSF %	Slump in.	28-day Compressive Strength psi
IA355+.BLK	0.35	5	5.5	0.0	3.5	6420
IA355+.EPG	0.35	5	5.5	0.0	3.5	6420
IA355+.EPO	0.35	5	5.5	0.0	3.5	6420
IA355+.UND	0.35	5	5.5	0.0	3.5	6420
IA355-.BLK	0.35	5	4.5	0.0	6	N/A
IA355-.EPO	0.35	5	4.5	0.0	2.25	N/A
IA405+.BLK	0.40	5	8	0.0	2.25	N/A
IA405+.EPG	0.40	5	8	0.0	2	6381
IA405+.EPO	0.40	5	8	0.0	2	N/A
IA405-.BLK	0.40	5	6	0.0	2	N/A
IA405-.BLK	0.40	5	6	0.0	1.5	6264
IA405-.EPG	0.40	5	6	0.0	3	6818
IA405-.EPO	0.40	5	5.5	0.0	2	6517
IB355+.BLK	0.35	5	6	7.5	2.5	5870
IB355+.EPD	0.35	5	6	7.5	1.75	N/A
IB355+.EPO	0.35	5	6	7.5	3	7699
IB355-.BLK	0.35	5	5.5	7.5	3	9906
IB358+.BLK	0.35	8	8	7.5	5.5	5930
IB358+.EPD	0.35	8	8	7.5	4	6476
IB358+.EPO	0.35	8	8	7.5	4	6476
IB358-.BLK	0.35	8	9	7.5	7	6331
IC355+.BLK	0.35	5	5.5	10.0	7	9114
IC355+.EPO	0.35	5	5.5	10.0	7	9114
IC355-.BLK	0.35	5	5.5	10.0	6	7035
IC358+.BLK	0.35	8	9.5	10.0	4.5	7442
IC358+.EPO	0.35	8	9.5	10.0	4.5	7442
IC358-.BLK	0.35	8	10	10.0	4.5	N/A
XA358-.BLK	0.35	5	N/A	0.0	4.5	6122
XA358-.EPO	0.35	5	N/A	0.0	4.5	6122
XB358-.BLK	0.35	8	N/A	7.5	4.5	8588
XB358-.EPO	0.35	8	N/A	7.5	4.5	8588
XC358-.BLK	0.35	8	N/A	10.0	4.5	9230
XC358-.EPO	0.35	8	N/A	10.0	4.5	9230

Table 5.6

actuator (cracks were induced after the curing process). The specimens were subjected to a two point, transverse load which created a constant moment region across the center 9 inches (22.9 cm.) of the specimen. Loads were increased until flexural crack widths of 0.50 to 1.40 mm. were introduced into the specimens (widths were measured under load). For the specimens containing no CSF, the applied loads were increased to a maximum of 7 kips per load point, resulting in a maximum applied moment of 126 kip·inches. Specimens containing 7.5% and 10% CSF had maximum applied loads of 8 and 9 kips per load point respectively, resulting in maximum applied moments of 144 and 162 kip·inches, respectively. The specimens containing CSF were subjected to increased loads due to the projected increase in strength associated with the addition of silica fume to concrete. The resulting increase in concrete tensile strength required a higher cracking moment for the same specimen geometry and loading condition.

The depth of cracks in the slab specimens averaged 4 inches over all the specimens, with a minimum measured depth of 2.25 inches and a maximum measured depth 6 inches. The widths of the cracks in the slab specimens decreased from the initially measured values after the load was removed. An average crack width of 0.48 mm. was measured on seven slab specimens at the conclusion of the experimental program (minimum value of .25 mm., maximum value of 0.60).

After cracking, the slab specimens were coated on four sides with the

methelmethacrylate sealant, and the top and bottom mats of reinforcing steel were wired together. A plexiglass dike was caulked into place around the top of the specimens, to hold the ponded salt water.

5.3.1. Experimental Corrosive Environment

Several steps were taken to promote a corrosive environment for the reinforcing steel in the concrete specimens. In some specimens, the concrete was placed in two lifts. The lift containing the anodic reinforcing steel was seeded with 20 pounds of chloride per cubic yard of concrete, and the lift containing the cathodic steel was cast with chloride free concrete. The seeded chloride was introduced into the concrete mix water as NaCl. The anodic reinforcing steel in these specimens was subjected to chloride levels that were over 10 times the concentrations that have been suggested to depassify the reinforcing steel [14]. In addition, the differential levels of chloride concentration between the two mats of reinforcing steel in these specimens created a larger potential difference between the two layers of steel, and thus a larger driving force for the corrosion process.

After a 28 day initial curing, all specimens were subjected to a cyclical wetting and drying period, in which a 15% salt water solution was ponded on top of the specimen for 4 days. After ponding, the specimens were vacuumed dry, scrubbed and rinsed with fresh water and left to dry for 3 days. The fresh water scrub and rinse prevented a salt crust from forming on the concrete surface which might have inhibited the absorption of chlorides

into the concrete.

The existence of macrocell corrosion in a large number of reinforced concrete applications (i.e. bridge decks and parking ramps) has been well established [7]. In order to enhance the macrocell corrosion of the reinforcing steel, all specimens were created with a potentially cathodic area of reinforcing steel that was twice that of the potentially anodic steel area. The oxygen reduction reaction occurring at the cathode has the potential to control the entire corrosion rate, therefore, by increasing the area of the cathodic electrode, we can realistically expect to increase the corrosion activity at the anode.

5.4 Experimental Measurement Techniques

The corrosion monitoring measurements of the test specimens were taken weekly beginning with the first salt water ponding cycle. Measurements were always taken at the end of the four day wet cycle. The measurement of resistance, current, and driving voltage were chosen as the significant parameters to monitor in this study. These three measured quantities in the experimental system should obey the following relationship discussed in Section 4.3.:

$$R=\frac{V}{i} \qquad (4.3)$$

Where: V: Potential Difference (volts)
i: Current (amperes)
R: Resistance (ohms)

This general statement is the definition of the resistance of a conductor, whether the V - i curve is linear (Ohm's Law) or not. For each specimen, all of the three variables listed above were monitored: a) potential difference, b) current, and c) resistance. These quantities were monitored externally, between the two mats of steel reinforcement. The significance of each of these variables can be described in terms fluid flow in a pipe.

The potential difference between the two layers of steel can be likened to a pressure difference between two points in the pipe, which drives the flow. The flow of fluid in a pipe (for example, liters/second) is directly analogous to the current. And finally, the resistance of an electrical system can be compared to the physical parameters of our imaginary pipe which would constrict or enhance the fluid flow (i.e. length, interior surface, cross section, etc...).

It is important to note that the current measurements taken in this experimental program cannot and do not represent the total corrosion current present in the reinforcing steel and concrete specimen, but only the macrocell

current between the two layers of steel. It is impossible to measure the current associated with any microcell corrosion activity that can, and most probably will, occur between adjacent portions of the same rebar in a given specimen. This fact does not alter the validity of the microcell current measurement used in this program as a qualitative measurement of the corrosion activity of one specimen or variable group compared to another specimen or variable group in this experiment. It is also generally accepted that the primary, and most damaging corrosion model present in corroding RC structures is a macrocell model [1,7].

Measurements of current, potential difference and also half cell potential were taken with a Keithley Model 614 Electrometer. This sensitive instrument allowed for the measurement of dc currents as low as 10 femto-amperes (10^{-15}A), with a minimal voltage burden, as well as voltages as low as 0.00001 V. Voltage burden can be described as the drop in voltage which occurs internally on a typical multimeter in order to take a measurement. If a conventional voltage meter were used instead of an electrometer, the voltage error introduced by the measureing device could exceed the driving voltage of the system.

In order to measure the potential difference between the two mats of reinforcement, the circuit between the two layers of steel must be open, and the voltmeter inserted in series between the two. However, upon opening the circuit, the potential of each steel layer polarizes away from the other, due to

the effect of the differential environments of each layer. A typical example of this behavior is illustrated by Figure 5.7, in which a single voltage measurement of specimen 129 is plotted. The data aquisition system used captured the "instant-off" voltage measurement for this specimen as 0.075 volts at 10 milliseconds. The potential difference between the two mats of steel continued to increase, as the rebars polarized away from one another.

To record the driving potentials of the specimens, the data collection procedure was triggered and controlled by a personal computer attached to a Keithley series 500 data acquisition system (DAS). The program instructed the DAS to begin recording voltage measurements from the specimen as soon as the circuit was opened. The Keithley data acquisition program enabled us to obtain voltage measurements in 10 millisecond intervals upon opening the circuit between the two layers of reinforcement.

From the resulting data files, the driving voltage could be determined in a consistent fashion for each specimen. In addition to the computer data, the first measurement appearing on the electrometer digital readout was manually recorded for a backup.

After obtaining the driving voltage measurements, the electrometer control was switched to obtain current readings. The data acquisition program sampled 50 current readings, at 10 millisecond intervals, computed the arithmetic average and standard deviation, and displayed the results for operator review. If the readings appeared stable, the mean result was

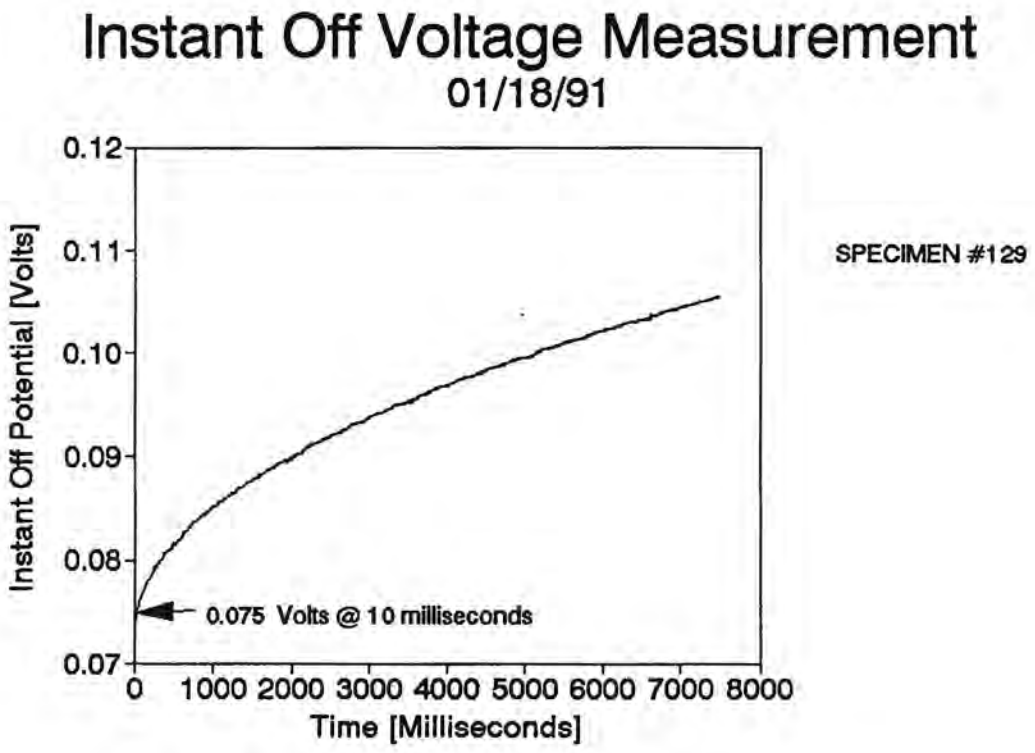
Instant Off Voltage Measurement
01/18/91
SPECIMEN #129
Instant Off Potential [Volts]
0.12
0.11
0.10
0.09
0.08
0.07
0.075 Volts @ 10 milliseconds
0
1000
2000
3000
4000
5000
6000
7000
8000
Time [Milliseconds]

Figure 5.7

appended to a computer data file. Data was also manually recorded at the time of the test for a backup. Plate 2a illustrates the data aquisition system used for this study.

Resistance between the two mats of steel was monitored with the use of a Nielson AC soil resistance meter. The resistance meter had the ability to measure resistance readings as low as 1 ohm, and as large as 1000000 ohms. The resistance meter was an analog device which was manually operated. An AC resistance meter was needed to determine the resistance between the two layers of steel in the presence of the DC corrosion current. Plate 2b shows the resistance meter connected to a slab specimen.

Copper-Copper Sulfate half-cell potentials were also measured in the specimens. As discussed in Section 4.1.2., half-cell potential mapping has been established by ASTM (ASTM C-876) as an acceptable test for the probable location of severe reinforcement steel corrosion activity [51]. While the test has considerable limitations, it is a workable method which given the proper implementation and interpretation, can be of significant use in determining corrosion activity in a concrete structure. Table 4.1 summarized the ASTM recommended interpretation of Cu-$CuSO_4$ half-cell readings.

A half-cell potential survey consists of measuring the electrochemical potential of embedded reinforcing steel against a that of a standardized half-cell (ie, Cu-$CuSO_4$, Ag-AgCl, or saturated calomel electrode) with a portable voltmeter. The voltmeter must be capable of recording potential voltages of

0.02 volts or less without interpolation, with a ±3% end-of-scale accuracy. In this experiment, the $Cu/CuSO_4$ half-cell potential was taken with a 1" diameter M.C. Miller model RE-7 half-cell electrode, attached to the Keithley Model 614 electrometer.

In the experimental measurements, the electrometer measured the potential difference between the $Cu\text{-}CuSO_4$ electrode and the top mat of the reinforcing steel. Every specimen had readings taken from two separate locations on the top surface for each measurement. The half-cell survey was taken while the specimen surface was moist. A water saturated pad between the electrode porous plug and the surface of the specimen insured electrical contact with the concrete. The reference half-cell used for the experimental measurements was routinely checked for accuracy with a duplicate half-cell used only for this purpose. In addition, the half-cell was recharged with a fresh saturated copper sulfate solution every 4 to 6 weeks, as recommended by the manufacturer.

The $Cu\text{-}CuSO_4$ half-cell potential measurement was included in this investigation in order to correlate this research with a commonly used field detection technique. The ASTM acknowledgement of this test has made half-cell potential mapping a tool which is used in both the U.S. and abroad [50]. Past research has established an empirical relationship between $Cu\text{-}CuSO_4$ half-cell readings and the measured macrocell corrosion current [15,52]. This relationship was presented as Equation (4.4). The data gathered for this

research will add additional information to the past work by providing data obtained from a similar test procedure, but using specimens which have different material variables.

5.5 Monitoring Cycle

The entire specimen population was subjected to a cycle of 4 days ponding with a 15% NaCl solution, and 3 days dry at laboratory room temperatures. In all data collection sessions, which were taken at the end of the four day ponding cycle, the following procedure was used:

1. The ponded salt solution on all specimens was vacuumed off. - CIRCUIT CLOSED

2. The specimens were given a fresh water rinse, scrubbed, and the remaining water was vacuumed off. - CIRCUIT CLOSED

3. The microcomputer-controlled data acquisition system was connected to the specimen to be monitored (in series between the two layers of steel). - CIRCUIT CLOSED

4. The electrometer was set for voltage readings. The driving voltage ("instant off voltage") data acquisition routine was run. The circuit was opened. - CIRCUIT OPEN

5. The circuit was closed. Driving voltage reading was reviewed. - CIRCUIT CLOSED

6. The electrometer was set for current readings. The current data acquisition routine was run. Current reading was reviewed. - CIRCUIT CLOSED

7. If half-cell readings were taken, the electrometer was set to read voltage. One electrometer lead was connected to the Cu-Cu SO_4 electrode, and the other electrometer lead was connected to the top layer of reinforcement. - CIRCUIT OPEN

a. The half-cell was placed on a wetted pad, at the first location on top of the specimen. - CIRCUIT OPEN

b. The half-cell potential voltage was manually recorded, the half-cell electrode moved to the second location on top of the specimen and the potential voltage was manually recorded again. - CIRCUIT OPEN

10. The microcomputer controlled data acquisition system was disconnected. - CIRCUIT CLOSED

11. The resistance monitor was attatched in series between the two layers of reinforcment, and the resistance value was manually recorded. - CIRCUIT CLOSED.

Instant off voltage, current, and resistance readings were taken weekly, while half-cell measurements were taken monthly. Many of the specimens that were initially seeded with chlorides had significant corrosion current readings as soon as the monitoring cycle began. Other specimens, such as those in unseeded concrete having epoxy-coated reinforcing steel showed no indication of corrosion current for many weeks.

5.6. Additional Test Specimens

After the initial specimens had all been under test for approximately 5 weeks, evidence of galvanic reaction between bars in the same mat appeared in a limited number of specimens. This prompted the casting of three more specimens, varying the bar configuration and electrical hookup, to enable the isolation of potential corrosion micrcocells between any two bars. These specimens were cast from normal concrete with a w/c ratio of 0.40, and an entrained air content of approximately 5%. Uncoated reinforcing steel was

placed at the same levels as in the previous specimens, however, one specimen had only one bar in each layer, one specimen had one bar in the top mat and two bars in the bottom mat, and the third specimen had two bars in both the top and bottom mat levels.

The electrical hook-up of these specimens allowed for measuring the current, resistance and driving voltage between two bars in the same mat, or to single out any two bars and compare the readings with the conventional readings between the two mats. Because the moisture content in the specimen could not be considered constant over an entire level, it was possible to have galvanic corrosion cells forming between bars in the same layer. This phenomenon could have a significant impact on the original assumption that each layer behaved as a single anode or cathode.

Chapter 6.0 Results and Discussion

6.1.0. Presentation of Results

Information gathered from the experimental data is expressed here in several formats, both tabular and graphic. Prior to discussing specific results, it is necessary to define the two methods used in generating the graphical representations of specimen behavior: average readings and individual readings.

In some cases, the graphical results refer to the average resistance or average current readings. As previously discussed in the experimental procedure section, each variable set tested was represented by three individual specimens. Each of these specimens was subjected to the same environment, for the same time period. Average readings are defined as the arithmetic mean of the absolute value of the weekly measured quantities from the three specimens within the same variable group.

Absolute values are needed for the current readings only. It will be shown that in certain specimens, for varying time periods, the assumed model behavior of anodic top steel to cathodic bottom steel was reversed. This resulted in negative current readings measured for these specimens. It is emphasized that the sign difference does not affect the magnitude of current, i.e., a current reading of -50 μ amps is not smaller than a current reading of +50 μ amps. The negative readings indicate only that the assumed direction of electron flow between the two mats of steel was reversed. The sign of

of corrosion in a given specimen. Rather, it only impacts the layer of reinforcement which behaved as the anode and lost material. Section 6.1.1.1. expands the discussion on specimens which exhibited this behavior.

Individual readings refer to the weekly specimen resistance, current, or instant-off measurements, or the half-cell readings on each of the individual specimens. These results will be presented in tabular form for the entire experimental time period. Some individual current and resistance readings are also presented in graphical format to show the variation or correlation of results among specimens of the same variable group.

6.1.1. Comparison of Behavior of Specimens within a Variable Group

The three specimens within any given variable group were cast together from the same mix, cured under the same conditions, and subjected to the same test environment for the same length of time (unless otherwise noted). In most cases, the specimens within a single variable group exhibited similar behavior.

Figures 6.1 - 6.4 show the correlation between the weekly resistance readings of the three specimens in each of the following groups:

6.1)	IA355+.BLK	(uncracked specimens, 0% CSF, w/c ratio of 0.35, 5% nominal air, initially seeded with salt, uncoated reinforcement)
6.2)	IA405+.BLK	(uncracked specimens, 0% CSF, w/c ratio of 0.40, 5% nominal air, initially seeded with salt, uncoated reinforcement)
6.3)	IB358-.BLK	(uncracked specimens, 7.5% CSF, w/c ratio of 0.35, 8% nominal air, not seeded with salt, uncoated reinforcement)

6.4) IC355+.BLK (uncracked specimens, 10% CSF, w/c ratio of 0.35, 8% nominal air, initially seeded with salt, uncoated reinforcement)

The above figures illustrate the type of consistent behavior among specimens in the same variable group found in roughly 85% of the experimental specimens. In approximately 15% of the cases, specimens of the same variable group exhibited widely varying behavior with regard to measured quantities. Figure 6.5 illustrates specimen group IA405-.EPO, which did not exhibit uniform behavior among the three specimens within the group.

6.1.1.1. Specimens Exhibiting Atypical Behavior.

As discussed in Sections 5.4 and 6.1, after roughly 5 weeks of testing, measurements obtained from a limited number of specimens indicated that the assumed model of anodic top steel and cathodic bottom steel behavior was not occurring. In order to study this behavior, three additional specimens were cast. This group of specimens had electrical connections which enabled measurements of current, resistance or driving voltage between any combination of bars in either mat.

These three specimens were subjected to the same laboratory conditions as the original specimens. Electrical measurements of current and resistance were made between the top and bottom mat as before, however, additional readings were then taken between every two bar combination. The results of this three group study indicated that corrosion current readings of the highest magnitude did not necessarily occur between the top and bottom

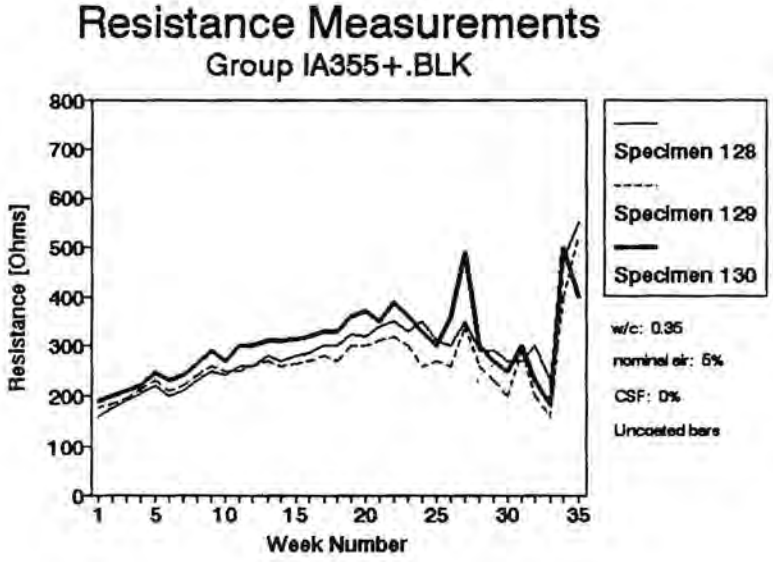
Resistance Measurements
Group IA355+.BLK
Resistance [Ohms]
800
700
600
500
400
300
200
100
0
1
5
10
15
20
25
30
35
Week Number
Specimen 128
Specimen 129
Specimen 130
w/c: 0.35
nominal air: 5%
CSF: 0%
Uncoated bars

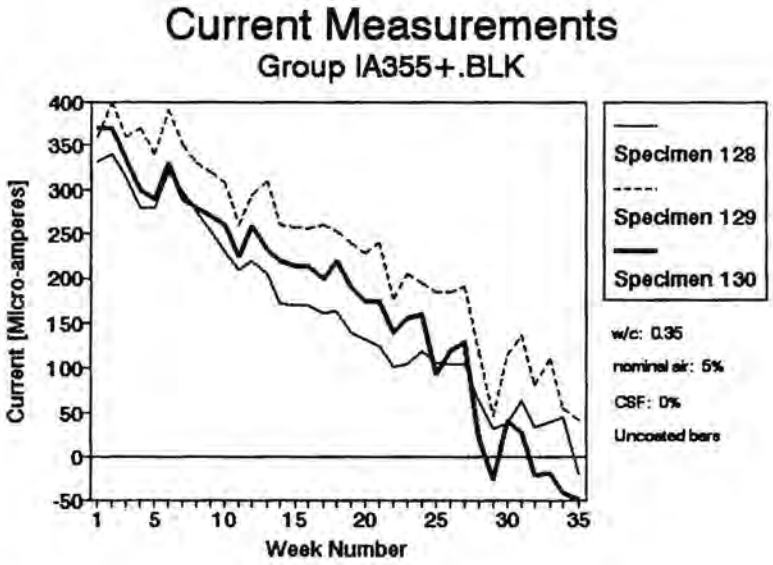
Current Measurements
Group IA355+.BLK
Current [Micro-amperes]
400
350
300
250
200
150
100
50
0
-50
1
5
10
15
20
25
30
35
Week Number
Specimen 128
Specimen 129
Specimen 130
w/c: 0.35
nominal air: 5%
CSF: 0%
Uncoated bars

Figure 6.1

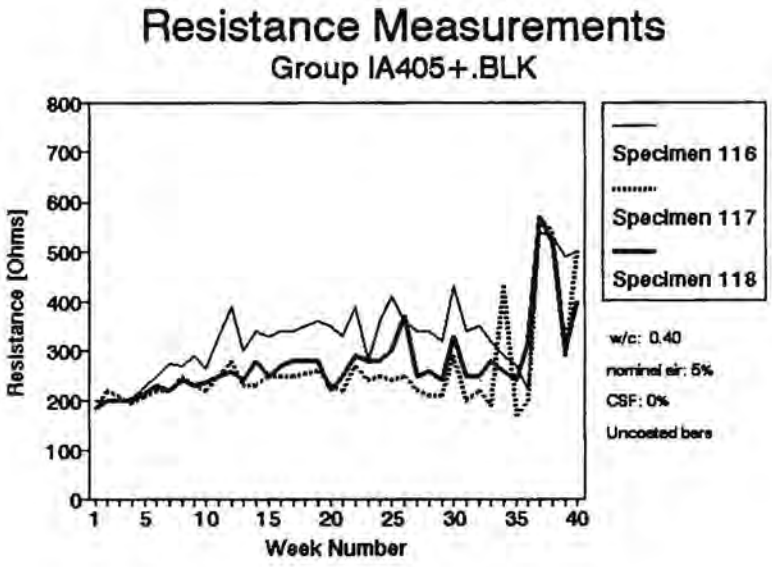
Resistance Measurements
Group IA405+.BLK
Resistance [Ohms]
800
700
600
500
400
300
200
100
0
1
5
10
15
20
25
30
35
40
Week Number
Specimen 116
Specimen 117
Specimen 118
w/c: 0.40
nominal air: 5%
CSF: 0%
Uncoated bars

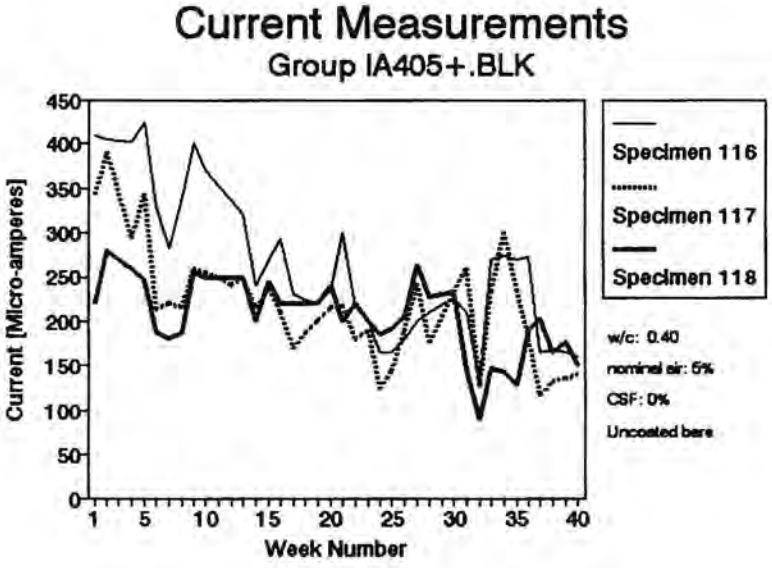
Current Measurements
Group IA405+.BLK
Current [Micro-amperes]
450
400
350
300
250
200
150
100
50
0
1
5
10
15
20
25
30
35
40
Week Number
Specimen 116
Specimen 117
Specimen 118
w/c: 0.40
nominal air: 5%
CSF: 0%
Uncoated bars

Figure 6.2

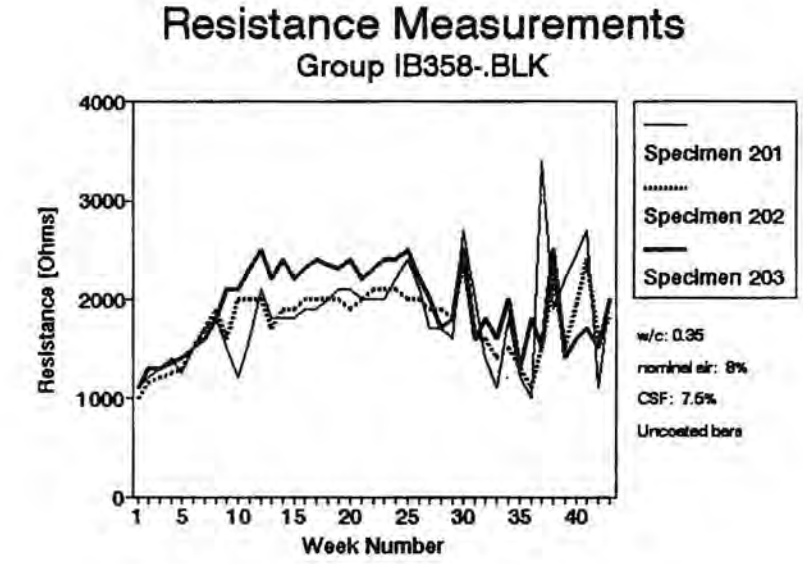
Resistance Measurements
Group IB358-.BLK
Resistance [Ohms]
4000
3000
2000
1000
0
1 5 10 15 20 25 30 35 40
Week Number
Specimen 201
Specimen 202
Specimen 203
w/c: 0.35
nominal air: 8%
CSF: 7.5%
Uncoated bars

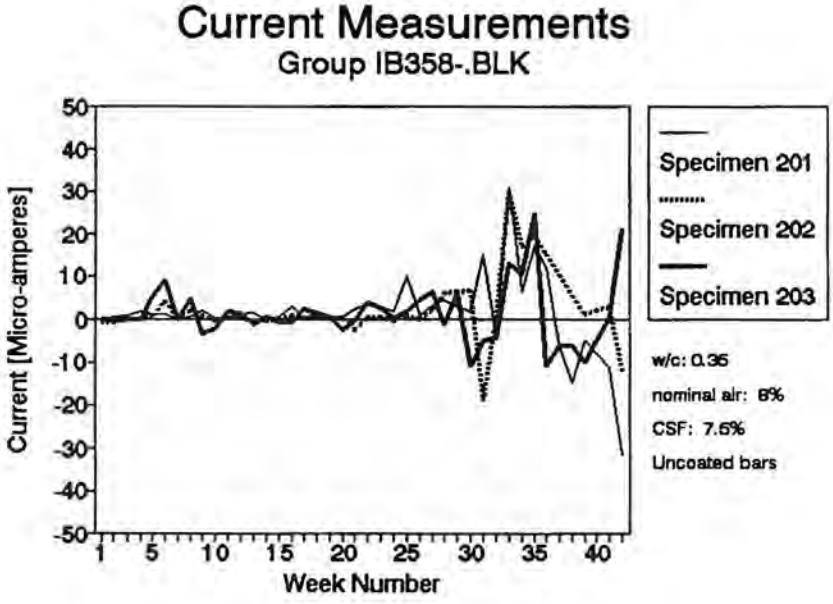
Current Measurements
Group IB358-.BLK
Current [Micro-amperes]
50
40
30
20
10
0
-10
-20
-30
-40
-50
1 5 10 15 20 25 30 35 40
Week Number
Specimen 201
Specimen 202
Specimen 203
w/c: 0.35
nominal air: 8%
CSF: 7.5%
Uncoated bars

Figure 6.3

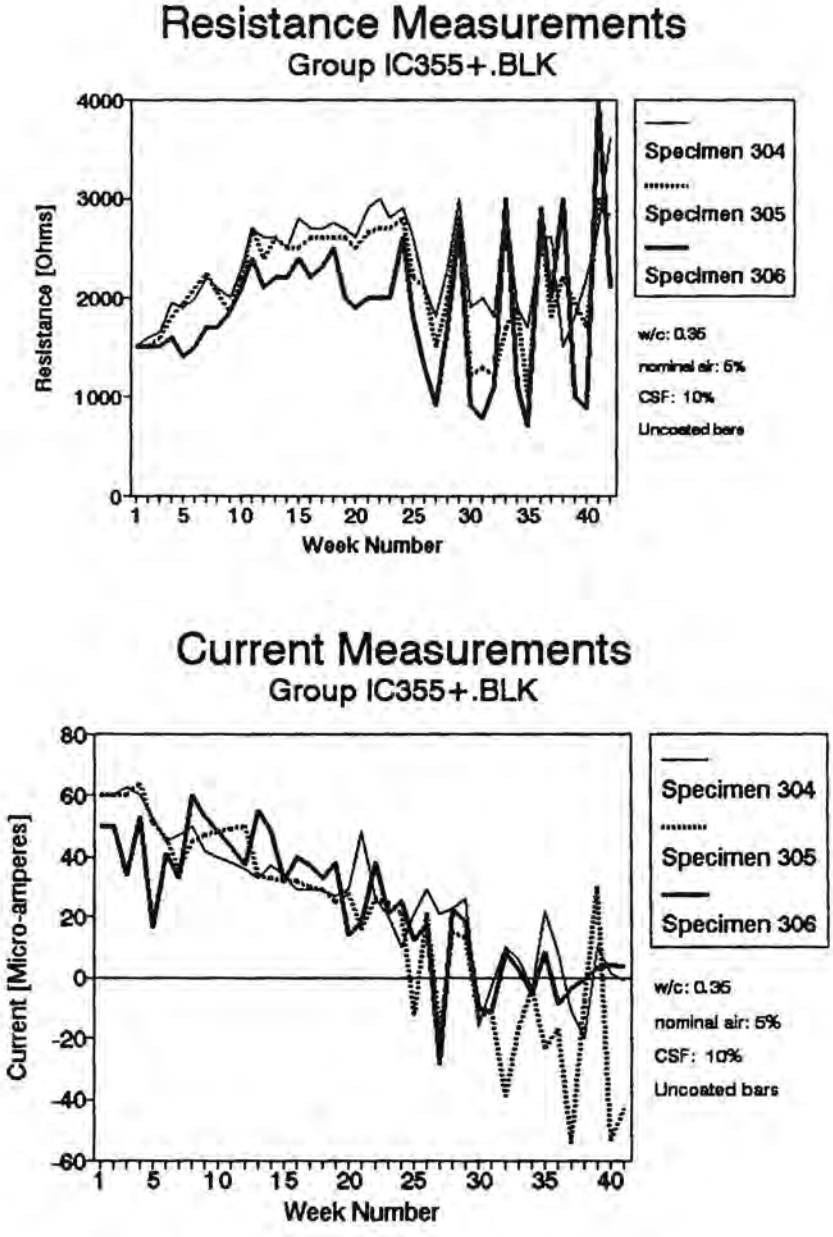
Resistance Measurements
Group IC355+.BLK
Resistance [Ohms]
4000
3000
2000
1000
0
1 5 10 15 20 25 30 35 40
Week Number
Specimen 304
Specimen 305
Specimen 306
w/c: 0.35
nominal air: 5%
CSF: 10%
Uncoated bars
Current Measurements
Group IC355+.BLK
Current [Micro-amperes]
80
60
40
20
0
-20
-40
-60
1 5 10 15 20 25 30 35 40
Week Number
Specimen 304
Specimen 305
Specimen 306
w/c: 0.35
nominal air: 5%
CSF: 10%
Uncoated bars

Figure 6.4

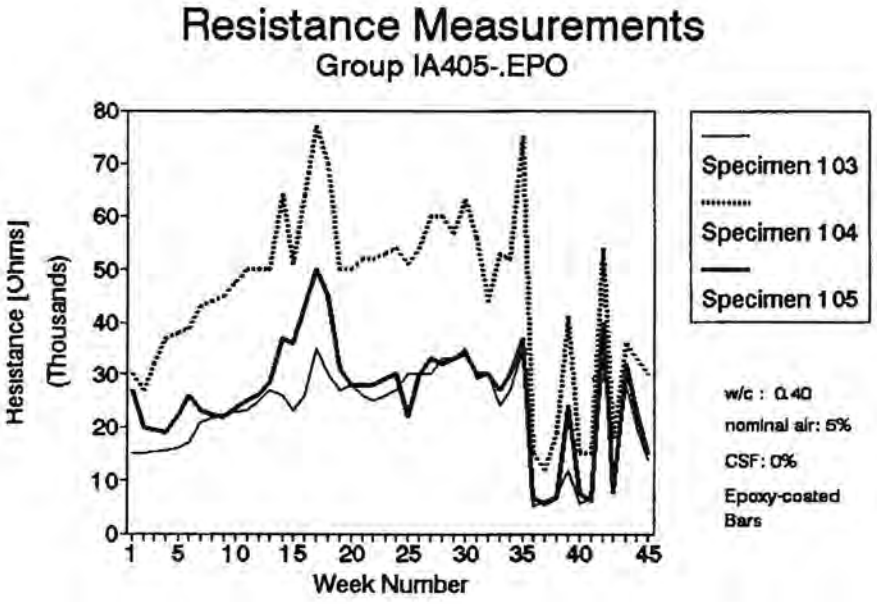
Resistance Measurements
Group IA405-.EPO
Resistance [Ohms]
(Thousands)
80
70
60
50
40
30
20
10
0
1 5 10 15 20 25 30 35 40 45
Week Number
Specimen 103
Specimen 104
Specimen 105
w/c : 0.40
nominal air: 5%
CSF: 0%
Epoxy-coated
Bars

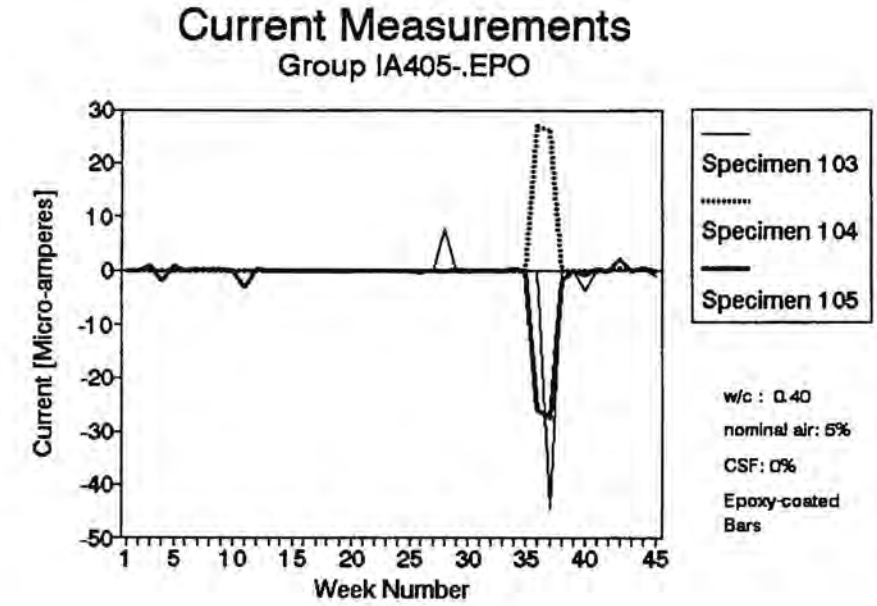
Current Measurements
Group IA405-.EPO
Current [Micro-amperes]
30
20
10
0
-10
-20
-30
-40
-50
1 5 10 15 20 25 30 35 40 45
Week Number
Specimen 103
Specimen 104
Specimen 105
w/c : 0.40
nominal air: 5%
CSF: 0%
Epoxy-coated
Bars

Figure 6.5

mats of steel, but in some cases occurred between bars in the same mat. In other words, it was possible for two bars in the bottom layer of steel to exhibit macrocell behavior where one bar became anodic to the other. The possibility of this occurrence was not considered during the experimental planning, but would be a consideration in further research using the same specimen geometry.

During the experimental test period, the behavior described above did not occur on a consistent basis, but was a sporadic occurrence. This may be due to differential zones of moisture saturation occurring in the specimen during the length of test as a result of humidity, or loss of ponding solution by evaporation. In some cases, peaks or irregularities in current or resistance readings were caused by incidents of accidental loss of ponding solution, where the resistance of the dry specimen was much greater than that of a saturated specimen. These events have been identified, and are noted where applicable. When a reading was identified as being irregular due to a specific cause, the reading was not used in computing the average current or resistance history for that specimen group.

6.2.0. Concrete Material Effects

The effects of air entrainment percentage, condensed silica fume percentage, reinforcing steel coating type, and initial chloride content on the measured corrosion activity of the test specimens are presented in this section.

6.2.1. Air Entrainment

The effect of the percentage of entrained air in the concrete matrix was included in this study because of the opposing properties that increased air percentages bring to the material. Increasing the percentage of entrained air in the concrete matrix increases the volume of air pockets in the concrete. This has the dual property of increasing the electrical resistance of the concrete and also increasing the porosity of the concrete. Increased electrical resistance should inhibit the corrosion mechanism. However, the increased porosity would allow chlorides, external moisture and oxygen a more readily accessible path to the level of the steel reinforcement, thus increasing the corrosion potential of the concrete.

It has been well established that for concretes exposed to freeze-thaw conditions, entrained air is necessary to provide frost resistance. ACI 318-89 Building Code Requirements for Reinforced Concrete requires frost resistant concrete (3/4 in. nominal maximum aggregate size) to have total air contents of 6% and 5% for severe and moderate exposure, respectively [61]. Some designers routinely specify air contents of up to 8% entrained air for concretes subjected to severe exposure. It is not a coincidence that concretes exposed to severe freeze-thaw conditions are also highly probable to be exposed to reinforcement corrosion from sources such as road de-icing salts.

The goal in this study was to determine if the difference between a 5%

and 8% entrained air content made any significant impact on the corrosion resistance of a concrete mix.

Based on the current and resistance readings of the experimental specimens in this program there was no evidence of a direct relationship between the corrosion resistant properties of concretes made with either 5% or 8% (nominal) entrained air. Figures 6.6, 6.7, and 6.8 show that for uncoated, coated, and damaged coated bars, there was not either a significant difference in the resistance or current readings between the air contents, nor was there a constant relationship between the two (i.e. 8% concrete was neither consistently higher or lower than 5% concrete). Refer to Table 5.5 for a complete listing of both nominal and actual entrained air percentages.

6.2.2. Condensed Silica Fume

Results from this study show a consistently significant increase in specimen resistance, and decrease in corrosion current of specimens with CSF compared with those of specimens without CSF. This trend was present in both the prism and cracked slab specimens, in both the seeded and unseeded cases, and was not dependent on bar coating.

These findings are consistent with past research. The addition of condensed silica fume (CSF) to the concrete matrix has been shown to produce a concrete which is dramatically less permeable to chloride ion intrusion [26,32]. This is a direct result of the pozzolanic reaction occurring

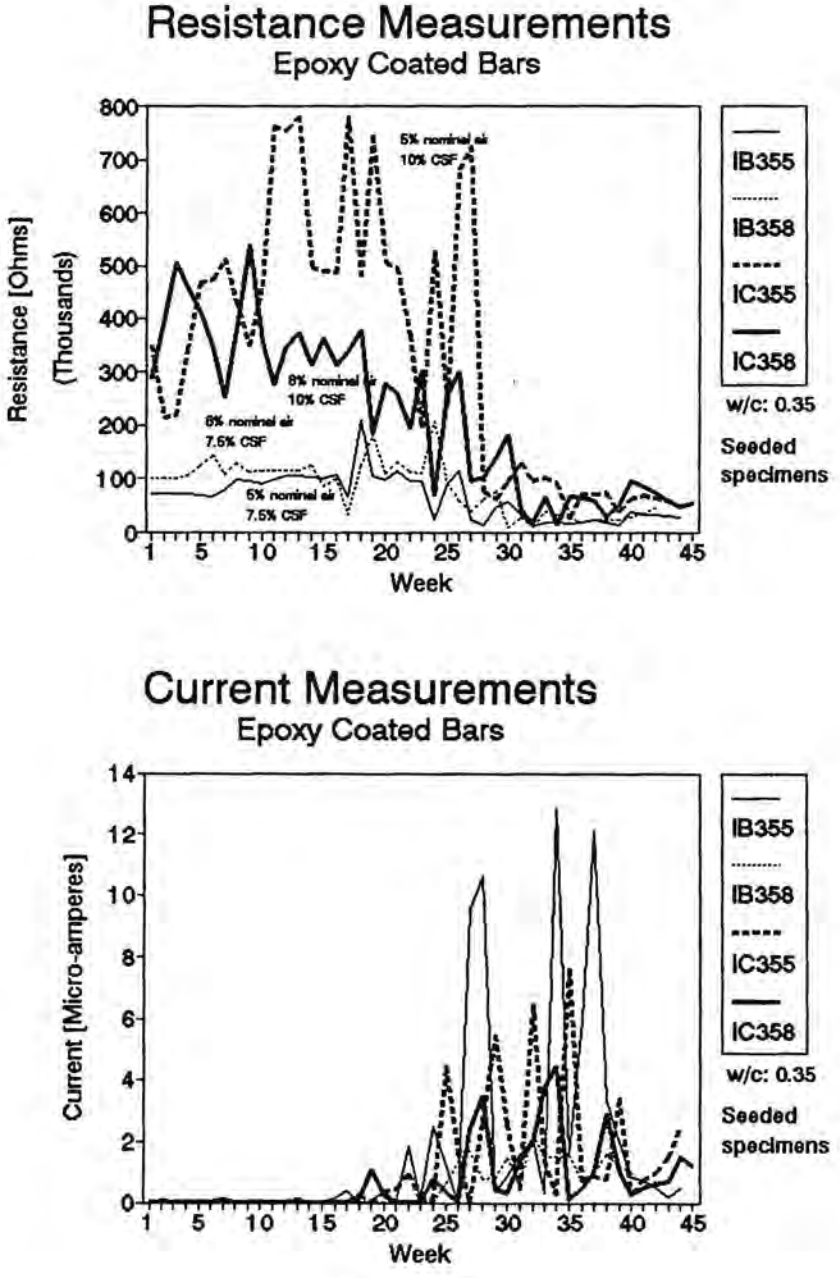
Resistance Measurements
Epoxy Coated Bars
Resistance [Ohms]
(Thousands)
800
700
600
500
400
300
200
100
0
1 5 10 15 20 25 30 35 40 45
Week
5% nominal air
10% CSF
8% nominal air
10% CSF
8% nominal air
7.5% CSF
5% nominal air
7.5% CSF
IB355
IB358
IC355
IC358
w/c: 0.35
Seeded
specimens
Current Measurements
Epoxy Coated Bars
Current [Micro-amperes]
14
12
10
8
6
4
2
0
1 5 10 15 20 25 30 35 40 45
Week
IB355
IB358
IC355
IC358
w/c: 0.35
Seeded
specimens

Figure 6.6

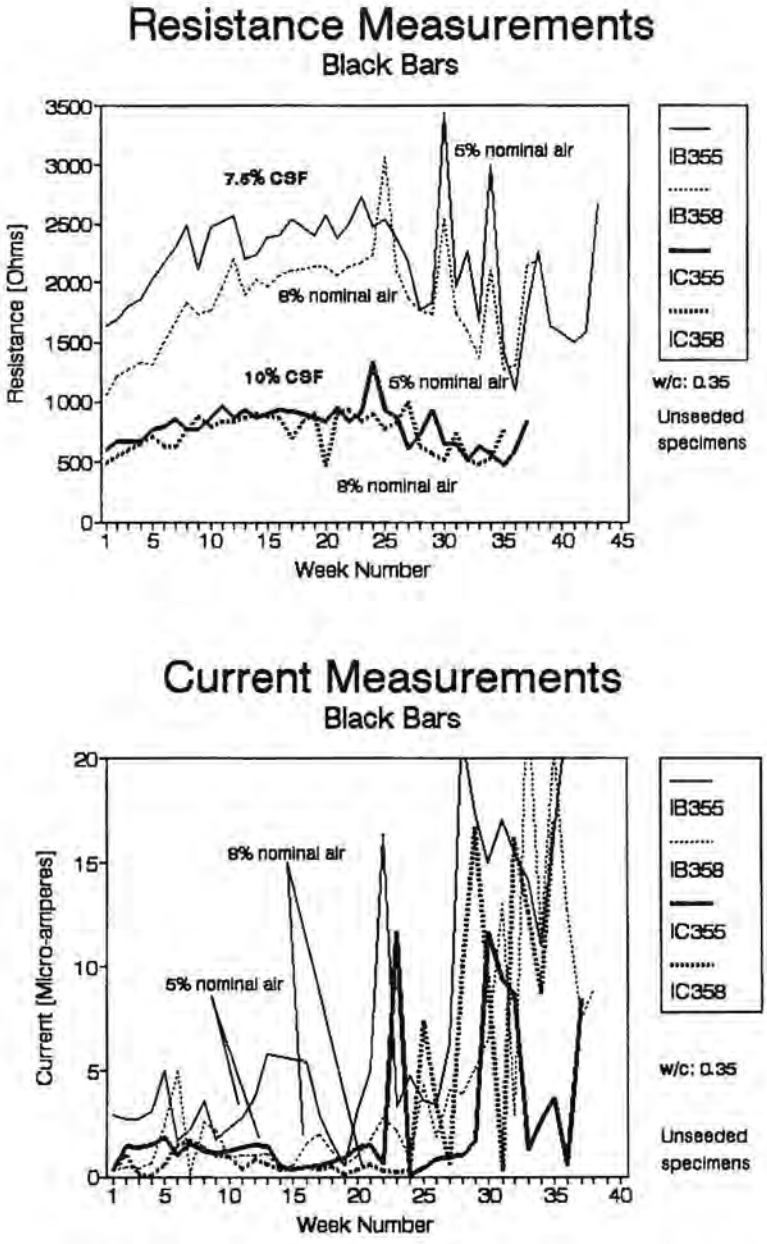
Resistance Measurements
Black Bars
Resistance [Ohms]
Week Number
7.5% CSF
10% CSF
5% nominal air
8% nominal air
IB355
IB358
IC355
IC358
w/c: 0.35
Unseeded specimens
Current Measurements
Black Bars
Current [Micro-amperes]
Week Number
8% nominal air
5% nominal air
IB355
IB358
IC355
IC358
w/c: 0.35
Unseeded specimens

Figure 6.7

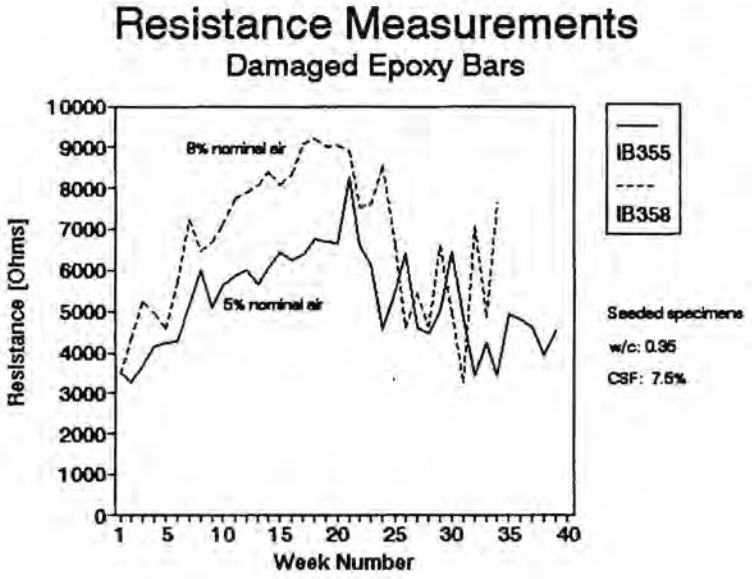
Resistance Measurements
Damaged Epoxy Bars
Resistance [Ohms]
10000
9000
8000
7000
6000
5000
4000
3000
2000
1000
0
8% nominal air
5% nominal air
1
5
10
15
20
25
30
35
40
Week Number
IB355
IB358
Seeded specimens
w/c: 0.35
CSF: 7.5%

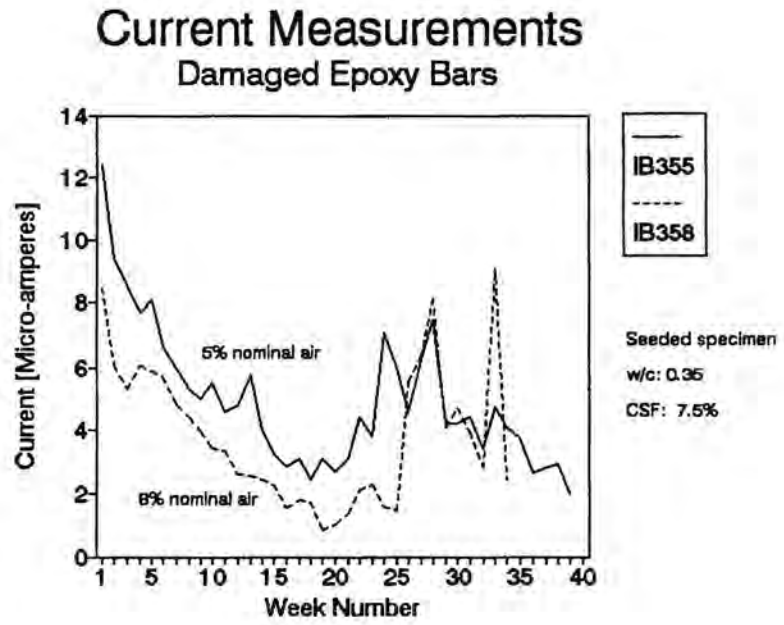
Current Measurements
Damaged Epoxy Bars
Current [Micro-amperes]
14
12
10
8
6
4
2
0
5% nominal air
8% nominal air
1
5
10
15
20
25
30
35
40
Week Number
IB355
IB358
Seeded specimen
w/c: 0.35
CSF: 7.5%

Figure 6.8

between the silica and the calcium hydroxide in concrete, as discussed in Section 3.2.1.

Further investigation on the effects of condensed silica fume on the corrosion of reinforcing steel in this study reveals an interesting trend. Figure 6.9 shows the average resistance and corrosion current measured for unseeded prism specimens containing uncoated reinforcing steel with the three variable quantities of CSF added to the mix (0, 7.5, 10% CSF).

As discussed in Section 6.1.1.1., Figure 6.9 illustrates an incident of abnormal readings for one specimen affecting the average behavior of the specimen group. The peaks on the resistance history graph for group IB355-.BLK occured as a result of one of the three specimens drying out during the test week, thus artificially increasing the average resistance for the entire group. Figure 6.10 shows the range of resistance values for group IB355-.BLK, with the artificially high values marked. Figure 6.11 is a corrected plot of the average resistance and corrosion current measured for unseeded prism specimens containing uncoated reinforcing steel with the three variable quantities of CSF added.

Figures 6.12 and 6.13 illustrate the behavior of seeded prism specimens, and unseeded cracked slab specimens containing uncoated reinforcing steel, with respect to variable quantities of CSF added to the mix.

The results indicate that there may be an optimum quantity of condensed silica fume that is effective in resisting the corrosion of reinforcing

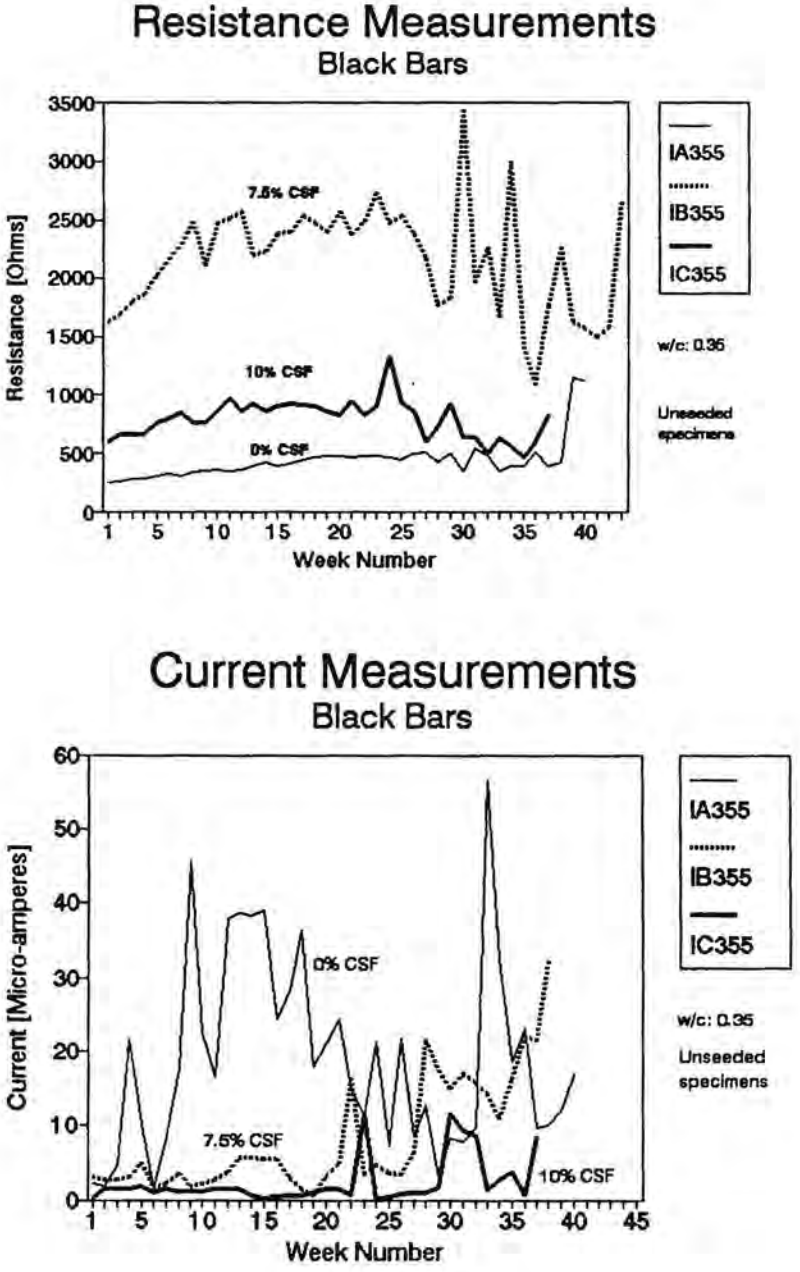
Resistance Measurements
Black Bars
Resistance [Ohms]
3500
3000
2500
2000
1500
1000
500
0
7.5% CSF
10% CSF
0% CSF
1 5 10 15 20 25 30 35 40
Week Number
IA355
IB355
IC355
w/c: 0.36
Unseeded specimens
Current Measurements
Black Bars
Current [Micro-amperes]
60
50
40
30
20
10
0
0% CSF
7.5% CSF
10% CSF
1 5 10 15 20 25 30 35 40 45
Week Number
IA355
IB355
IC355
w/c: 0.35
Unseeded specimens

Figure 6.9

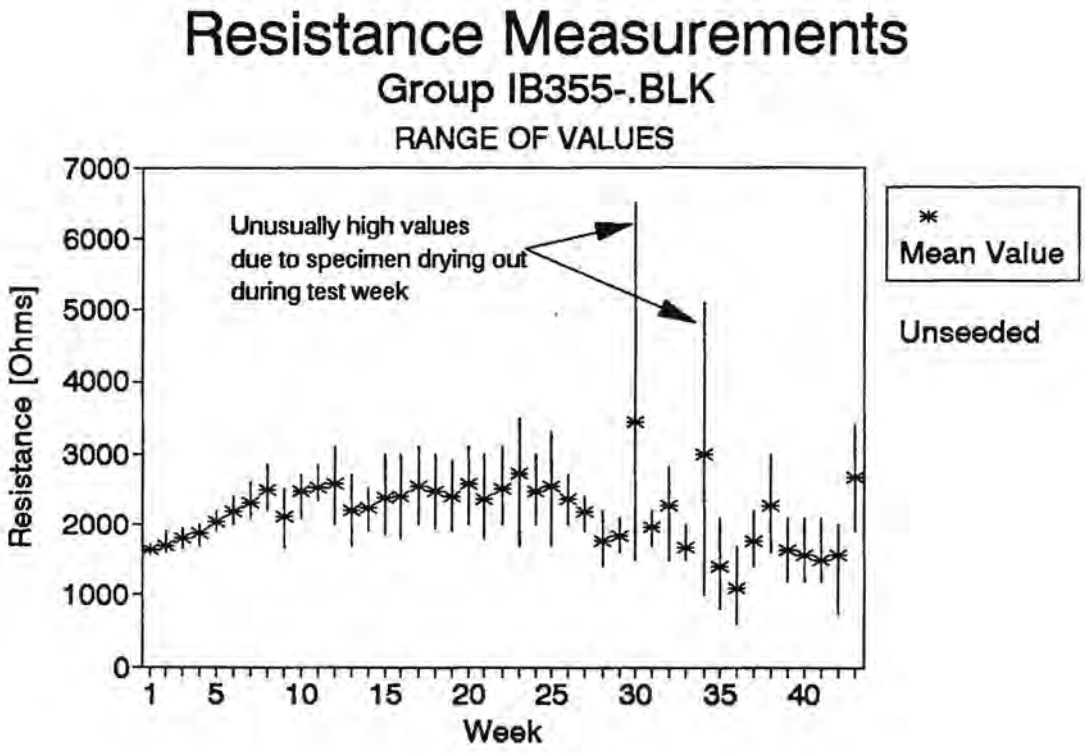
Resistance Measurements
Group IB355-.BLK
RANGE OF VALUES
Resistance [Ohms]
7000
6000
5000
4000
3000
2000
1000
0
Unusually high values
due to specimen drying out
during test week
1
5
10
15
20
25
30
35
40
Week
*
Mean Value
Unseeded

Figure 6.10

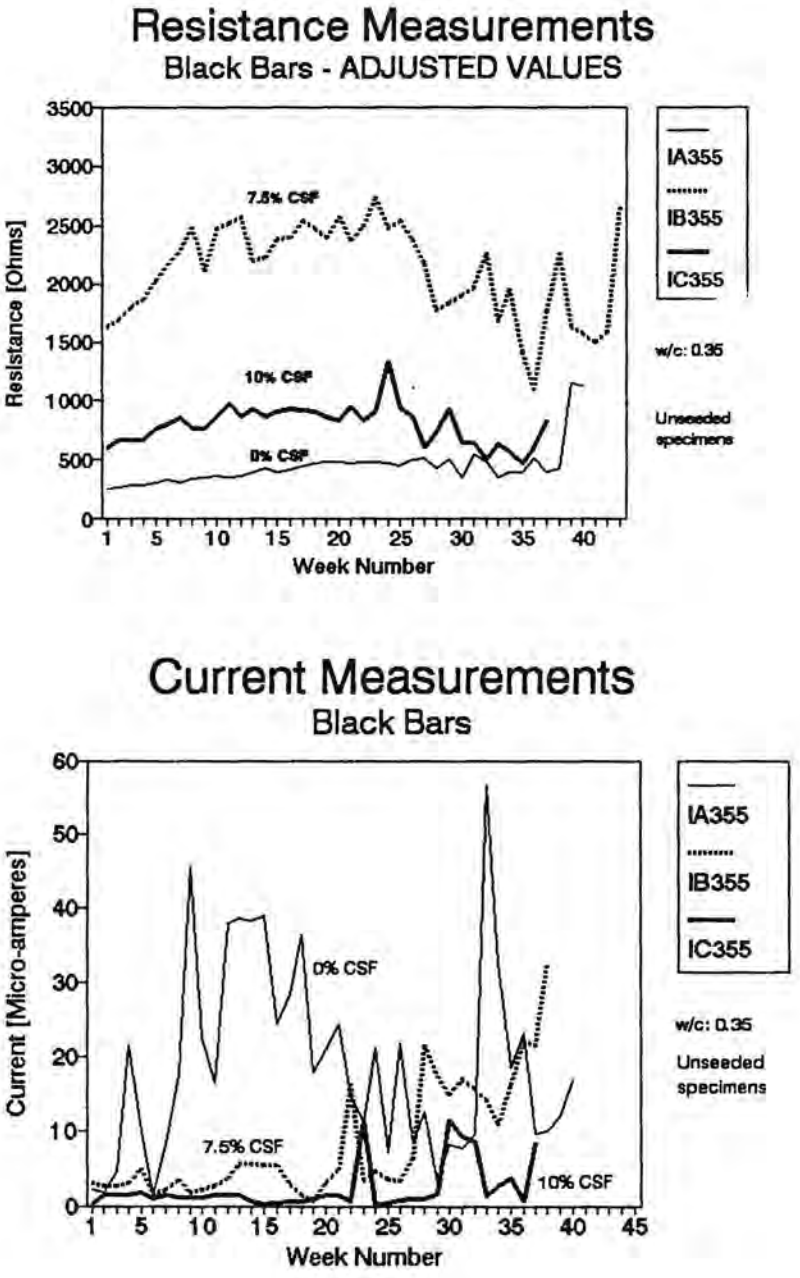
Resistance Measurements
Black Bars - ADJUSTED VALUES
Resistance [Ohms]
3500
3000
2500
2000
1500
1000
500
0
7.5% CSF
10% CSF
0% CSF
1 5 10 15 20 25 30 35 40
Week Number
IA355
IB355
IC355
w/c: 0.35
Unseeded specimens
Current Measurements
Black Bars
Current [Micro-amperes]
60
50
40
30
20
10
0
0% CSF
7.5% CSF
10% CSF
1 5 10 15 20 25 30 35 40 45
Week Number
IA355
IB355
IC355
w/c: 0.35
Unseeded specimens

Figure 6.11

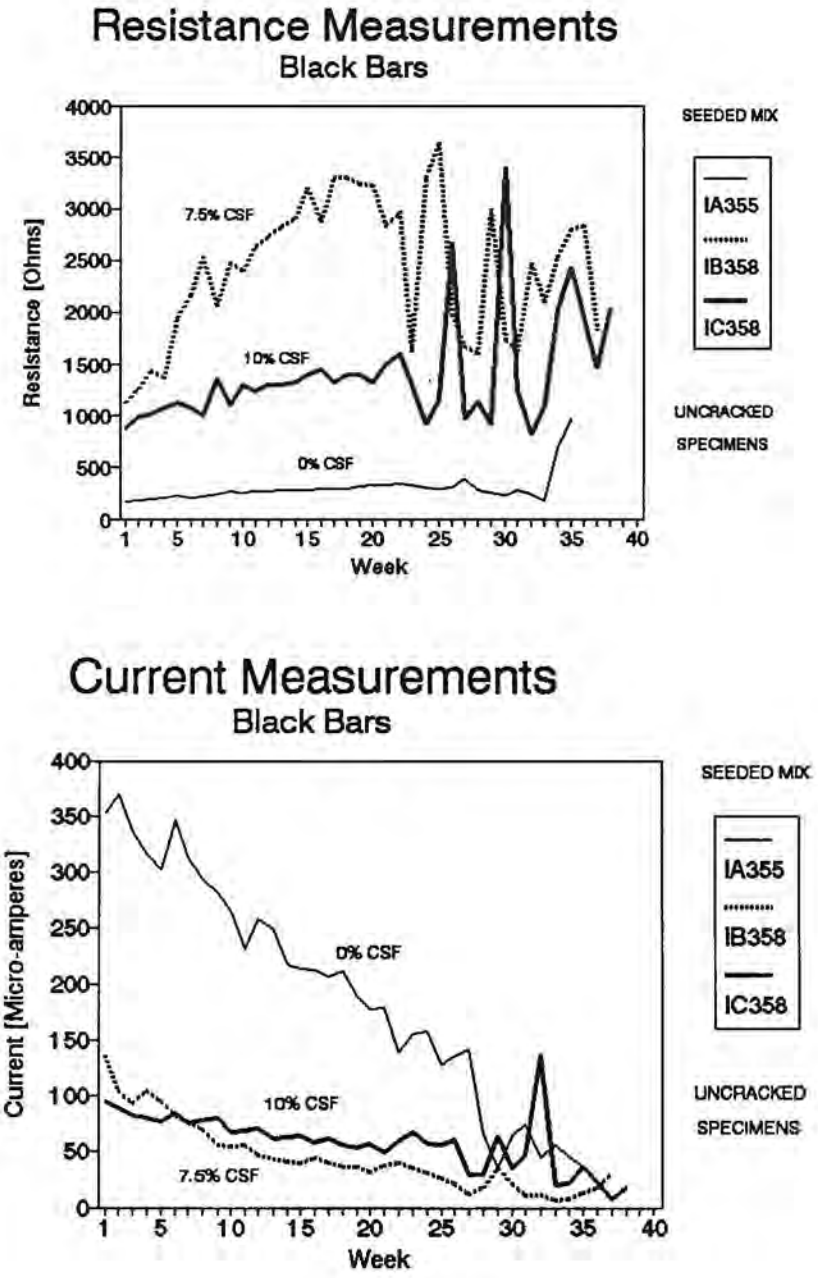
Resistance Measurements
Black Bars
Resistance [Ohms]
4000
3500
3000
2500
2000
1500
1000
500
0
7.5% CSF
10% CSF
0% CSF
1 5 10 15 20 25 30 35 40
Week
SEEDED MIX
IA355
IB358
IC358
UNCRACKED
SPECIMENS
Current Measurements
Black Bars
Current [Micro-amperes]
400
350
300
250
200
150
100
50
0
0% CSF
10% CSF
7.5% CSF
1 5 10 15 20 25 30 35 40
Week
SEEDED MIX
IA355
IB358
IC358
UNCRACKED
SPECIMENS

Figure 6.12

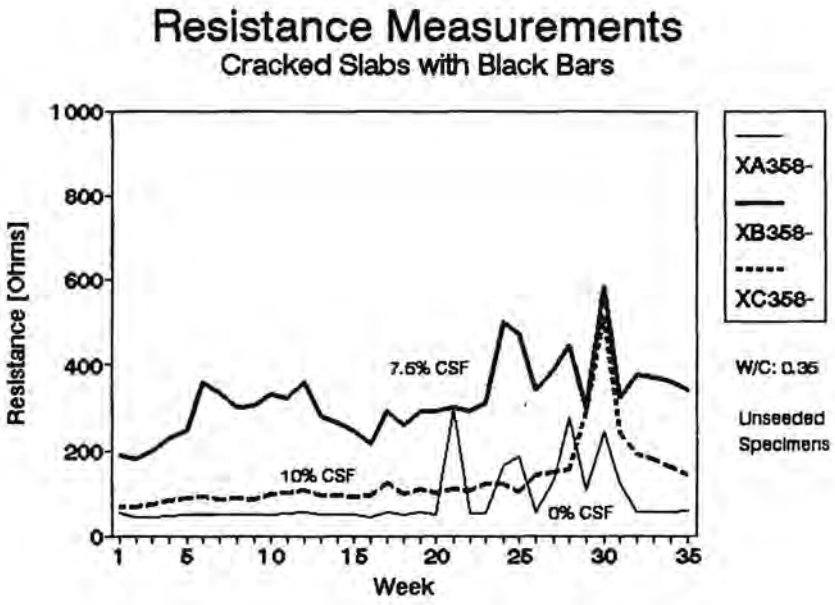
Resistance Measurements
Cracked Slabs with Black Bars
Resistance [Ohms]
1000
800
600
400
200
0
1
5
10
15
20
25
30
35
Week
7.5% CSF
10% CSF
0% CSF
XA358-
XB358-
XC358-
W/C: 0.35
Unseeded
Specimens

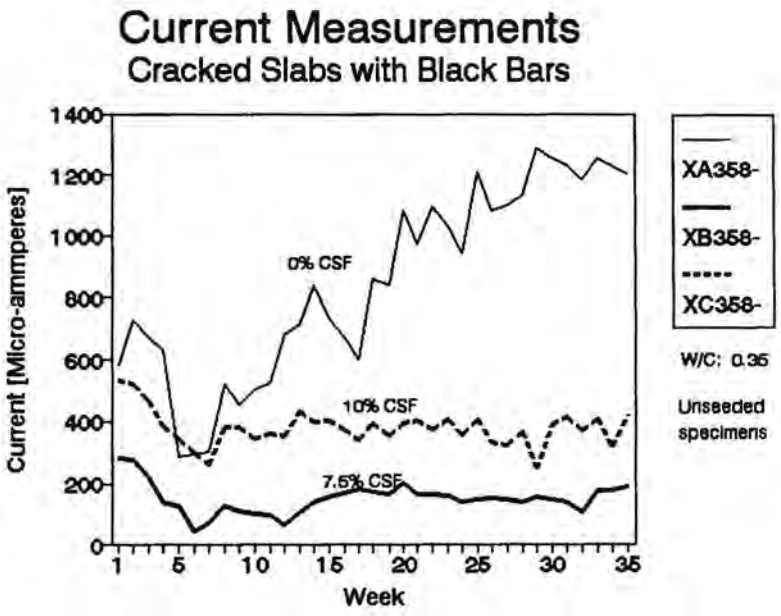
Current Measurements
Cracked Slabs with Black Bars
Current [Micro-ammperes]
1400
1200
1000
800
600
400
200
0
1
5
10
15
20
25
30
35
Week
0% CSF
10% CSF
7.5% CSF
XA358-
XB358-
XC358-
W/C: 0.35
Unseeded
specimens

Figure 6.13

steel in concrete. The difference in resistance readings between the two levels of CSF concrete may be attributed to differential saturation percentages in the specimens (saturated concrete has a much lower resistivity than that of dry concrete). However, given the test conditions, the differences in moisture content should not be consistent among all the specimens indicating this trend.

6.2.2.1. pH Measurements of Condensed Silica Fume Concrete

The addition of condensed silica fume to concrete has been shown to reduce the pH of concrete pore water solutions. The drop in pH values depends on the added quantity of CSF; however, pH values as low as 10.0 have been reported in concretes having 30% silica fume by mass of cementitious material [60]. A drop in the pH value of the concrete surrounding reinforcing steel leads to a reduction in the threshold concentration of chlorides needed to initiate depassivation of the steel, and therefore begin the corrosion process.

Additional research into the effects of chlorides added to concrete containing microsilica reports that as the level of microsilica increases, the fraction of chloride available in the pore water also increases [28]. In other words, as the concentration of CSF increases, the concrete's ability to complex chlorides out of solution decreases. It is suggested that this effect is due to the lower pH value of CSF concrete, which increases the solubility and decreases the quantity of calcium aluminate (CA), the cement component

which is credited with having the ability to bind chloride ions.

Results from this experiment indicated that specimens containing 10% CSF had incidences of higher measured corrosion currents over those containing 7.5% CSF. This prompted an investigation of the pH values for the two concretes as a possible explanation for the behavior.

Powder samples were taken from specimens containing each of the three quantities of CSF (0%, 7.5%, 10%), at the level of the top and bottom mats of reinforcing steel by a power drill. The pH investigation considered both specimens that initially contained chlorides in the top level of steel, and those that were initially chloride free. The samples were taken at the conclusion of the experimental program. One gram of powdered concrete was mixed with 10 ml deionized water, and the pH values were measured using an Orion pH meter. The results of this study are presented in Figure 6.14 and Table 6.1.

Results from this limited test support the fact that concretes containing CSF as a pozzolanic admixture tend to lower pH values. The lowest recorded pH value of 11.4 was exhibited at the top level of reinforcing steel in a specimen containing 10% CSF and no initial chlorides. A maximum recorded pH value of 12.1 was obtained in two of the specimens containing 0% CSF, one with, and one without initial chlorides present in the top level.

Statistically, the results of this test alone are not represented here as being conclusive evidence that an increase in CSF percentage allows for

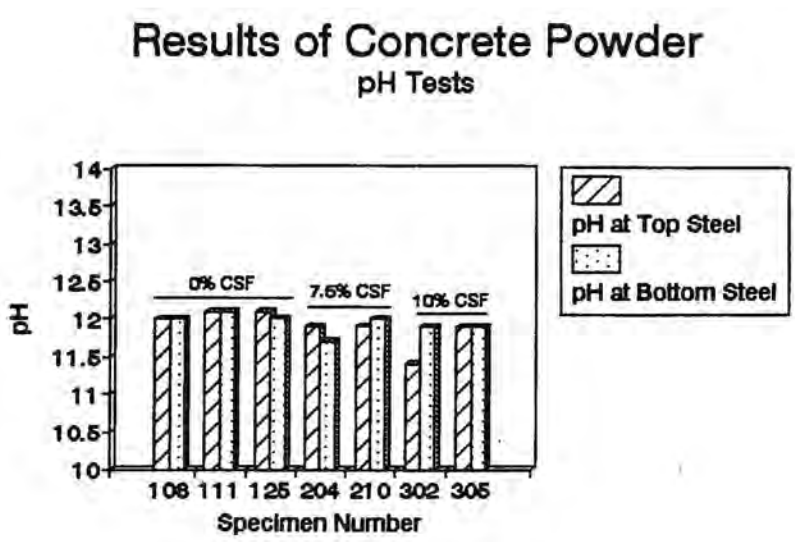

Figure 6.14

Specimen Number	Variable Group	pH Depth 1-1.5"	pH Depth 5.5-6"
108	IA405-.EPG	12.0	12.0
111	IA405+.EPG	12.1	12.1
125	IA355-.EPG	12.1	12.0
204	IB355-.BLK	11.9	11.7
210	IB355+.BLK	11.9	12.0
302	IC355-.BLK	11.4	11.9
305	IC355+.BLK	11.9	11.9

Results of Concrete Powder pH Tests

Table 6.1

increased corrosive activity. Especially since the seeded specimen containing 10% CSF returned pH values no lower than the 7.5% specimens. However, the trend shown here tends to support previous research results of the chemistry of CSF added concrete with regard to pH [22,28,60]. These results, combined with the established link between pH and corrosion activity [56], tend to reinforce the hypothesis presented in Section 6.2.2. on the existence of an optimum quantity of CSF which could be added to concrete as a corrosion inhibitor.

6.2.3. Effect of Reinforcing Steel Coatings on Corrosion Activity

The specimens containing reinforcing steel bars coated with epoxy coatings exhibited significantly higher resistance measurements, and lower current measurements than those specimens having uncoated bars. Undamaged epoxy coatings not only protect the reinforcing steel from the corrosion initiating chlorides, but insulate the steel from the electrochemical reaction as well. These advantages of epoxy coated reinforcement have been known since the early 1970's. Therefore, these results were predictable. The goal in selecting reinforcing bar coating types as a variable in this experiment was to compare the relative performance of the coatings.

6.2.3.1. Coated vs. Uncoated Bars

The differences in resistance and current measurements from the experimental specimens having coated reinforcing bars and those having uncoated bars were consistent across all mix design types. Figures 6.15 -

6.17 show the average (over each specimen group) resistance and current measurement histories of the uncracked specimens which were initially seeded with chloride as discussed in Section 5.1. The specimens containing epoxy coated steel exhibited resistance values that were consistently two orders of magnitude larger than those of the uncoated bars. Accordingly, the differences in the corrosion current measured from these specimens were also great. In many cases, the epoxy coated specimens registered currents < 1 μ ampere, which for the purposes of this experiment were negligible. At current levels this low, the galvanic reaction between the measurement and specimen connections begins to affect the readings.

6.2.3.2. Epoxy vs. Epoxy Grit Bars

Figure 6.15 shows a significant difference in the average specimen resistance readings between the specimens having epoxy coated bars (Scotchcote® 213) and those with epoxy grit coated bars (Armstrong C-701) for mix design IA355+ (uncracked specimens, 0% CSF, 0.35 w/c ratio, 5% nominal air, initially seeded with chloride). Figure 6.18 illustrates a similar difference in resistance seen for the unseeded prisms having mix design IA405- (uncracked specimens, 0% CSF, 0.40 w/c ratio, 5% nominal air, unseeded). The other mix design set that included both the epoxy and epoxy grit coated bars (IA405+) had generally higher resistance readings for the epoxy grit specimens, but the differences between the two systems were not of the same magnitude as those observed for the first two examples.

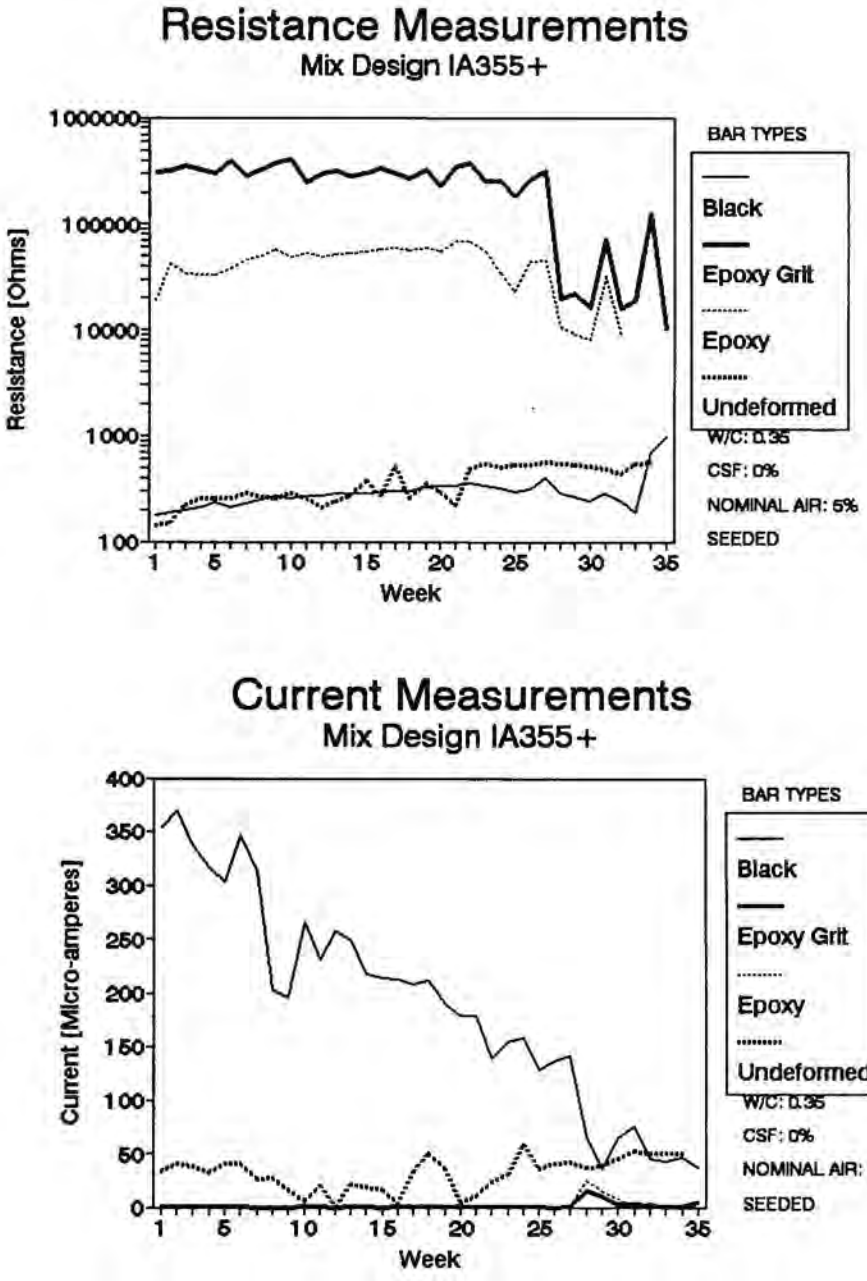
Resistance Measurements
Mix Design IA355+
Resistance [Ohms]
1000000
100000
10000
1000
100
1
5
10
15
20
25
30
35
Week
BAR TYPES
Black
Epoxy Grit
Epoxy
Undeformed
W/C: 0.35
CSF: 0%
NOMINAL AIR: 5%
SEEDED
Current Measurements
Mix Design IA355+
Current [Micro-amperes]
400
350
300
250
200
150
100
50
0
1
5
10
15
20
25
30
35
Week
BAR TYPES
Black
Epoxy Grit
Epoxy
Undeformed
W/C: 0.35
CSF: 0%
NOMINAL AIR: 5%
SEEDED

Figure 6.15

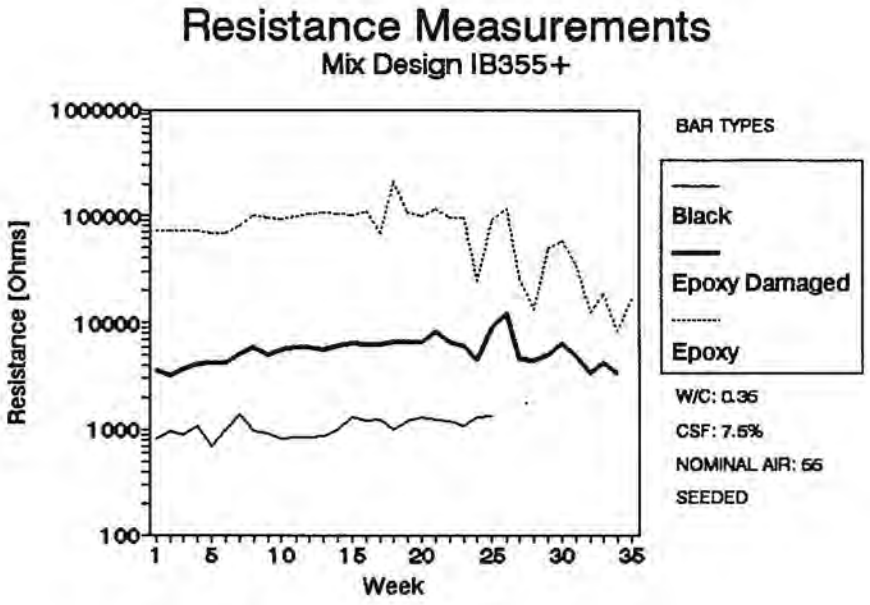
Resistance Measurements
Mix Design IB355+
Resistance [Ohms]
1000000
100000
10000
1000
100
1
5
10
15
20
25
30
35
Week
BAR TYPES
Black
Epoxy Damaged
Epoxy
W/C: 0.35
CSF: 7.5%
NOMINAL AIR: 6%
SEEDED

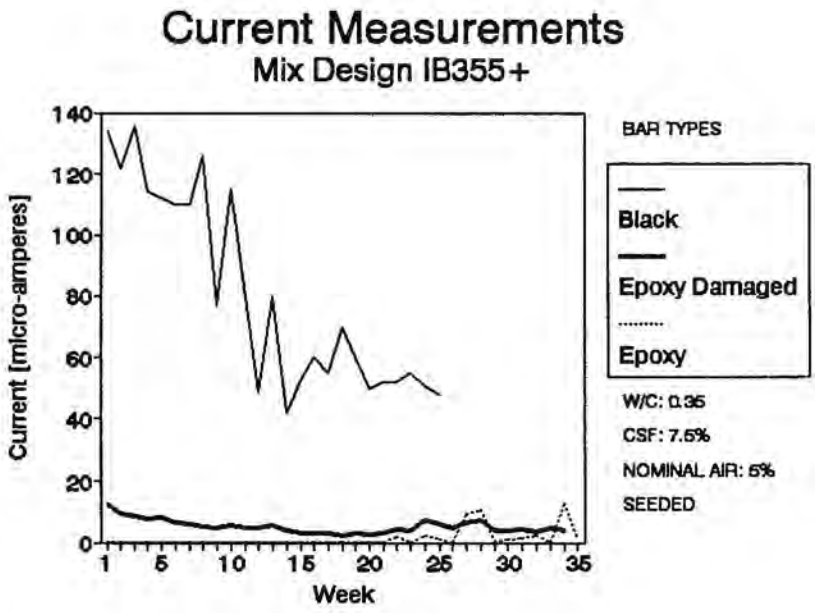
Current Measurements
Mix Design IB355+
Current [micro-amperes]
140
120
100
80
60
40
20
0
1
5
10
15
20
25
30
35
Week
BAR TYPES
Black
Epoxy Damaged
Epoxy
W/C: 0.35
CSF: 7.5%
NOMINAL AIR: 6%
SEEDED

Figure 6.16

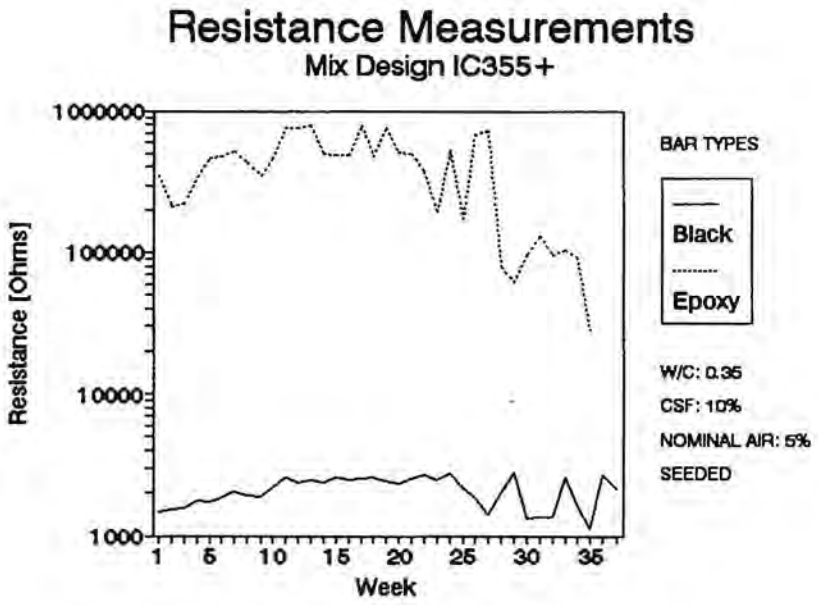
Resistance Measurements
Mix Design IC355+
Resistance [Ohms]
1000000
100000
10000
1000
1
5
10
15
20
25
30
35
Week
BAR TYPES
Black
Epoxy
W/C: 0.35
CSF: 10%
NOMINAL AIR: 5%
SEEDED

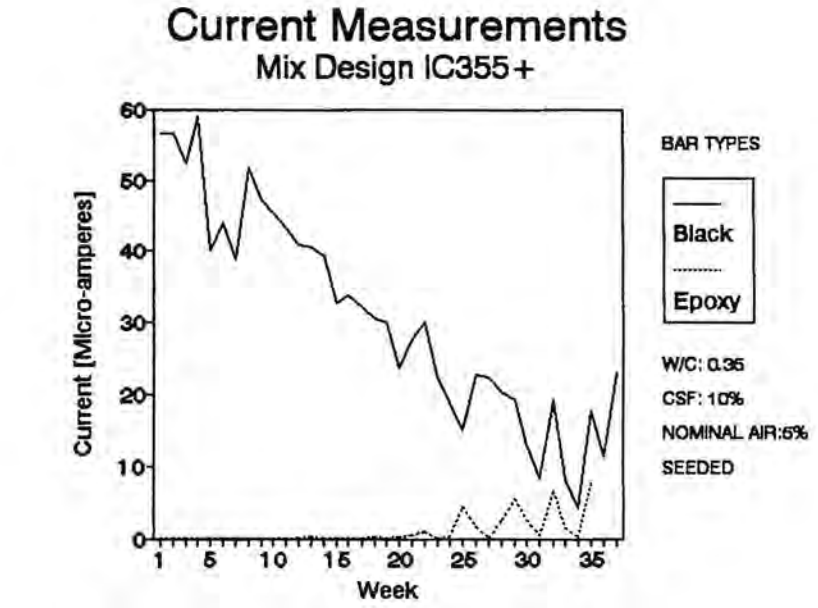
Current Measurements
Mix Design IC355+
Current [Micro-amperes]
60
50
40
30
20
10
0
1
5
10
15
20
25
30
35
Week
BAR TYPES
Black
Epoxy
W/C: 0.35
CSF: 10%
NOMINAL AIR:5%
SEEDED

Figure 6.17

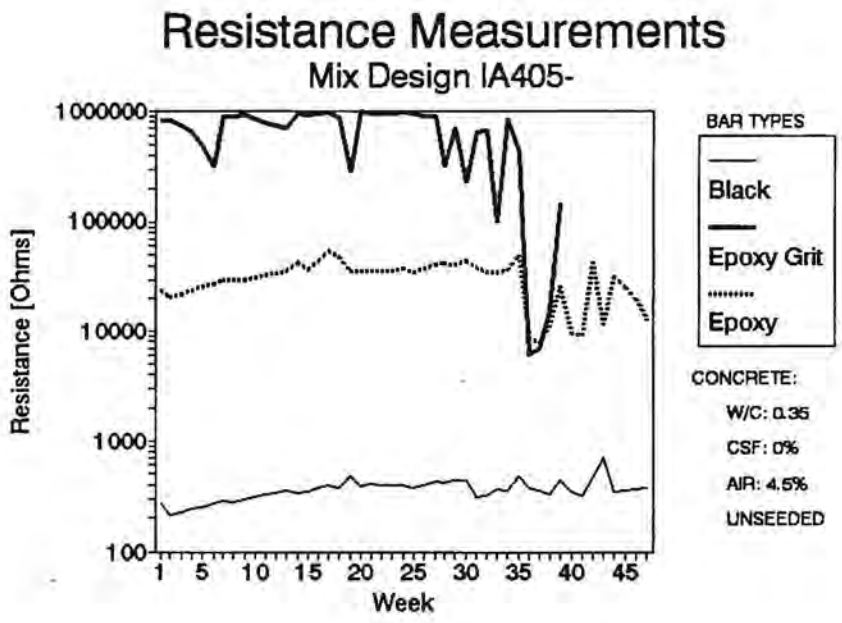
Resistance Measurements
Mix Design IA405-
Resistance [Ohms]
1000000
100000
10000
1000
100
1 5 10 15 20 25 30 35 40 45
Week
BAR TYPES
Black
Epoxy Grit
Epoxy
CONCRETE:
W/C: 0.35
CSF: 0%
AIR: 4.5%
UNSEEDED

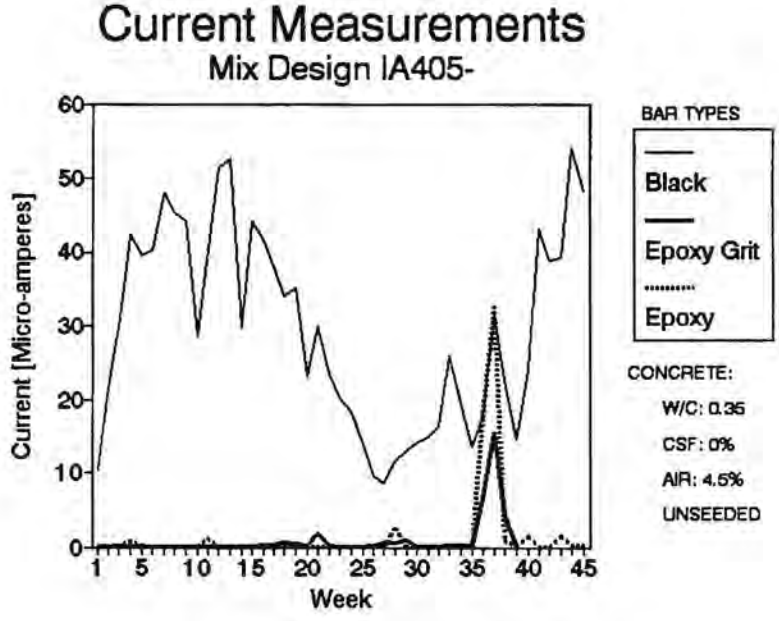
Current Measurements
Mix Design IA405-
Current [Micro-amperes]
60
50
40
30
20
10
0
1 5 10 15 20 25 30 35 40 45
Week
BAR TYPES
Black
Epoxy Grit
Epoxy
CONCRETE:
W/C: 0.35
CSF: 0%
AIR: 4.5%
UNSEEDED

Figure 6.18

Because the average current readings in these cases were all very small, the differences between the two coatings with respect to current measurements is both less dramatic and less meaningful. The difference in the resistance measurements is most likely due to the fact that the epoxy grit coated bars were undeformed, and therefore the coating has both a smooth surface to cover, and was less apt to have been damaged in transport. The epoxy coated reinforcing steel bars were regular deformed bars. The coating on these bars is more susceptible to damage on ribs and lugs which can occur in transport from abrasion on adjacent bars with deformations. The scratch and holiday survey data taken prior to casting the specimens and reported in Section 5.1 substantiates this fact. The epoxy grit coated undeformed bars had a lower number of holidays than the epoxy-coated deformed bars.

6.2.3.3. Effects of Damaged Epoxy Coating

In specimen group IB355+ and IB358+, the epoxy coating on the reinforcing steel was intentionally damaged to simulate a service condition where the rebar is placed without the coating being repaired. The extent of damage is described along with other variables in Section 5.1. The average current and resistance readings measured for these specimens are shown in Figures 6.16 and 6.19. Note that the behavior of these specimens was essentially the same for both mix designs.

The results of this experimental program indicate that the damaged reinforcing steels exhibited approximately a magnitude of order reduction in

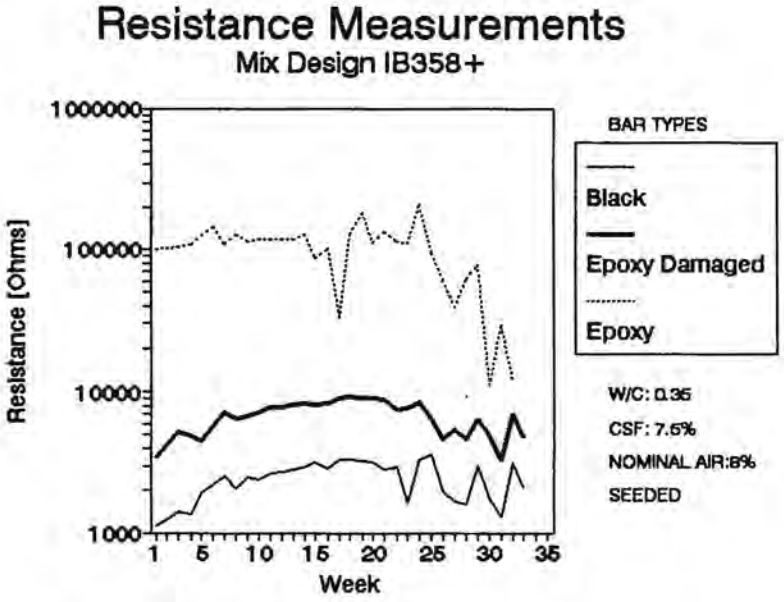
Resistance Measurements
Mix Design IB358+
Resistance [Ohms]
1000000
100000
10000
1000
1 5 10 15 20 25 30 35
Week
BAR TYPES
Black
Epoxy Damaged
Epoxy
W/C: 0.35
CSF: 7.5%
NOMINAL AIR:6%
SEEDED

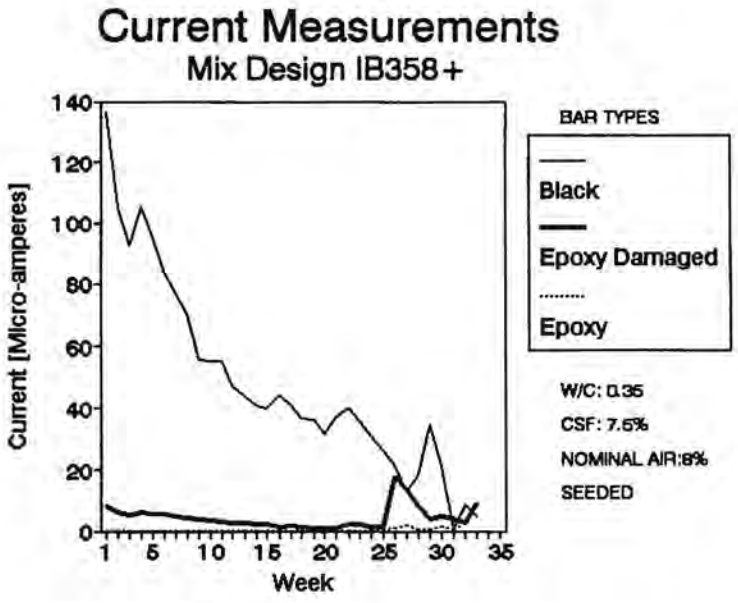
Current Measurements
Mix Design IB358+
Current [Micro-amperes]
140
120
100
80
60
40
20
0
1 5 10 15 20 25 30 35
Week
BAR TYPES
Black
Epoxy Damaged
Epoxy
W/C: 0.35
CSF: 7.5%
NOMINAL AIR:6%
SEEDED

Figure 6.19

average specimen resistance over the "as received" epoxy coated bars. However, the damaged epoxy bars still provided roughly a fivefold increase in resistance over the specimens containing uncoated bars.

Corrosion currents obtained from the damaged epoxy bar systems were almost constant over the entire test period. While the "as-received" epoxy bar systems recorded insignificant corrosion currents, the damaged epoxy bar systems had corrosion currents that were measurable ($\approx$ 10 microamperes). These measurements seemed to indicate the presence of a corrosion cell. But compared to the uncoated reinforcing steel systems with initial corrosion currents measured at over 130 microamperes, the damaged coating systems seemed to still offer a significant amount of protection.

It is possible that the comparison of the electrical measurements taken during this experimental program are not the most significant factor in the performance of the damaged epoxy system. This is due to the possibility of the existence of microcell corrosion occurring at the damaged sites. While the experimentally measured resistance is relatively high, and the measured current low as compared to the readings from uncoated bars, micro-cell corrosion (i.e. localized pitting) could be occurring at these uncoated sites. As previously discussed, the results of localized pitting corrosion can be much more severe than the results of generalized corrosion occurring over a larger area due to the greater loss of steel section which occurs in pitting. Refer to Section 7.4.2. for a discussion on the visual inspection of the reinforcement,

after the experimental program was completed.

6.3.0. Comparison of Cracked vs. Uncracked Specimen Behavior

Figures 6.20 and 6.21 illustrate the dramatic impact that cracks in the concrete cover have on the corrosion of steel in concrete with an averaged current history for one variable group of uncracked prisms and cracked slabs. The mix design shown is constant in both the cracked and uncracked specimens. In both the uncracked and cracked samples, the epoxy-coated reinforcing steel specimens exhibited measured corrosion currents consistently below 10 microamperes, therefore the effect of cracks in these samples was negligible. However, in the specimens having uncoated reinforcing steel, the cracked slabs experienced corrosion currents that were over two orders of magnitude higher than the uncracked specimens with the same mix design.

Both of the variable groups compared in Figures 6.20 And 6.21 contained no initial chlorides. However, the cracked specimens measured significant corrosion currents at the first reading, while the uncracked specimens underwent several weeks of ponding before showing any significant current activity. This confirms the assumption that cracked concrete allows the corrosion process to initiate much faster than the uncracked concrete. Refer to Section 6.4.2.1. for the results of visual inspections of the reinforcing steel at the completion of the experimental program.

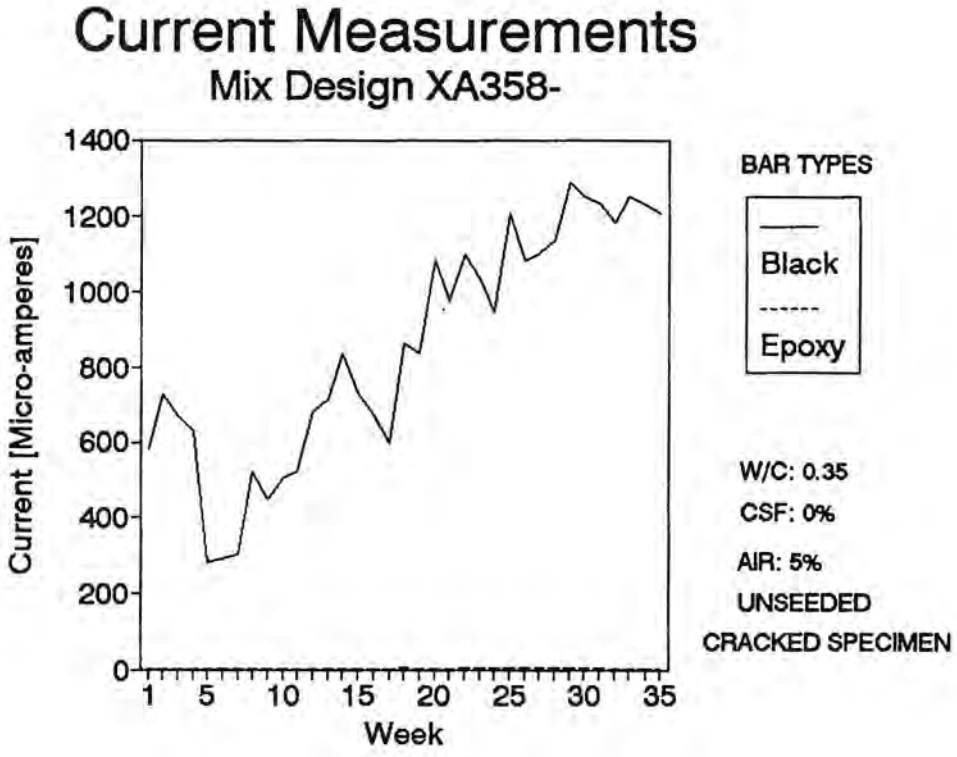
Current Measurements
Mix Design XA358-
Current [Micro-amperes]
1400
1200
1000
800
600
400
200
0
1
5
10
15
20
25
30
35
Week
BAR TYPES
Black
Epoxy
W/C: 0.35
CSF: 0%
AIR: 5%
UNSEEDED
CRACKED SPECIMEN

Figure 6.20

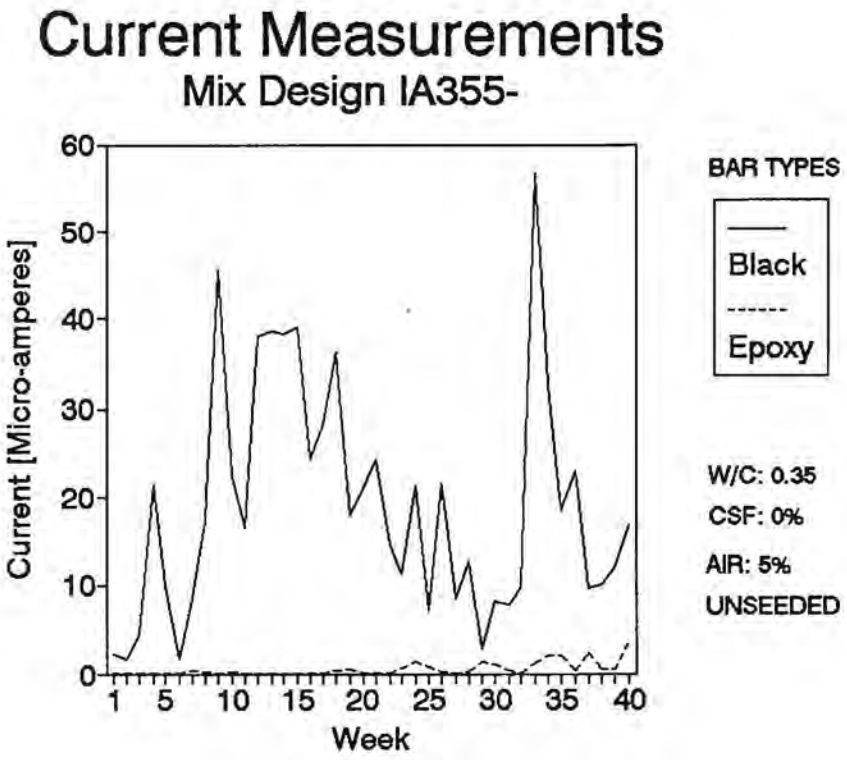
Current Measurements
Mix Design IA355-
Current [Micro-amperes]
60
50
40
30
20
10
0
1 5 10 15 20 25 30 35 40
Week
BAR TYPES
Black
Epoxy
W/C: 0.35
CSF: 0%
AIR: 5%
UNSEEDED

Figure 6.21

6.4.0. Physical Investigations

Results from chloride ion concentration tests and visual inspection of the reinforcing steel at the completion of the experimental program are presented in this section.

6.4.1. Chloride Ion Concentration Results

Concrete powder samples were taken from ten specimens at the conclusion of the test period. There were a total of 7 powder samples taken from each specimen. Samples were taken at 0.5 inch depths from 0 to 1.5 inches from each of two locations on the top of the specimens. One sample was taken at the level of the bottom reinforcing steel (between the depth of 5.5 and 6 inches from top) from each specimen. Figure 6.22 illustrates the sample locations for each specimen.

These powder samples were obtained in a manner consistent with the procedure outlined in the FHWA report number FHWA-RD-77-85, "Sampling and Testing for Chloride Ion in Concrete." The area over each sample hole was brushed clean with a wire brush, and the region was carefully vacuumed prior to the sample collection process. The concrete specimens were drilled with a rotary impact drill with depth indicators on the drill bit. Concrete powder was collected with a vacuum equipped with a filter to capture the powder at the end of the nozzle. Powder specimens were sealed in plastic sample bags for transport to the laboratory. The hole was thoroughly vacuumed clean prior to each additional depth sampling.

Sample Locations for Chloride Ion Tests

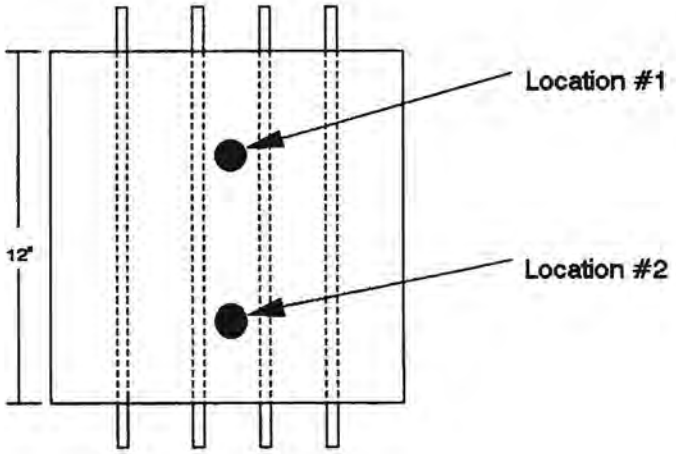

Plan View - Prism Specimen

Figure 6.22

The specimens tested for chloride ion content included both seeded and unseeded test specimens. Because the seeded specimens contained a significant amount of chloride (introduced as NaCl in the mix water), the chloride content was known to exceed the ACI recommended levels for chloride. These specimens were tested for water soluble chloride. The unseeded specimens were tested for acid soluble chloride content. The results of the chloride analysis follow in Tables 6.2, 6.3, and 6.4.

The results tabulated are given in parts per million by weight of concrete. Table 6.2 lists the acid soluble chloride content results from seven unseeded specimens. Table 6.3 lists the water soluble chloride content results from three specimens that were initially seeded with 20 lbs./cu. yd. of chloride ion (as NaCl) in the top (assumed anodic) lift. Table 6.4 compares the acid soluble chloride content to water soluble chloride content for the same unseeded specimen (specimen 100, variable group IA405-.BLK).

The results of the chloride content investigation illustrate several important facts about the initial assumptions made in this experimental program. As assumed in the experimental model, the chloride ion concentrations decrease with depth, producing an environment with a significant chloride concentration differential between the level of the top and bottom steel bars. This is consistent in all but two isolated cases (specimen 105, location 1, and specimen 204, location 1), where the test indicated a higher concentration of chlorides at the level of the bottom steel than the top

Acid Soluble Chloride Content Results

PPM by weight of concrete
Unseeded Specimens

Specimen Number	105		110		100	
Variable Group	IA405-.EPO		IA355-.BLK		IA405-.BLK	
Location	1	2	1	2	1	2
Depth [inches]						
0.0-0.5	5476	5731	6179	6413	6635	5751
0.5-1.0	2921	3390	2735	2863	3569	3981
1.0-1.5 (Top steel)	577	747	1347	2216	498	1379
5.5-6.0 (Bottom steel)	1972		236		221	
Specimen Number	201		204			
Variable Group	IB358-.BLK		IB355-.BLK			
Location	1	2	1	2		
Depth						
0.0-0.5	6982	6585	5800	3992		
0.5-1.0	2414	2200	1020	870		
1.0-1.5 (Top steel)	612	637	202	427		
5.5-6.0 (Bottom steel)	192		473			
Specimen Number	310		301			
Variable Group	IC358-.BLK		IC355-.BLK			
Location	1	2	1	2		
Depth						
0.0-0.5	6260	3562	6626	6022		
0.5-1.0	2045	816	2787	2274		
1.0-1.5 (Top steel)	811	935	430	797		
5.5-6.0 (Bottom steel)	207		233			

Corrosion threshold 289 ppm by weight of concrete [12]

Table 6.2

Water Soluble Chloride Content Results

PPM by weight of concrete
Seeded Specimens

Specimen Number	117		216		315	
Variable Group	IA405+.BLK		IB355+.BLK		IC355+.BLK	
Location	1	2	1	2	1	2
Depth [inches]						
0.0-0.5	7840	8356	8188	6932	8515	8296
0.5-1.0	5978	6301	5720	5784	8496	4612
1.0-1.5 (Top steel)	5087	5327	4082	4407	5879	4418
5.5-6.0 (Bottom steel)	3386		528		155	

Table 6.3

Acid vs. Water Soluble Chloride Content Results

PPM by weight of concrete
Unseeded Specimen

Specimen Number 100 Variable Group IA405-.BLK	ACID SOLUBLE		WATER SOLUBLE	
Location	1	2	1	2
Depth [inches]				
0.0-0.5	6635	5751	6438	5395
0.5-1.0	3569	3981	3418	3747
1.0-1.5 (Top steel)	498	1379	465	1268
5.5-6.0 (Bottom steel)	221		157	

Table 6.4

steel. There was no ready explanation for this observation.

As discussed in Section 5.2, the specimens that were seeded with salt at the level of the top steel had initial concentrations of chlorides over 10 times the level needed to depassify the reinforcing steel, suggested by Clear, et al. [12]. The results of the chloride investigation indicate that the reinforcing steels in top level of the unseeded specimens were also subjected to chloride concentrations that could initiate corrosion.

The minimum chloride concentration present at the level of the top steel mat in the specimens tested was 202 ppm by weight of concrete (specimen 204, location 1). Based on a design concrete unit weight of 3900 lbs./cu. yd., with a cement factor of 6.49, this value corresponds with a concentration of 1290 ppm by weight of cement. This chloride concentration level was only 70% of the corrosion threshold limit (289 ppm) proposed by Clear, et al. [12]. However, the second sample location on the same specimen returned a concentration value of 427 ppm by weight of concrete, which is almost 1.5 times the threshold value indicated by Clear, et al. Table 6.2 indicates that from samples taken at the level of top steel (1.0 - 1.5 inch depth), the chloride concentrations of all of the unseeded test specimens were significantly higher (factors ranged from 1.5 - 7.5 times greater) than the minimum levels needed to initiate the corrosion process.

As discussed in Section 3.2.1.2, higher w/c ratios are expected to correspond with higher concrete permeabilities. On this basis, one would

expect that the specimens containing a w/c ratio of 0.40 would have a higher chloride content than those having a w/c ratio of 0.35 (assuming the same exposure conditions). The results listed in Table 6.2 for unseeded specimens 105 and 110 are not consistent with the expected results, based on the assumed relative permeabilities. Of the two specimens, specimen 105 (w/c = 0.40) had larger chloride concentrations at the 0.5-1.0 inch, and 5.5-6.0 inch levels. Specimen 110 (w/c = 0.35) had larger chloride concentrations at the 0.0-0.5 inch, and 1.0-1.5 inch levels. Note that the tested chloride value of specimen 105 at the level of the bottom steel (1972 ppm) was almost three times the average value measured at the level of the top steel. The magnitude of this value suggests either test or sample collection error, or initial concrete mix contamination at the level of the bottom reinforcing steel. If the relative chloride concentrations between the top and bottom mats of steel in this specimen were correct, one would expect a reversed corrosion cell to occur, which was not observed.

Table 6.3 lists the water soluble chloride contents for the seeded specimens sampled. Comparison of the chloride levels present in the two samples containing condensed silica fume (specimen 216 - 7.5% CSF, specimen 315 - 10% CSF) shows in the top 1.5 inches of concrete, the 10% CSF specimen contains a significantly larger quantity of chlorides than the 7.5% CSF specimen. For both specimens, the concrete contained in this level was initially seeded with chlorides, to promote a corrosive environment.

As discussed in Section 6.2.2.1, as the concentration of microsilica increases, the concrete's ability to complex chlorides out of solution decreases. One explanation for the higher level of chlorides present in the 10% CSF specimens 301 and 315 (Tables 6.2 and 6.3, respectively) may be the decreased capacity of the calcium aluminate in the 10% CSF concrete to bind chlorides.

Table 6.4 lists both the acid and water soluble chloride content results from the initially unseeded specimen number 100 (group IA405-.BLK). The acid soluble concentrations are a closer representation of the total chlorides present in the concrete, and as such, are consistently larger than the water soluble concentrations. The average difference between the acid soluble and water soluble chloride concentration at all locations and depths approximately 9%. The magnitude of the difference between the two tests at any given location decreases with depth, however the percentage difference between the results of the two tests increases with depth.

6.4.2. Reinforcing Steel Visual Inspections

At the end of the testing period, representative samples of the specimens were broken open and the reinforcing steel was visually inspected for evidence of corrosion damage. The samples were broken open by a jack hammer, and the concrete was removed from the reinforcing steel with a small hand held hammer when necessary. Care was taken to preserve the integrity of reinforcing steel coatings when appropriate. As the reinforcing

steel bars were removed from the samples, their relative positions in the samples were noted, and the top and bottom level bars were kept separate. The results of the visual inspections will be discussed in order of the severity of corrosion observed.

Visual inspections of the black reinforcing steel bars, taken from various specimens, both seeded and unseeded, showed the bottom steel bars remained almost uniformly clear of visible corrosion products. This observation corresponds well with the assumed cathodic behavior of the bottom mat of reinforcing steel (discussed in Chapter 3.0). Certain specimens exhibited considerable corrosion products on the top two steel bars. This observation substantiates the assumed experimental model of the top steel becoming anodic to the bottom steel.

6.4.2.1. Visual Inspection of Uncoated Reinforcement

One cracked slab (specimen 421, group XC358-.BLK) containing uncoated reinforcing steel was opened for examination of the rebar at the conclusion of the experimental program. This specimen had exhibited some of the highest current readings obtained during the experimental program (see Figure 6.19). Additionally, the specimen had extensive rust stains on both the top and side surfaces. Examination of the two anodic bars in this specimen revealed significant corrosion products in localized areas generally corresponding to the locations of the cracks in the slab. The four cathodic bars were all free of corrosion products, except for a 1.0 - 1.5 inch region

adjacent to the exterior faces of the specimens, where the bars projected out from the concrete.

The corroded anodic areas on specimen 421 were all roughly 3 to 4 inches in length, and extended around the entire circumference of the bar. At one corrosion site the extensive scaling had clearly reduced the cross-sectional area of the bar. Caliper measurements indicated that this single corroded location had a diameter that was reduced approximately 0.015 inches from the two nearest corrosion free locations on the bar. Given a #4 bar, having a nominal diameter of 0.5 inches, this corresponded with a 3% reduction in diameter, and almost a 6% reduction in cross-sectional area. A close-up photograph of this corroded region is included here as Plate 3a.

Seeded specimens 117, 216 and 315, all were found to have corrosion products along the entire length of each anodic steel bar. Specimen 117 was from the uncracked specimen group containing 0% CSF, having a w/c of 0.40, 5% nominal air, initially seeded with chloride and containing uncoated reinforcing steel. This specimen had moderate corrosion products evenly distributed over the entire length of each anodic (top level) bar, with several areas of heavy corrosion having diameters < 1/4 inch. There were several distinct "pits" having diameters between 1/32 - 1/8 inch, corroding on each of the two bars. Specimen 216 from group IB358+.BLK, had moderate general corrosion products along the entire length of both anodic bars. There was severe corrosion product covering an approximate 6 inch length of each

bar. The corrosion product in this area had moderate scaling. Specimen 315 from group IC358+.BLK, had moderate general corrosion product along the entire length of both anodic bars. There was minor scaling in several locations. The four cathodic bars associated with each of these respective specimens were free from corrosion product, save minor general corrosion immediately adjacent to the exterior surface of the specimen. Figure 6.23 shows plots of the resistance and corrosion current history of each of these specimens.

Figure 6.23 shows clearly that current levels measured from the heavily corroded specimen 117 were 2 to 3 times those measured from specimens 216 or 315. The heightened current readings from this specimen correlate well with the increased corrosion product found on the top level (anodic) rebars. The plot of current history for specimens 216 and 315 shows a similar magnitude of corrosion current for most of the experimental test period, with specimen 216 exhibiting a consistently higher current level for the first 6 weeks of test. The visual results discussed above again confirm the measured corrosion current readings, as indicated by both specimens experiencing similar corrosion products over the entire length of the anodic bars. The initially higher currents measured on specimen 216 may correspond to the localized area of severe corrosion product evident on these anodic bars, and not on the anodic bars of specimen 315. Plate 4 records the final conditions of the bars from the specimens described above.

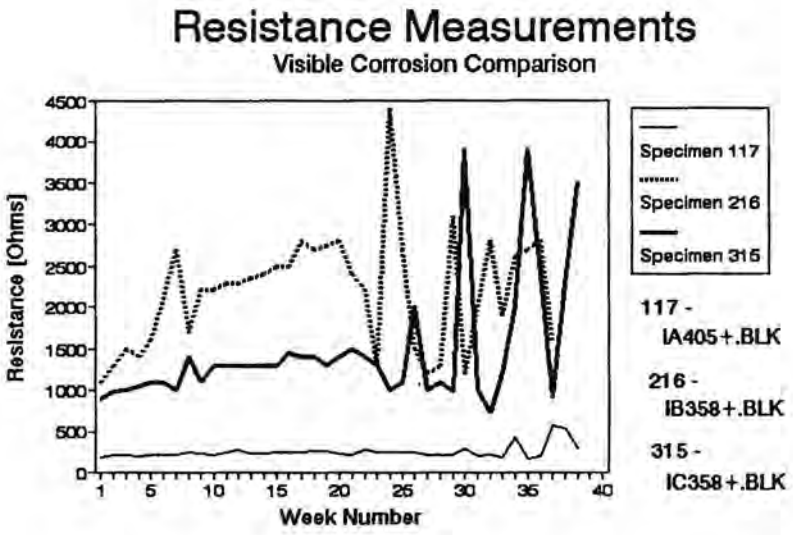

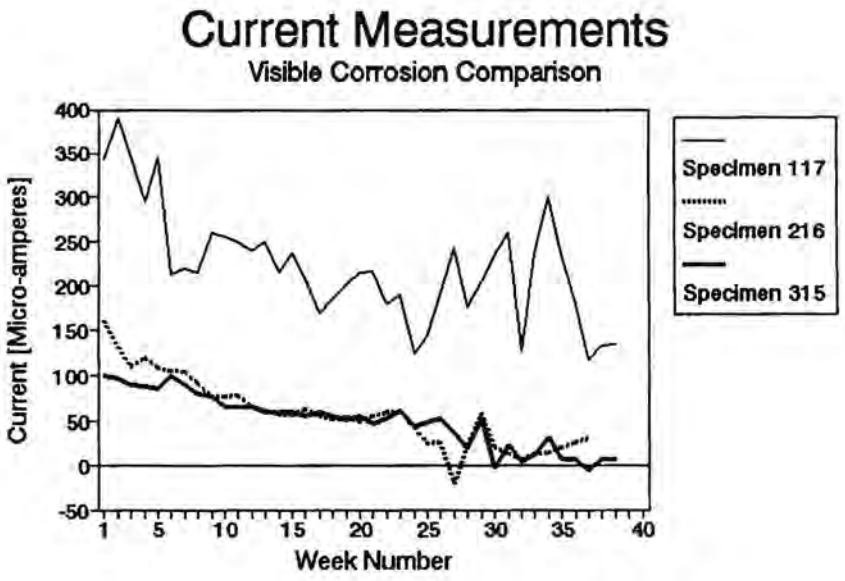

UNCOATED REINFORCING STEEL HAVING SIGNIFICANT CORROSION PRODUCTS ON ANODIC BARS

Figure 6.23

Uncoated reinforcing steels contained in specimens 100 and 110 exhibited a limited amount of corrosion product on the top level bars. Both of these specimens were uncracked prisms, containing 0% CSF, 5% nominal air, and no initial chlorides. Specimen 100 had a w/c ratio of 0.40, while specimen 110 had a w/c ratio of 0.35. One anodic bar from Specimen 100 had a generalized corrosion area of approximately one inch in length over the top half of the bar located near the center of the specimen. This bar also had light corrosion product at the bar ends near the concrete face. Specimen 110 had negligible corrosion products near the end of one anodic bar, and evidence of minimal corrosion product on select parts of the other anode.

Again, the cathodic (bottom) bars taken from these specimens were generally free from corrosion products. Specimen 100, however, did have one cathodic bar with limited corrosion product surrounding the bar at approximately 2 inches into the specimen.

Figure 6.24 plots the measured resistance and current history of these two specimens. It is interesting to note that the measured current level of these two specimens was below 50 microamperes throughout most of the experimental period. These relatively low current readings (as compared to readings measured on the chloride seeded specimens) again correspond to the limited amounts of corrosion product evident on the reinforcing steel at the end of the test. Significant in the visual observation however, was the presence of the corrosion product on one of the cathodic bars.

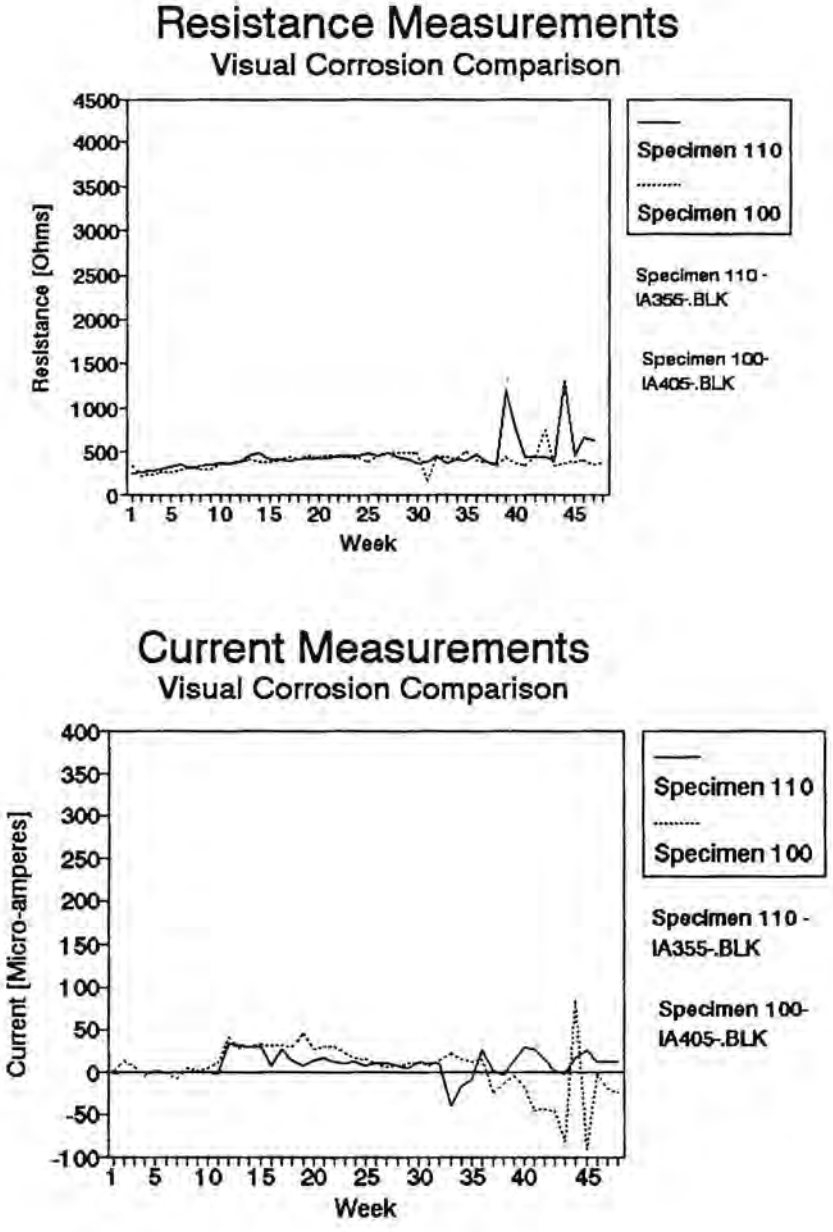

Uncoated Reinforcing Steel Having No Significant Corrosion Products

Figure 6.24

As evident on Figure 6.24, specimen 100 returned small negative current readings early in the experimental test, positive current readings throughout the middle test period and then, at week 36, negative current readings increasing in magnitude. As previously discussed, the negative readings indicated that the assumed corrosion cell model of anodic top steel and cathodic bottom steel had reversed. Since corrosion product can only form at anodic sites, the presence of corrosion product on one of the assumed cathodic bars confirms that the relative electrochemical status between the top and bottom of the reinforcing steel bars had been reversed.

6.4.2.2. Visual Inspection of Epoxy-Coated Reinforcement

Visual inspection of two specimens with epoxy-coated bars showed no indication of either debonded coatings or corrosion products. In many cases, the initial marks made on the bar to highlight scratches or holidays were clearly visible. Even in these areas where the coating was known to be broken, there was no corrosion activity visible.

Specimen 108 (group IA405-.EPG), was an uncracked specimen with Armstrong C-701 epoxy-grit coated reinforcing steel from Florida Wire and Cable company. As shown on Figure 6.25, this specimen exhibited extremely high resistance and low current readings. Those readings were consistent with the lack of visible corrosion activity. Specimen 105 (group IA405-.EPO), was another uncracked specimen containing Scotchcote® 213 epoxy-coated reinforcing steel. The current and resistance values measured on this

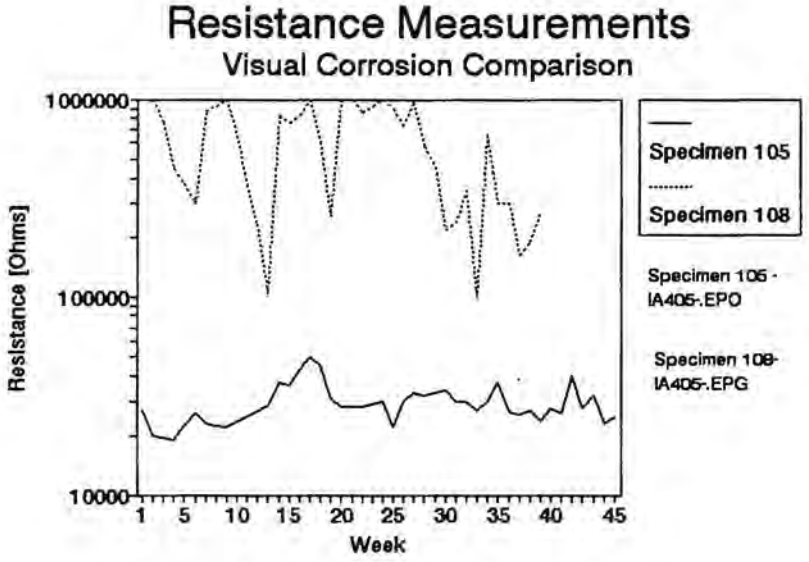

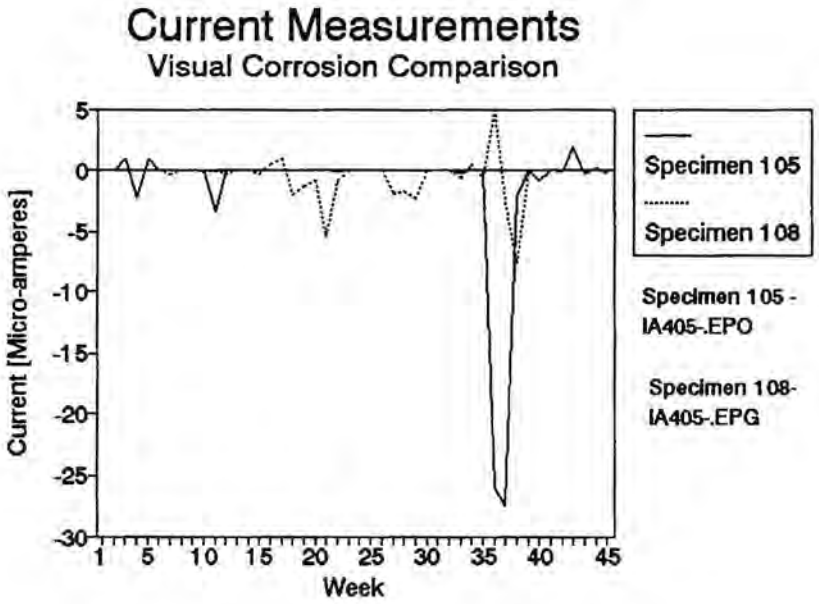

Coated Reinforcing Steel Having No Visual Corrosion Products

Figure 6.25

specimen are also plotted in Figure 6.25. Although the resistance readings on specimen 105 were high relative to readings from specimens containing uncoated bars, they were approximately an order of magnitude lower than those measured on specimen 108 (epoxy-grit specimen). The corrosion current of specimen 105 was still very low (generally below 1 microamp), which was consistent with specimen 108. The variations in specimen resistance values, assuming the saturation levels of the concretes were comparable, could be due to the difference in holidays, or breaks in the coatings, which expose the steel.

Specimens 222 and 223 (group IB358+.EPD) contained reinforcing steel bars in both top and bottom levels that had been intentionally damaged (as described in Section 5.2). At the conclusion of the test period, visual inspections of the rebar in these specimens revealed a very small amount of corrosion product around the perimeter of one of the twelve total damaged sections on the set of anodic bars in specimen 222 and around two of the twelve total damaged sections on the set of anodic bars in specimen 223. The cathodic bars in the lower level of steel in both of these specimens were free from any signs of corrosion (See Plate 3b). There were no signs of delamination of the epoxy coating in any of the bars in these samples. Based on these observations, it appears that the test specimens which had current readings below 50 microamperes throughout the test period experienced no significant corrosion of reinforcing steel.

6.5. Comparison of Cu-$CuSO_4$ Half-Cell Potential with Measured Current

The tabulated results of Cu-$CuSO_4$ half-cell potential readings measured on the specimens in this experimental program are presented in Appendix B. As discussed in Section 5.4., one purpose of the half-cell readings was to reference the ASTM C-876 specification for locating probable corrosion areas of steel in concrete. The other purpose of the half-cell readings was to compare the results of this study with those of Pfeifer, Landgren and Zoob, [15] who developed an empirical linear relationship between half-cell potential readings and corrosion current measured on specimens with similar geometry and bar orientation, but having different mix designs. The Pfeifer et al. study determined that equation (4.4) represented the relationship between half-cell potential and corrosion current based on 209 readings from 52 different concrete specimens.

$$I = -774.2P - 184.2 \qquad (4.4)$$

Where: I = corrosion current (microamperes)
P = Cu\$CuSO_4$ half-cell potential (volts)

Figure 6.26 shows the plot of current vs. averaged half-cell readings taken from all of the specimens in this study. Figure 6.24 also illustrates the empirical relationship between these two readings as determined by Pfeifer, Landgren and Zoob.

Based on the visual examination of reinforcing steel bars taken from specimens in the University of Minnesota study, it was determined that

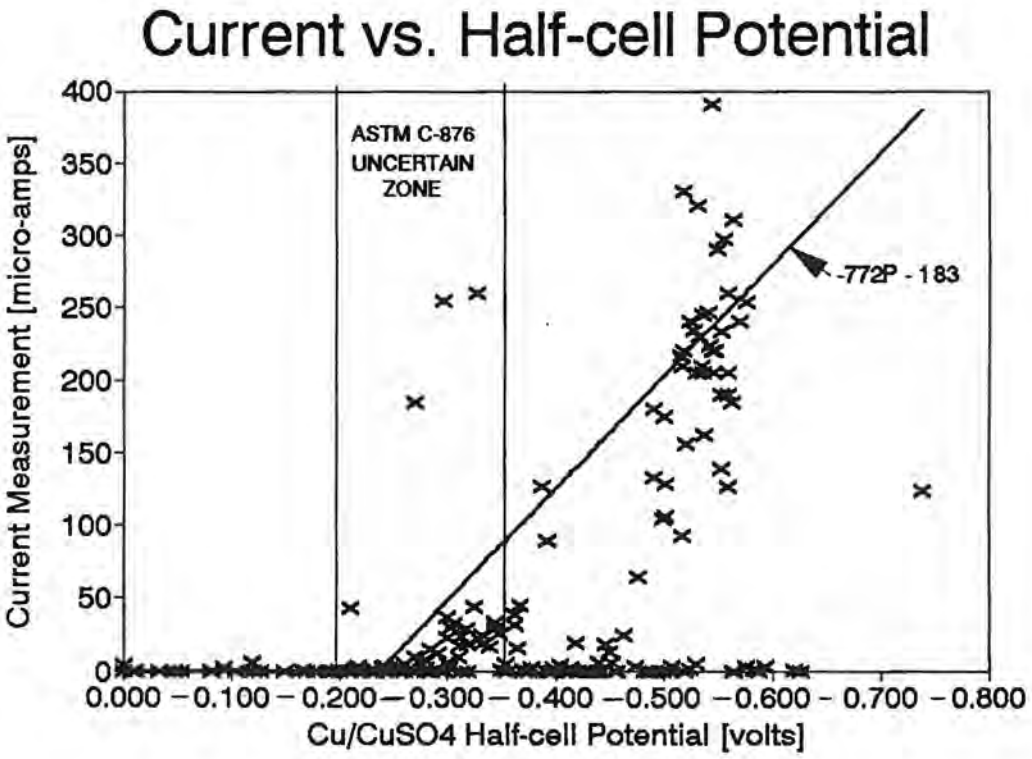
Current vs. Half-cell Potential
ASTM C-876
UNCERTAIN
ZONE
-772P - 183
Current Measurement [micro-amps]
400
350
300
250
200
150
100
50
0
0.000 −0.100 − 0.200 − 0.300 − 0.400 −0.500 −0.600 - 0.700 −0.800
Cu/CuSO4 Half-cell Potential [volts]

Figure 6.26

currents < 50 microamperes were generally indicative of insignificant corrosion activity. Figure 6.26 indicates that the current readings of specimens having half-cell potential measurements between -0.20 and -0.35 fall generally below the 50 microampere level, however a few of the readings in this range had significant current measurements. No half-cell readings greater (more positive) than -0.20 were associated with corrosion currents greater than 1 microampere. This observation corresponds well with the ASTM recommended interpretation of copper-copper sulfate half-cell readings on RC, as previously listed in Table 4.1. ASTM suggests that half-cell readings between the range of -0.20 and -0.35 are uncertain with respect to the probability of corrosion activity.

The University of Minnesota results also correlated well with the linear relationship between current and half-cell potential as determined by Pfeiffer, Landgren and Zoob. Note that in the ASTM uncertain zone (between -0.20 and -0.35 volts) the measured current readings from the specimens in this experiment generally lie below the Pfeiffer et al. line. At half-cell readings more negative than -0.35 volts, the Pfeiffer et al. line represents a fairly good approximation of the mean current measurements recorded. The results seem to indicate that the Pfeiffer et al. relationship between half-cell potential and current in a RC specimen bounds most current values for potentials in the ASTM uncertain zone, however there were a few limited results that indicated a much higher current. The relationship seems to give a reasonable

indication of average currents for potential readings more negative than -0.35 volts.

Chapter 7.0 Conclusions and Recommendations

An experimental program designed to investigate the effects of various material properties on the corrosion of reinforcing steel in concrete was conducted at the University of Minnesota. The University of Minnesota (U of M) study developed a test procedure which assumed a macrocell corrosion model, with 96 specimens undergoing an accelerated corrosion process for periods ranging from 35 to 48 weeks. The impact of the following variables on the corrosion of reinforcing steel in concrete was monitored in this program:

1. Water/cementitious ratio.
2. Addition of condensed silica fume.
3. Percentage of entrained air in the concrete.
4. Type of reinforcing steel and coating.
5. Cracked concrete.

Based on the results of this investigation (see Chapter 6.0), the following conclusions and recommendations are given:

1). The macrocell corrosion model used in this test, where one layer of reinforcement acted as the corrosion cell anode, and another layer acted as the cathode, was found to be a good assumption in approximately 85% of the total specimen population. In most of the specimens tested, the chloride concentration gradient formed between the top and bottom layers of steel allowed the top mat of reinforcement to become anodic to the bottom mat. This resulted in corrosion product (if any) being formed on the anodic bars, while the cathodic bars in the specimens remained free of corrosion

product.

For roughly 15% of the specimens, differential concentration cells of either oxygen, moisture, chlorides or some combination of the three, were formed within the concrete in such a way as to reverse the assumed direction of the corrosion cell. This was initially evinced by negative current and potential readings between the top and bottom layers of steel. The reversal was confirmed by the monitoring of additional specimens designed to enable the measurement of current between bars on the same level in order to detect the development of corrosion macrocells within a single layer of steel (see Section 5.4 and Section 6.1.1.1). Visual inspection of the steel bars from a specimen that exhibited negative current and driving potential readings (see Section 6.4.2) confirmed the existence of corrosion products on one of the bottom bars that had been assumed to be cathodic. Future researchers using similar specimen geometry may wish to consider the possibility for this type of occurrence.

2). Based on the analysis of concrete powder samples taken from various specimens at the conclusion of this experimental program, there is evidence that the reinforcing steel in the top levels of the specimens in this study was subjected to chloride concentrations in excess of the established values needed to initiate corrosion. Therefore, the salt water ponding and drying cycle used in this study was effective in establishing an environment in which the reinforcing steel could corrode. However, significant corrosion

occurred only in those specimens which were initially seeded with chlorides at the level of the top steel, or in those specimens which were cracked.

3). The effects of w/c ratios on the corrosion of reinforcing steel in concrete have been established by past researchers (See Section 3.2.1.2.). The results of the U of M study corresponded to previously published conclusions. Specifically, specimens which had higher w/c ratios exhibited lower resistances and increased corrosion currents over those having lower w/c ratios (all other variables constant).

4). Based on the current and resistance readings from the experimental program, no evidence of a direct relationship between the corrosion resistant properties of concretes made with either 5% or 8% (nominal) entrained air was found. There was neither a consistent, or significant difference among specimens containing either of the nominal entrained air percentages investigated. It is possible that the benefits and disadvantages of entrained air in concrete tend to cancel one another out.

5). Results from this study show a consistently significant increase in specimen resistance, and decrease in corrosion current of specimens with condensed silica fume (CSF) in the concrete mix compared with those of specimens without CSF. This behavior was independent of bar coating, initial chloride content, cracked or uncracked concrete.

6). Based on the current and resistance readings of three independent variable groups (containing 21 individual specimens), the results of the

University of Minnesota study display a significant trend of increased corrosion current and decreased specimen resistance in those groups containing 10% CSF over those containing 7.5% CSF. These results indicate there may be an optimum quantity of condensed silica fume which could be added to concrete as a corrosion inhibitor.

7). Concrete powder samples taken from specimens at the conclusion of the experimental program support the fact that concretes containing condensed silica fume as a pozzolanic admixture have a lower pH than those without CSF. In the samples tested for this study, as the percentage of CSF in concrete increased, there was a trend for the pH of the concrete powder sample to decrease. A link between lower concrete pH and the initiation of reinforcing steel corrosion has previously been established (see Section 6.2.2.1). These results could explain the existence of an optimum quantity of CSF in concrete for the protection of reinforcing steel from corrosion. As discussed in Section 3.2.1.1., the addition of CSF offers increased corrosion protection by decreasing the concrete permeability. There may be a level of CSF concentration where the benefits of decreased concrete permeability are offset by the disadvantages of lower concrete pH.

8). Uncoated reinforcing steel specimens showed substantially decreased resistance and increased corrosion current over those of epoxy-coated reinforcing steels. In most cases, the epoxy-coated specimens registered current measurements of less than 1 μ ampere, which were

negligible for this experiment.

9). Specimens containing the epoxy grit coated rods showed a significant increase in resistance over those containing epoxy-coated deformed bars in two of three mix designs. In the third mix design variable combination, the differences in the resistance levels were negligible. This result was attributed to the epoxy grit coated rods having fewer coating scratches and holidays than the epoxy coated deformed bars. The ribs and lugs of the epoxy coated bars were more likely to be susceptible to damage from adjacent bars in transport. There may also be inherent differences in the uniformity of coating application on smooth bars verses deformed bars. However, the results were not likely due to the quality of the reinforcing steels, because both types of steel exhibited similar current/resistance behavior in the uncoated reinforcement study.

10). Intentionally damaged epoxy-coated reinforcing steel (as described in Section 5.1) still offered a significant amount of corrosion protection over uncoated reinforcing steel. The concern of localized corrosion occurring at the area of exposed bar, leading to a significant loss of section, was not observed in the University of Minnesota study. Visual inspection of the bars with intentionally damaged coating showed only light corrosion products forming at isolated exposed steel areas on the top level steel bars. No signs of epoxy-coating delamination or corrosion migration under the coating was evinced during the period of this study. It may be of interest to

investigate the effects of damaged coatings for a more prolonged exposure and testing period.

11). The University of Minnesota study specimens having cracked concrete with uncoated reinforcement promoted corrosion cells initiation immediately upon exposure to the chloride ponding solution. Uncracked, initially chloride free specimens having uncoated reinforcement were subjected to several weeks of ponding before returning any significant measured corrosion currents.

Among specimens having the same mix designs and uncoated reinforcing steels, the cracked concrete specimens experienced corrosion currents that were over two orders of magnitude higher than the uncracked specimens. Visual inspection of the uncoated reinforcing steel in a cracked specimen indicated isolated regions of severe corrosion in the top bars which corresponded to the location of the cracks. The uncoated anodic bars in the unseeded, uncracked specimens examined did not have the type of severe corrosion exhibited on the cracked specimens. The results of the University of Minnesota study indicate that the existence of cracks in concrete can lead to a most damaging corrosion environment. Further research into the corrosion of reinforcing steel in concrete should seriously consider the effects of concrete cracks.

12). The results of Cu-$CuSO_4$ half-cell potential readings vs. current from the University of Minnesota study have been compared with those of

previous researchers (as described in Section 6.5). Given similar specimen geometry and reinforcing steel orientation, but different concrete mix designs and reinforcing steels, there is a reasonable agreement between the results of the U of M study and a published empirical relationship between Cu-$CuSO_4$ half-cell potential and current readings.

In conclusion, the most significant variables determined in the University of Minnesota experimental program were the concentration levels of CSF, the significance of concrete cracking, and the lack of any notable corrosion resulting in specimens with high levels of chloride contamination, containing bars with significantly damaged epoxy-coatings.

Recommendations for future research programs include the investigation into the effects of cyclically loaded specimens on the corrosion of reinforcing steel in concrete. The combination of steel reinforcement subjected to near-yielding stresses, and cracked concrete in a corrosive environment may provide insight on the corrosion process in actual service conditions. The investigation of cyclical loading on the integrity of coated reinforcement may also be of interest. Other suggestions for future research would be a comprehensive investigation on a wider variety of CSF concentrations, extended test periods, and epoxy grit coating on deformed bars.

References

[1] Clear, K., Virmani, Y., "Solving Rebar Corrosion Problems in Concrete, Research Update: Methods and Materials", **Solving Rebar Corrosion Problems in Concrete,** National Association of Corrosion Engineers, Houston, 1982.

[2] Escalante, E., Ito, S., "Measuring the Rate of Corrosion of Steel in Concrete," **A Compilation of Papers on Rebar Corrosion - 1976-1982,** National Association of Corrosion Engineers, Houston, 1984.

[3] Whiting, D., "Concrete Materials, Mix Design, Construction Practices and Their Effects on the Corrosion of Reinforcing Steel," **A Compilation of Papers on Rebar Corrosion - 1976-1982,** National Association of Corrosion Engineers, Houston, 1984.

[4] Wheat, H.G., Eliezer, Z., "Comments on the Identification of a Chloride Threshold in the Corrosion of Steel in Concrete," **Corrosion,** February 1987, pp. 126-128.

[5] Flick, L.D., Lloyd, J.P., "Corrosion of Steel in Internally Sealed Concrete Beams Under Load," **Corrosion of Reinforcing Steel in Concrete,** ASTM STP 713 D, E. Tonini & J.M. Gaidis, Eds., American Society for Testing and Materials, Philadelphia, 1980.

[6] Cornet, I., Bresler, B., "Critique of Testing Procedures Related to the Performance of Galvanized Steel Reinforcement in Concrete," **Corrosion of Reinforcing Steel in Concrete,** ASTM STP 713 D, E. Tonini & J.M. Gaidis, Eds., American Society for Testing and Materials, Philadelphia, 1980.

[7] Slater, J.E., **Corrosion of Metals in Association with Concrete,** ASTM STP 818, American Society for Testing and Materials, Philadelphia, 1983.

[8] Locke, C.E., "Corrosion of Steel in Portland Cement Concrete: Fundamental Studies," **Corrosion Effect of Stray Currents and the Techniques for Evaluating Corrosion of Rebars in Concrete,** ASTM STP 906, V. Chaker, Ed., American Society for Testing and Materials, Philadelphia, 1986.

[9] Andrade, C., et. al, "The Determination of the Corrosion Rate of Steel Embedded in Concrete by the Polarization Resistance and AC Impedance Methods," **Corrosion Effect of Stray Currents and the Techniques for Evaluating Corrosion of Rebars in Concrete**, ASTM STP 906, V. Chaker, Ed., American Society for Testing and Materials, Philadelphia, 1986.

[10] Clear, K.C., et. al., **Time-to-Corrosion of Reinforcing Steel in Concrete Slabs**, Vol.I. FHWA-RD: 73/32., Federal Highway Administration, Washington D.C., 1973.

[11] Clear, K.C., et. al., **Time-to-Corrosion of Reinforcing Steel in Concrete Slabs**, Vol. II. FHWA-RD: 73/33., Federal Highway Administration, Washington D.C., 1973.

[12] Clear, K.C., et. al., **Time-to-Corrosion of Reinforcing Steel in Concrete Slabs**, Vol. III. FHWA-RD: 76/70., Federal Highway Administration, Washington D.C., 1976.

[13] Clear, K.C., et. al., **Time-to-Corrosion of Reinforcing Steel in Concrete Slabs**, Vol. IV. FHWA-RD: 82/028., Federal Highway Administration, Washington D.C., 1978.

[14] Clear, K.C., et. al., **Time-to-Corrosion of Reinforcing Steel in Concrete Slabs**, Vol. V. FHWA-RD: 83/012., Federal Highway Administration, Washington D.C., 1979.

[15] Pfeifer, D.W., **Protective Systems for New Prestressed and Substructure Concrete**, FHWA-RD: 86/193., Federal Highway Administration, Washington D.C., 1980.

[16] Jabar, T., Braun Engineering Company, Minneapolis, MN, personal conversation.

[17] Hinatsu, J.T., Graydon, W.F., Foulkes, F.R., "Voltammetric Behavior of Iron in Cement. I. Development of a Standard Procedure for Measuring Voltammograms," **Journal of Applied Electrochemistry**, Volume 19, 1989, pp. 868-876.

[18] Gouda, V.K., Mourad, H.M., "Galvanic Cells Encountered in The Corrosion of Steel Reinforcement -I. Differential pH Cells," **Corrosion Science**, Volume 14, 1974, pp. 681-690.

[19] Gouda, V.K., Mourad, H.M., "Galvanic Cells Encountered in The Corrosion of Steel Reinforcement -II. Differential Salt Concentration Cells," **Corrosion Science**, Volume 15, 1975, pp. 307-315.

[20] Gouda, V.K., Mourad, H.M., "Galvanic Cells Encountered in The Corrosion of Steel Reinforcement -III. Differential Surface Condition Cells," **Corrosion Science**, Volume 15, 1975, pp. 317-328.

[21] Gouda, V.K., Mourad, H.M., "Galvanic Cells Encountered in The Corrosion of Steel Reinforcement -IV. Differential Aeration Cells," **Corrosion Science**, Volume 15, 1975, pp. 329-336.

[22] Parker, D.G., "Microsilica Concrete. Part 1: The Material." **Concrete**, Volume 19-H10, 1985, pp 21-22.

[23] Mindess, S., Young, J.F., **Concrete**, Prentice-Hall, Englewood Cliffs, New Jersey, 1981.

[24] Rasheeduzzafar, et. al., "Influence of Cement Composition on the Corrosion of Reinforcement and Sulfate Resistance of Concrete," **ACI Materials Journal**, Volume 87, No. 2., 1990.

[25] Dehghanian C., Locke C., "Electrochemical Behavior of Steel in Concrete as a Result of Chloride Diffusion into Concrete: Part 2", **Corrosion - NACE**, Volume 38, No. 9, September, 1982.

[26] Cohen, M.D., Olek, J., "Silica Fume in PCC: The Effects of Form on Engineering Performance," **Concrete International**, Volume 11, No. 11, 1989.

[27] Hope, B.B., Ip, A.K., "Chloride Corrosion Threshold in Concrete," **ACI Materials Journal**, Volume 84, No. 4, 1987.

[28] Fédération International de la Précontrainte, **Condensed Silica Fume in Concrete**, Thomas Telford Ltd., London, 1988.

[29] Young, J.F., "A Review of the Pore Structure of Cement Paste and Concrete and its Influence on Permeability", **Permeability of Concrete**, ACI SP-108, D. Whiting, A. Walitt, Ed., American Concrete Institute, Detroit, 1988.

[30] Marusin, S.L., "Influence of Superplasticizers, Polymer Admixtures, and Silica Fume in Concrete on Chloride Ion Permeability," **Permeability of Concrete**, ACI SP-108, D. Whiting, A. Walitt, Ed., American Concrete Institute, Detroit, 1988.

[31] Ozyildirim, C., Halstead, W., "Resistance to Chloride Ion Penetration of Concretes Containing Fly Ash, Silica Fume, or Slag," **Permeability of Concrete**, ACI SP-108, D. Whiting, A. Walitt, Ed., American Concrete Institute, Detroit, 1988.

[32] Perraton, D., et. al., "Permeabilities of Silica Fume Concrete," **Permeability of Concrete**, ACI SP-108, D. Whiting, A. Walitt, Ed., American Concrete Institute, Detroit, 1988.

[33] Coggins, F., French, K., "Material Properties of a Twenty-Year-Old Prestressed Bridge Girder Obtained By Nondestructive Testing," Structural Engineering Report No. 89-03., Department of Civil and Mineral Engineering, University of Minnesota, July 1989.

[34] Clifton, J.R., Knab, L.I., "Service Life of Concrete", NISTIR 89-4086, United States Department of Commerce National Institute of Standards and Technology, Gaithersburg, MD, 1989.

[35] Monteiro, P.J.M., Gjorv, O.E., Mehta, P.K., "Microstructure of the Steel-Cement Interface in the Presence of Chloride," **Cement and Concrete Research**, Volume 15, pp. 781-784, 1985.

[36] Feldman, R.F., Huang Cheng-yi, "Resistance of Mortars Containing Silica Fume to Attack by a Solution Containing Chlorides," **Cement and Concrete Research**, Volume 15, pp. 411-420, 1985.

[37] Alonso, C., Andrade, C., González, J.A., "Relation Between Resistivity and Corrosion Rate of Reinforcements in Carbonated Mortar Made With Several Cement Types," **Cement and Concrete Research**, Volume 8, pp. 687-698, 1988.

[38] Gaynor, R., "Understanding Chloride Percentages," **Corrosion, Concrete and Chlorides, Steel Corrosion in Concrete: Causes and Restraints**, ACI SP-102, Frances W.Gibson, ed., American Concrete Institute, Detroit, MI, 1987.

[39] Hime, W., Erlin, B., "Some Chemical and Physical Aspects of Phenomena Associated with Chloride-Induced Corrosion", **Corrosion, Concrete and Chlorides, Steel Corrosion in Concrete: Causes and Restraints,** ACI SP-102, Frances W. Gibson, ed., American Concrete Institute, Detroit, MI, 1987.

[40] Fraczek, J., "A Review of Electrochemical Principles as Applied to Corrosion of Steel in a Concrete or Grout Environment," **Corrosion, Concrete and Chlorides, Steel Corrosion in Concrete: Causes and Restraints,** ACI SP-102, Frances W. Gibson, ed., American Concrete Institute, Detroit, MI, 1987.

[41] Poston, R. W., **Improving Durability of Bridge Decks by Transverse Prestressing,** unpublished Doctorial Thesis, The University of Texas at Austin, December, 1984.

[42] **Corrosion of Steel in Concrete,** Report of the Technical Committee 60-CSC, The International Union of Testing and Research Laboratories for Materials and Structures (RILEM), P. Schiessl, editor, Chapman and Hall, London, 1988.

[43] Webster, T.E., "ACI Forum: Influence of Chlorides in Reinforced Concrete," **Corrosion, Concrete and Chlorides, Steel Corrosion in Concrete: Causes and Restraints,** ACI SP-102, Frances W. Gibson, ed., American Concrete Institute, Detroit, MI, 1987.

[44] Fontana, M.G., **Corrosion Engineering,** McGraw-Hill, Inc., New York, NY, 1986.

[45] Clear, K.C., "Measuring the Rate of Corrosion of Steel in Field Concrete Structures," paper prepared by Kenneth C. Clear, Inc., Sterling, VA, January 1989.

[46] Chin, D., "A Calcium Nitrite-Based, Non-Corrosive, Non-Chloride Accelerator," **Corrosion, Concrete and Chlorides, Steel Corrosion in Concrete: Causes and Restraints,** ACI SP-102, Frances W. Gibson, ed., American Concrete Institute, Detroit, MI, 1987.

[47] Smith, P., "Effects of Two Non-Chloride Accelerating Agents on Setting Characteristics of Portland Cement Mortars," **Corrosion, Concrete and Chlorides, Steel Corrosion in Concrete: Causes and Restraints,** ACI SP-102, Frances W. Gibson, ed., American Concrete Institute, Detroit, MI, 1987.

[48] Bickley, J.A., "Potential for Carbonation of Concrete in Canada" **Paul Klieger Symposium on Performance of Concrete**, ACI SP-122, David Whiting, ed., American Concrete Institute, Detroit, MI, 1990.

[49] Somayaji, S., Keeling, D., Heidersbach, R., "Corrosion of Reinforcing Steel in Concrete Exposed to Marine and Freshwater Environments", **Paul Klieger Symposium on Performance of Concrete**, ACI SP-122, David Whiting, ed., American Concrete Institute, Detroit, MI, 1990.

[50] Berkeley, K.G.L. , Pathmanaben, S., **Cathodic Protection of Reinforcement Steel in Concrete**, Butterworth & Co., London, 1990.

[51] ASTM C 876-87, "Standard Test Method for Half-Cell Potentials of Uncoated Reinforcing Steel in Concrete", **ASTM Book of Annual Standards 1990**.

[52] Holm, J., "Comparison of the Corrosion Potential of Calcium Chloride and a Calcium Nitrate Based Non-Chloride Accelerator - a Macro-Cell Corrosion Approach", **Corrosion, Concrete and Chlorides, Steel Corrosion in Concrete: Causes and Restraints**, ACI SP-102, Frances W.Gibson, ed., American Concrete Institute, Detroit, MI, 1987.

[53] Gautefall, O., Vennesland, O, "Effects of Cracks on the Corrosion of Embedded Steel in Silica-Concrete Compared to Ordinary Concrete", **Nordic Concrete Research**, Publication No. 2, Oslo, December, 1983.

[54] Feliu, S., Gonzãlez, J.A., Feliu, S., Jr., Andrade, C., "Relationship Between Conductivity of Concrete and Corrosion of Reinforcing Bars", **British Corrosion Journal**, Vol. 24, No. 3, 1989, pp. 195-198.

[55] Jang, J.W., Iwasaki, I., "Rebar Corrosion Under Simulated Concrete Conditions Using Galvanic Current Measurements", A paper submitted to: Transportation Research Board, 2101 Constitution Avenue, N.W., Washington, D.C., 1991.

[56] Pourbaix, M., **Lectures On Electrochemical Corrosion**, Plenum Press, New York, N.Y., 1973.

[57] Wranglén, G., **An Introduction to Corrosion and Protection of Metals**, Chapman and Hall, New York, N.Y., 1985.

[58] Litvan, G.G., "Deterioration of Parking Structures", **Durability of Concrete, Vol I**, ACI SP-126, V.M. Malhotra, ed., American Concrete Institute, Detroit, MI, 1991.

[59] **Highway Statistics, 1989**, United States Department of Transporation, Federal Highway Administration, Washington D.C., p. 135.

[60] Takagi, N., Miyagawa, T., Amasaki, S., Kojima, T., "Chloride Corrosion of Reinforcing Steel in Silica Fume Concrete Exposed to Marine Environment", **Durability of Concrete, Vol. I**, ACI SP-126, V.M. Malhotra, ed., American Concrete Institute, Detroit, MI, 1991.

[61] **Building Code Requirements for Reinforced Concrete**, ACI 318-89, American Concrete Institute, Detroit, MI, 1989.

[62] Denda, D., "Parking Garage Repair and Retrofit: How Big is the Underlying Problem?", **Concrete Technology Today**, Volume 12, Number 2, July 1991, pp. 4-5.

[63] Clifton, J., Beeghly, H., Mathey, R., **Nonmetallic Coatings for Concrete Reinforcing Bars**, FHWA-RD-74-18, National Bureau of Standards, Washington, D.C., 1974.

[64] ASTM D 3963M-87, "Standard Specification for Epoxy-Coated Reinforcing Steel", **ASTM Book of Annual Standards 1990**.

Appendix A

week number	resistance r [ohms]	current i [ampere	i.off v [volts]	v=ir theory [volts]	resistance r [ohms]	current i [ampere	i.off v [volts]	v=ir theory [volts]	resistance r [ohms]	current i [ampere	i.off v [volts]	v=ir theory [volts]
	specimen 100				specimen 101				specimen 102			
1	340	1.0	-	0.0003	240	10.0	-	0.0024	230	20.0	-	0.0046
5	270	2.0	-	0.0005	260	22.0	-	0.0057	230	95.0	-	0.0219
10	350	3.8	0.001	0.0013	310	8.5	0.003	0.0026	280	73.6	0.020	0.0206
15	390	32.8	0.014	0.0128	330	-39.0	-0.013	-0.0129	330	60.5	0.010	0.0200
20	430	27.0	0.014	0.0116	360	-11.5	-0.003	-0.0041	370	31.0	0.002	0.0115
25	380	15.0	0.008	0.0057	370	-3.7	-0.001	-0.0014	370	23.0	0.009	0.0085
30	480	10.0	0.006	0.0048	430	-7.4	-0.004	-0.0032	400	25.0	0.066	0.0100
35	500	11.4	0.005	0.0057	530	-7.5	-0.003	-0.0040	430	22.0	0.008	0.0095
40	370	-16.5	-0.004	-0.0061	350	-34.0	-0.013	-0.0119	330	22.0	0.007	0.0073
45	390	-90.0	-0.470	-0.0351	370	-40.3	-0.017	-0.0149	340	13.0	0.017	0.0044
	specimen 103				specimen 104				specimen 105			
1	15000	0.0001	-	0.0000	30000	0.0010	-	0.0000	27000	0.001	-	0.0000
5	16000	0.0090	-	0.0001	38000	0.0100	-	0.0004	22500	1.000	-	0.0225
10	22750	-0.0060	-0.0020	-0.0001	47500	-0.0012	0.0016	-0.0001	23500	-0.050	-0.0100	-0.0012
15	23000	0.0030	0.0013	0.0001	51000	-0.0015	-0.0030	-0.0001	36000	-0.018	-0.0030	-0.0006
20	28000	0.0250	0.0010	0.0007	50000	-0.0010	-0.0030	-0.0001	28000	0.036	0.0080	0.0010
25	30000	0.0000	0.0001	0.0000	51000	0.0002	0.0010	0.0000	22000	0.010	0.0060	0.0002
30	35000	0.0035	0.0010	0.0001	63000	0.0005	0.0001	0.0000	34000	0.020	0.0200	0.0007
35	35000	-0.0075	-0.0020	-0.0003	75000	-0.0001	-0.0001	-0.0000	37000	0.004	0.0001	0.0001
40	5800	-3.8000	-0.0220	-0.0220	15000	-0.1200	-0.0020	-0.0018	7600	-0.780	-0.0070	-0.0059
45	14000	-1.0000	-0.0010	-0.0140	30000	-0.4600	-0.0980	-0.0138	15000	-0.230	-0.0090	-0.0035
	specimen 106				specimen 107				specimen 108			
1	750000	0.0005	-	0.0004	760000	0.0080	-	0.0061	1000000	0.0010	-	0.0010
5	600000	0.0007	-	0.0004	500000	0.0080	-	0.0040	375000	0.0002	-	0.0001
10	1000000	0.0003	0.0060	0.0003	900000	-0.0008	-0.0100	-0.0007	650000	-0.0350	-0.1100	-0.0228
15	1000000	0.0067	0.0060	0.0067	1000000	-0.0054	-0.0600	-0.0054	750000	-0.3000	-0.1700	-0.2250
20	1000000	0.0011	0.0050	0.0011	1000000	0.0018	0.0600	0.0018	1000000	-0.8600	-0.2700	-0.8600
25	1000000	0.0005	0.0010	0.0005	1000000	0.0002	0.0200	0.0002	890000	0.0008	0.0100	0.0007
30	600000	-0.0447	-0.0600	-0.0268	62000	-0.0060	-0.0150	-0.0004	22000	0.0056	0.0440	0.0001
35	500000	-0.1100	-0.2200	-0.0550	500000	0.0080	0.0250	0.0040	300000	-0.6500	-0.2500	-0.1950

week number	resistance r [ohms]	current i [ampere	i.off v [volts]	v=ir theory [volts]	resistance r [ohms]	current i [ampere	i.off v [volts]	v=ir theory [volts]	resistance r [ohms]	current i [ampere	i.off v [volts]	v=ir theory [volts]
	specimen 110				specimen 111				specimen 112			
1	250	1.7	-	0.0004	250	1.7	-	0.0004	245	3.2	-	0.0008
5	320	0.0	-	0.0000	300	10.0	0.0050	0.0030	285	20.0	0.0070	0.0057
10	370	0.1	0.0000	0.0000	350	47.1	0.0200	0.0165	380	20.0	0.0080	0.0076
15	410	30.0	0.0100	0.0123	390	80.0	0.0300	0.0312	390	7.0	0.0040	0.0027
20	420	13.0	0.0060	0.0055	550	15.0	0.0100	0.0083	460	35.0	0.0200	0.0161
25	480	8.0	0.0030	0.0038	390	1.5	0.0020	0.0006	460	12.0	0.0100	0.0055
30	360	12.0	0.0055	0.0043	340	8.6	0.0100	0.0029	350	-4.2	-0.0029	-0.0015
35	400	-9.6	-0.0050	-0.0038	340	-6.0	-0.0020	-0.0020	430	40.0	0.0110	0.0172
40	750	28.2	0.0120	0.0212	1800	13.5	0.0190	0.0243	820	8.7	0.0040	0.0071
	specimen 113				specimen 114				specimen 115			
1	115000	0.0001	-	0.0000	80000	-0.0010	-	-0.0001	71000	0.0125	-	0.0009
5	85000	0.0300	-	0.0026	100000	0.0010	-	0.0001	80000	0.0005	-	0.0000
10	90000	-0.0900	-0.0200	-0.0081	150000	-0.0400	-0.0400	-0.0060	1000000	-0.3500	-0.0200	-0.3500
15	180000	0.0010	-0.0001	0.0002	150000	0.0020	0.0006	0.0003	1000000	0.0020	0.0020	0.0020
20	210000	0.0820	0.0800	0.0172	180000	0.0145	0.0020	0.0026	180000	0.0210	0.0290	0.0038
25	210000	-0.5000	-0.1000	-0.1050	170000	-0.1000	-0.0500	-0.0170	1000000	-0.0800	-0.0700	-0.0800
30	190000	0.4000	0.0600	0.0760	200000	0.5000	0.0800	0.1000	1000000	0.1000	0.0800	0.1000
35	34000	-0.2000	-0.0970	-0.0068	50000	-0.0400	-0.0038	-0.0020	34000	-0.7500	-0.0390	-0.0255
40	170000	-0.4100	-0.0800	-0.0697	200000	-0.2500	-0.0700	-0.0500	50000	-0.8900	-0.0640	-0.0445
	specimen 116				specimen 117				specimen 118			
1	200	410.0	0.0900	0.0820	185	344.0	0.0900	0.0636	185	220.0	0.0500	0.0407
5	227	425.0	0.0900	0.0965	207	345.0	0.0700	0.0714	215	246.0	0.0500	0.0529
10	265	370.0	0.0900	0.0981	220	255.0	0.0500	0.0561	235	250.0	0.0500	0.0588
15	330	270.0	0.0800	0.0891	250	236.0	0.0400	0.0590	250	245.0	0.0500	0.0613
20	350	235.0	0.0900	0.0823	230	215.0	0.0600	0.0495	220	240.0	0.0800	0.0528
25	410	165.0	0.0670	0.0677	240	144.0	0.0350	0.0346	300	192.0	0.0520	0.0576
30	430	226.0	0.1000	0.0972	290	234.0	0.0300	0.0679	330	234.0	0.0900	0.0772
35	270	270.0	0.0330	0.0729	170	235.0	0.0440	0.0400	240	129.0	0.0340	0.0310
40	500	160.0	0.0780	0.0800	500	140.0	0.0640	0.0700	400	150.0	0.0570	0.0600

week number	resistance r [ohms]	current i [ampere	i.off v [volts]	v=ir theory [volts]	resistance r [ohms]	current i [ampere	i.off v [volts]	v=ir theory [volts]	resistance r [ohms]	current i [ampere	i.off v [volts]	v=ir theory [volts]
	specimen 119				specimen 120				specimen 121			
1	400000	0.001	-	0.0004	1000000	0.001	-	0.0010	1000000	0.000	-	0.0000
5	180000	2.080	0.3100	0.3744	345000	0.002	0.0090	0.0007	235000	0.003	0.0110	0.0006
10	47000	3.200	0.3000	0.1504	17000	-1.500	-0.0200	-0.0255	200000	-0.010	-0.0800	-0.0020
15	11000	2.610	0.0320	0.0287	35000	-3.800	-0.1900	-0.1330	1000000	0.010	0.0100	0.0100
20	44000	0.017	0.0030	0.0007	40000	0.280	0.0200	0.0112	1000000	0.010	0.0100	0.0100
25	140000	0.018	0.0140	0.0025	60000	-0.720	-0.0600	-0.0432	131000	-0.016	-0.0140	-0.0021
30	29000	-0.07	-0.0110	-0.0020	49000	-1.500	-0.1100	-0.0735	100000	-0.010	-0.0020	-0.0010
35	43000	1.000	0.0500	0.0430	38000	0.420	0.0140	0.0160	27000	1.500	0.0220	0.0405
	specimen 122				specimen 123				specimen 124			
1	250000	0.001	-	0.0002	1000000	0.001	-	0.0010	1000000	0.000	-	0.0003
5	540000	-0.003	-0.0300	-0.0014	700000	0.000	-	0.0001	900000	0.011	0.0220	0.0099
10	275000	0.001	0.0010	0.0003	1000000	0.001	0.001	0.0010	500000	0.003	0.0010	0.0013
15	210000	-0.029	-0.0100	-0.0061	490000	0.000	0.001	0.0000	260000	0.000	0.0030	0.0001
20	410000	0.004	0.0500	0.0014	1000000	0.000	0.000	0.0000	250000	0.001	0.0500	0.0001
25	230000	0.003	0.0100	0.0008	500000	0.000	0.018	0.0001	33000	0.006	0.0280	0.0002
30	500000	0.003	0.0050	0.0016	100000	-0.000	-0.027	-0.0000	100000	0.050	0.0170	0.0050
35	25000	-1.120	-0.0220	-0.0280	52000	1.300	0.055	0.0676	27000	0.970	0.0300	0.0262
40	32000	1.970	0.0670	0.0630	49000	-1.300	-0.022	-0.0637	45000	-1.850	-0.0610	-0.0833
	specimen 125				specimen 126				specimen 127			
1	19000	0.007	0.0700	0.0001	18500	0.014	0.0050	0.0003	20000	0.037	0.0100	0.0007
5	57000	0.140	0.0400	0.0080	19000	0.060	0.0010	0.0011	23000	0.010	0.0030	0.0002
10	96000	-0.019	-0.0100	-0.0018	23000	0.060	0.0300	0.0014	30000	0.035	0.0020	0.0011
15	110000	0.009	0.0010	0.0010	28000	0.014	0.0010	0.0004	28000	-0.100	-0.0030	-0.0028
20	99000	-0.010	-0.0070	-0.0010	34000	0.008	0.0010	0.0003	33000	0.007	0.0010	0.0002
25	16000	6.400	0.0630	0.1024	27000	-0.110	0.0075	-0.0030	26000	-0.100	0.1270	-0.0026
30	8800	-8.000	-0.0600	-0.0704	7100	-12.200	-0.1200	-0.0866	7700	-3.300	-0.0300	-0.0254
35	58000	-1.400	-0.1100	-0.0812	16000	-0.410	-0.0190	-0.0066	29000	-1.400	-0.0600	-0.0406
40	34000	0.650	0.0480	0.0221	17900	-0.040	-0.0020	-0.0007	14000	-0.420	-0.0640	-0.0059

week numbe	resistance r [ohms]	current i [amper	i.off v [volts]	v=ir theory [volts]	resistance r [ohms]	current i [amper	i.off v [volts]	v=ir theory [volts]	resistance r [ohms]	current i [amper	i.off v [volts]	v=ir theory [volts]
	specimen 128				specimen 129				specimen 130			
1	160	332.0	0.060	0.0531	175	360.0	0.050	0.0630	190	370.0	0.070	0.0703
5	220	280.0	0.060	0.0616	230	340.0	0.070	0.0782	245	290.0	0.070	0.0711
10	240	230.0	0.060	0.0552	250	309.0	0.070	0.0773	270	260.0	0.070	0.0702
15	280	170.0	0.050	0.0476	265	258.0	0.070	0.0684	315	215.0	0.070	0.0677
20	320	132.0	0.049	0.0422	300	228.0	0.069	0.0684	370	175.0	0.069	0.0648
30	270	38.0	0.010	0.0103	200	115.5	0.230	0.0231	250	40.5	0.012	0.0101
35	620	-19.2	-0.007	-0.0119	1100	42.0	0.007	0.0462	1200	-49.0	-0.042	-0.0588
	specimen 131				specimen 132				specimen 133			
1	110000	0.0004	0.0400	0.0000	290000	0.0011	0.0200	0.0003	515000	0.0061	0.0200	0.0031
5	160000	0.0008	0.0010	0.0001	140000	0.0010	0.0100	0.0001	600000	0.0055	0.0100	0.0033
10	310000	-0.0005	-0.0300	-0.0002	330000	0.0004	0.0300	0.0001	570000	0.0004	0.0040	0.0002
15	195000	0.0000	0.0000	0.0000	250000	0.0001	0.0000	0.0000	450000	0.0002	0.0000	0.0001
20	190000	-0.0030	-0.0140	-0.0006	240000	-0.0017	-0.0010	-0.0004	250000	-0.0020	-0.0800	-0.0005
25	170000	-0.0200	-0.0190	-0.0034	150000	-0.0075	-0.0210	-0.0011	220000	-0.0800	-0.1560	-0.0176
30	20000	-0.8300	-0.0300	-0.0166	13000	4.5000	0.0400	0.0585	15000	-3.2000	-0.0500	-0.0480
35	12000	-0.5800	-0.0390	-0.0070	62000	-2.0000	-0.0150	-0.1240	12000	-6.4100	-0.0700	-0.0769
	specimen 201				specimen 202				specimen 203			
1	1100	0.22	-	0.0002	1000	0.44	-	0.0004	1100	0.13	-	0.0001
5	1250	1.16	-	0.0015	1300	1.00	-	0.0013	1400	5.10	0.0070	0.0071
10	1200	0.26	0.0001	0.0003	2000	-0.32	-0.0005	-0.0006	2100	-2.04	-0.0040	-0.0043
15	1800	0.60	0.0002	0.0011	1900	-0.19	-0.0002	-0.0004	2200	-0.70	-0.0010	-0.0015
20	2100	0.41	0.0005	0.0009	1900	0.21	0.0002	0.0004	2400	-2.50	-0.0060	-0.0060
25	2400	10.00	0.0110	0.0240	4300	1.00	0.0010	0.0043	2500	2.00	0.0100	0.0050
30	2700	1.80	0.0040	0.0049	2400	6.80	0.0260	0.0163	2500	-11.00	-0.0150	-0.0275
35	1200	17.30	0.0060	0.0208	1300	19.70	0.0230	0.0256	1300	25.00	0.0380	0.0325
40	2450	-8.00	-0.0100	-0.0196	1950	2.10	0.0030	0.0041	1600	-5.00	-0.0070	-0.0080

week number	resistance r [ohms]	current i [amper	i.off v [volts]	v=ir theory [volts]	resistance r [ohms]	current i [amper	i.off v [volts]	v=ir theory [volts]	resistance r [ohms]	current i [amper	i.off v [volts]	v=ir theory [volts]
	specimen 204				specimen 205				specimen 206			
1	1700	8.23	0.0130	0.0140	1600	0.36	-	0.0006	1600	0.25	-	0.0004
5	2200	13.00	0.0020	0.0286	1900	2.00	0.0030	0.0038	2000	0.00	0.0001	0.0000
10	2600	6.10	0.0140	0.0159	2700	0.40	0.0006	0.0011	2100	-0.28	-0.0007	-0.0006
15	3000	2.30	0.0060	0.0069	1850	13.00	0.0200	0.0241	2300	1.30	0.0020	0.0030
20	3100	3.00	0.0070	0.0093	2000	6.00	0.0100	0.0120	2600	0.45	0.0009	0.0012
25	3300	3.50	0.0100	0.0116	1700	7.30	0.0150	0.0124	2600	0.00	0.0000	0.0000
30	6500	5.00	0.0300	0.0325	1500	30.00	0.0250	0.0450	2300	10.00	0.0200	0.0230
35	2100	-7.10	-0.0160	-0.0149	820	6.20	0.0140	0.0051	1300	35.50	0.0650	0.0462
40	2100	-18.00	-0.0400	-0.0378	1400	3.90	0.0100	0.0055	1200	-4.00	-0.0040	-0.0048
	specimen 207				specimen 208				specimen 209			
1	110000	0.018	-	0.0020	55000	0.032	0.0090	0.0018	55000	0.024	0.0040	0.0013
5	95000	0.070	0.0200	0.0067	59000	0.062	0.0100	0.0037	54000	0.010	0.0400	0.0005
10	100000	0.010	0.0070	0.0010	77000	0.010	0.0030	0.0008	100000	0.070	0.0100	0.0070
15	120000	-0.012	-0.0050	-0.0014	87000	0.020	0.0010	0.0017	100000	0.120	0.0500	0.0120
20	79000	-1.200	-0.0120	-0.0948	98000	-0.010	-0.0300	-0.0010	120000	-0.002	-0.0020	-0.0002
25	90000	-0.800	-0.1000	-0.0720	83000	1.000	0.1000	0.0830	100000	1.900	0.1000	0.1900
30	24000	-2.470	-0.1200	-0.0593	51000	0.100	0.0170	0.0051	100000	0.130	0.0360	0.0130
35	15000	0.630	0.0040	0.0095	23000	1.800	0.0290	0.0414	11000	2.300	0.0800	0.0253
	specimen 210				specimen 211				specimen 212			
1	3500	6.70	0.0300	0.0235	4000	17.20	0.2200	0.0688	3100	13.40	0.0400	0.0415
5	3700	8.40	0.0600	0.0311	4500	7.30	0.0500	0.0329	4500	8.60	0.0400	0.0387
10	5000	4.10	0.0290	0.0205	6500	4.00	0.0300	0.0260	5300	8.50	0.0700	0.0214
15	5400	3.10	0.0240	0.0167	7200	3.50	0.0260	0.0252	6700	3.20	0.0240	0.0214
20	5700	2.50	0.0200	0.0143	7300	3.50	0.1400	0.0256	7000	2.10	0.0190	0.0147
25	10000	1.00	0.1000	0.0100	6000	12.00	0.0700	0.0720	5500	5.00	0.0200	0.0275
30	6200	8.80	0.0440	0.0546	7100	3.00	0.0800	0.0213	6000	3.60	0.0300	0.0216
35	5600	1.20	0.0070	0.0067	4700	-0.58	-0.0020	-0.0027	4500	9.50	0.0190	0.0428

week number	resistance r [ohms]	current i [amper	i.off v [volts]	v=ir theory [volts]	resistance r [ohms]	current i [amper	i.off v [volts]	v=ir theory [volts]	resistance r [ohms]	current i [amper	i.off v [volts]	v=ir theory [volts]
	specimen 213											
1	820	134	0.1030	0.1099								
5	690	112	0.0055	0.0773								
10	830	115	0.0250	0.0955								
15	1300	53	0.0400	0.0689								
20	1300	50	0.0500	0.0650								
	specimen 216				specimen 217				specimen 218			
1	1150	113.0	0.0600	0.1300	1100	160.0	0.0500	0.1760	-	-	-	-
5	2650	90.0	0.1500	0.2385	1600	109.0	0.0900	0.1744	1600	86.0	0.1200	0.1376
10	2300	55.0	0.1300	0.1265	2200	77.0	0.1100	0.1694	2700	34.0	0.0900	0.0918
15	2800	43.0	0.1200	0.1204	2500	57.0	0.1400	0.1425	4300	20.0	0.0600	0.0860
20	3200	35.1	0.1000	0.1123	2800	49.5	0.1400	0.1386	3700	11.2	0.0440	0.0414
25	3000	40.0	0.0400	0.1200	2700	25.0	0.0700	0.0675	5200	14.0	0.0700	0.0728
30	1500	13.3	0.0190	0.0200	1200	20.7	0.0280	0.0248	2500	30.0	0.0740	0.0750
35	2300	12.0	0.0300	0.0276	2700	20.0	0.0510	0.0540	3000	7.0	0.0200	0.0210
	specimen 219				specimen 220				specimen 221			
1	42000	0.080	0.0200	0.0034	98000	0.000	0.0000	0.0000	160000	0.0005	0.0000	0.0001
5	80000	0.010	0.0010	0.0008	105000	0.005	0.0000	0.0005	190000	0.0020	0.0000	0.0004
10	100000	-0.006	-0.0040	-0.0006	100000	-0.003	-0.0010	-0.0003	150000	0.0060	0.0200	0.0009
15	120000	0.022	0.0070	0.0026	30000	0.001	0.0010	0.0000	110000	0.0012	0.0070	0.0001
20	100000	0.010	0.0030	0.0010	110000	-0.001	-0.1200	-0.0001	120000	-0.0010	-0.0320	-0.0001
25	50000	-0.380	-0.0266	-0.0190	100000	-1.000	-0.2500	-0.1000	130000	-0.5700	-0.2000	-0.0741
30	6600	-3.100	-0.0700	-0.0205	15000	-0.250	-0.0300	-0.0038	12000	-1.0000	-0.0470	-0.0120
35	2100	-3.600	-0.1000	-0.0076	33000	-0.300	-0.0200	-0.0099	46000	-0.7000	-0.0200	-0.0322
	specimen 222				specimen 223				specimen 224			
1	3000	9.1	0.0300	0.0273	3000	7.30	0.0300	0.0219	4400	9.0	0.0200	0.0396
5	4700	4.1	0.0300	0.0193	4200	7.00	0.0400	0.0294	4800	6.5	0.0350	0.0312
10	7500	1.7	0.0100	0.0128	5800	4.40	0.0300	0.0255	8000	4.2	0.0300	0.0336
15	9000	0.9	0.0090	0.0081	6900	1.60	0.0020	0.0110	9000	2.0	0.0200	0.0180
20	9500	0.9	0.0100	0.0086	7400	0.25	0.0800	0.0019	9700	3.0	0.0300	0.0291
25	7000	-19.0	-0.1200	-0.1330	4500	-12.00	-0.0830	-0.0540	5500	3.7	0.0220	0.0204
30	2700	-8.4	-0.0580	-0.0226	3400	0.35	0.0070	0.0012	3700	3.0	0.0100	0.0111
35	7800	8.5	-0.0770	0.0663	6500	-3.45	-0.0019	-0.0224	6800	1.3	0.0610	0.0085

week number	resistance r [ohms]	current i [ampere	i.off v [volts]	v=ir theory [volts]	resistance r [ohms]	current i [ampere	i.off v [volts]	v=ir theory [volts]	resistance r [ohms]	current i [ampere	i.off v [volts]	v=ir theory [volts]
	specimen 301				specimen 302				specimen 303			
1	1600	1.0	-	0.0016	1600	1.00	-	0.0016	1800	1.0	-	0.0018
5	1800	13.0	0.010	0.0234	2100	4.00	0.007	0.0084	2300	5.5	0.008	0.0127
10	2300	17.0	0.040	0.0391	2400	2.00	0.008	0.0048	2600	3.5	0.008	0.0091
15	2400	11.5	0.028	0.0276	2500	1.00	0.001	0.0025	2700	1.0	0.020	0.0027
20	2300	7.8	0.004	0.0179	2500	5.20	0.012	0.0130	2500	4.0	0.010	0.0100
25	2500	10.0	0.024	0.0250	2300	6.20	0.014	0.0143	2800	1.1	0.069	0.0031
30	1600	10.0	0.018	0.0160	2000	-35.00	0.063	-0.0700	1900	-35.0	-0.042	-0.0665
35	1200	5.7	0.005	0.0068	1500	0.27	0.011	0.0004	1400	-11.1	-0.020	-0.0155
40	2300	1.0	0.001	0.0023	2000	-7.50	-0.010	-0.0150	2000	-16.5	-0.010	-0.0330
	specimen 304				specimen 305				specimen 306			
1	1500	60.0	-		1500	60.0	-	0.0900	1500	50.0	-	0.0750
5	1900	52.5	0.110	0.0998	1950	51.0	0.090	0.0995	1400	16.5	0.010	0.0231
10	2300	40.0	0.100	0.0920	2200	48.0	0.100	0.1056	2100	48.0	0.100	0.1008
15	2800	34.0	0.090	0.0952	2500	32.0	0.070	0.0800	2400	32.0	0.048	0.0768
20	2600	29.0	0.034	0.0754	2500	28.0	0.000	0.0700	1900	13.7	0.170	0.0260
25	2600	21.0	0.065	0.0546	2200	-12.0	-0.026	-0.0264	1800	12.0	0.013	0.0216
30	1900	-16.0	-0.012	-0.0304	1200	-13.0	-0.100	-0.0156	900	-10.0	-0.078	-0.0090
35	1700	21.9	0.040	0.0372	1000	-22.9	-0.030	-0.0229	700	8.4	0.007	0.0059
40	2200	1.4	0.008	0.0031	1700	-53.0	-0.069	-0.0901	880	4.1	0.003	0.0036
	specimen 307				specimen 308				specimen 309			
1	590000	0.050	0.050	0.0295	295000	-0.003	-0.002	-0.0009	160000	0.005	0.010	0.0008
5	1000000	0.000	0.000	0.0000	263333	-0.030	-0.018	-0.0079	140000	-0.003	-0.002	-0.0004
10	210000	-0.020	-0.002	-0.0042	1000000	-0.006	-0.004	-0.0060	180000	0.003	0.003	0.0005
15	600000	0.002	0.001	0.0009	620000	0.004	0.003	0.0025	245000	0.000	0.000	0.0000
20	240000	-0.010	-0.020	-0.0024	1000000	-0.800	-0.190	-0.8000	280000	-0.250	-0.070	-0.0700
25	270000	-0.020	-0.005	-0.0054	350000	-1.850	-0.110	-0.6475	100000	-11.500	-0.250	-1.1500
30	200000	-0.010	-0.020	-0.0020	70000	-0.350	-0.010	-0.0245	22000	-7.290	-0.040	-0.1604
35	64000	-1.700	-0.150	-0.1088	12000	-3.700	-0.039	-0.0444	7000	-17.500	-0.110	-0.1225
40	74000	1.000	0.080	0.0740	80000	1.100	0.030	0.0880	31000	2.000	0.07	0.0620

week number	resistance r [ohms]	current i [amper	i.off v [volts]	v=ir theory [volts]	resistance r [ohms]	current i [amper	i.off v [volts]	v=ir theory [volts]	resistance r [ohms]	current i [amper	i.off v [volts]	v=ir theory [volts]
	specimen 310				specimen 311				specimen 312			
1	1350	0.00	-	0.0000	1350	0.10		0.0001	1450	1.0		0.0015
5	2100	-0.25	-	-0.0005	2050	0.23	0.0002	0.0005	2150	1.7	0.002	0.0037
10	2400	-0.90	-0.002	-0.0022	2200	0.60	0.0010	0.0013	2400	2.7	0.006	0.0065
15	3050	0.00	0.001	0.0000	2900	1.00	0.0040	0.0029	2650	1.0	0.003	0.0027
20	2000	-3.30	-0.003	-0.0066	2100	4.40	0.0012	0.0092	1400	-0.9	-0.002	-0.0012
25	2100	-7.80	-0.006	-0.0164	1900	-22.00	-0.0110	-0.0418	2300	-22.0	-0.020	-0.0506
30	2000	2.40	0.005	0.0048	1700	33.00	0.0530	0.0561	1500	-27.8	-0.039	-0.0417
35	2500	21.70	0.040	0.0543	2500	-5.38	-0.0040	-0.0135	2300	-50.8	-0.078	-0.1168
40	2600	9.00	0.031	0.0234	1700	1.20	0.0100	0.0020	1400	-20.0	-0.030	-0.0280
	specimen 313				specimen 314				specimen 315			
1	885	90	-	0.0797	885	95	-	0.0841	885	100	-	0.0885
5	1150	71	0.080	0.0817	1150	76	0.090	0.0874	1100	86	0.100	0.0946
10	1300	65	0.080	0.0845	1300	74	0.100	0.0962	1300	66	0.090	0.0858
15	1600	60	0.078	0.0960	1300	73	0.030	0.0949	1300	59	0.080	0.0767
20	1400	52	0.070	0.0728	1200	65	0.090	0.0780	1400	56	0.023	0.0784
25	1200	47	0.061	0.0564	1200	75	0.085	0.0900	1100	48	0.060	0.0528
30	2900	35	0.049	0.1015	3400	67	0.118	0.2278	3900	-3	-0.017	-0.0117
35	2200	21	0.020	0.0462	1200	81	0.080	0.0972	3900	8	0.020	0.0320
	specimen 316				specimen 317				specimen 318			
1	405000	0.010	-	0.0041	260000	0.0040	-		200000	0.0001	-	0.0000
5	250000	-0.022	-0.040	-0.0055	550000	-0.0027	-0.040	-0.0015	440000	-0.0006	-0.005	-0.0003
10	350000	-0.004	-0.080	-0.0014	360000	0.0043	0.001	0.0015	360000	0.0001	0.001	0.0000
15	480000	-0.001	-0.020	-0.0006	350000	-0.1500	-0.090	-0.0525	260000	-0.0025	-0.030	-0.0007
20	300000	-0.690	-0.190	-0.2070	240000	-0.0024	-0.022	-0.0006	300000	-0.0030	-0.050	-0.0009
25	270000	0.010	0.003	0.0027	240000	0.0100	0.003	0.0024	270000	0.1000	0.040	0.0270
30	160000	-0.900	-0.012	-0.1440	200000	0.0023	0.048	0.0005	190000	-0.1100	-0.057	-0.0209
35	35000	-0.100	-0.010	-0.0035	120000	-0.0700	-0.040	-0.0084	48000	-0.2500	-0.020	-0.0120

week number	resistance r [ohms]	current i [ampere	i.off v [volts]	v=ir theory [volts]	resistance r [ohms]	current i [ampere	i.off v [volts]	v=ir theory [volts]	resistance r [ohms]	current i [ampere	i.off v [volts]	v=ir theory [volts]
	specimen 401				specimen 402				specimen 403			
1	-	-	-	-	190	280	0.001	0.0532	-	-	-	-
5	-	-	-	-	245	125	0.030	0.0306	-	-	-	-
10	360	50	0.020	0.0181	260	88	0.020	0.0229	370	165	0.060	0.0611
15	240	160	0.034	0.0384	230	85	0.021	0.0196	270	227	0.062	0.0613
20	240	166	0.041	0.0398	250	41	0.010	0.0103	390	400	0.085	0.1560
25	300	108	0.011	0.0324	800	26	0.008	0.0210	320	300	0.092	0.0960
30	590	92	0.060	0.0543	500	30	0.021	0.0150	670	320	0.150	0.2144
	specimen 411				specimen 412				specimen 413			
1	-	-	-	0.0000	4000	0.00	0.001	0.0000	8000	0.00	0.003	0.0000
5	-	-	-	0.0000	4000	0.15	0.001	0.0006	9000	0.01	0.001	0.0001
10	21000	0.23	0.020	0.0048	4500	-0.20	-0.040	-0.0009	14000	-0.00	-0.002	-0.0000
15	15000	-0.50	-0.036	-0.0075	6800	-2.00	-0.066	-0.0136	9700	-1.20	0.050	-0.0116
20	9100	0.65	0.030	0.0059	5100	2.10	0.008	0.0107	8300	0.35	0.030	0.0029
25	12000	-2.71	-0.096	-0.0325	8500	1.58	0.045	0.0134	17000	0.17	0.015	0.0029
30	11000	0.15	0.001	0.0017	42000	0.92	0.020	0.0386	14000	1.12	0.023	0.0157
	specimen 421				specimen 422				specimen 423			
1	51	500	0.020	0.0255	52	600	0.030	0.0312	55	650	0.030	0.0358
5	50	261	0.010	0.0131	51	320	0.001	0.0163	53	275	0.012	0.0146
10	48	700	0.040	0.0336	55	465	0.030	0.0256	49	350	0.020	0.0172
15	47	920	0.009	0.0432	50	690	0.040	0.0345	50	580	0.030	0.0290
20	50	1268	0.064	0.0634	48	1050	0.052	0.0504	50	940	0.057	0.0470
25	460	1530	0.109	0.7038	500	1177	0.022	0.5885	480	920	0.040	0.4416
30	180	1600	0.220	0.2880	300	1495	0.330	0.4485	160	967	0.150	0.1547

week number	resistance r [ohms]	current i [ampere	i.off v [volts]	v=ir theory [volts]	resistance r [ohms]	current i [ampere	i.off v [volts]	v=ir theory [volts]	resistance r [ohms]	current i [ampere	i.off v [volts]	v=ir theory [volts]
	specimen 431				specimen 432				specimen 433			
1	4300	0.03	0.003	0.0001	2900	0.04	0.030	0.0001	4600	0.00	0.020	0.0000
5	4000	0.22	0.001	0.0009	3100	0.05	0.001	0.0002	4100	0.21	0.001	0.0009
10	3400	-0.09	-0.014	-0.0003	3500	-1.50	-0.030	-0.0053	4200	-20.00	-0.200	-0.0840
15	2500	-1.20	-0.011	-0.0030	2700	-2.90	-0.031	-0.0078	2700	-2.40	-0.010	-0.0065
20	2100	0.93	0.010	0.0020	1800	5.64	0.049	0.0102	2100	1.76	0.016	0.0037
25	3000	3.09	0.021	0.0093	3500	7.92	0.028	0.0277	2600	1.33	0.009	0.0035
30	7900	2.71	0.020	0.0214	6400	2.10	0.011	0.0134	2200	3.32	0.020	0.0073
	specimen 441				specimen 442				specimen 443			
1	72	625	0.030	0.0450	68	470	0.040	0.0320	68	502	0.030	0.0341
5	91	450	0.052	0.0410	85	260	0.020	0.0221	86	315	0.030	0.0271
10	97	490	0.060	0.0475	98	220	0.046	0.0216	100	330	0.030	0.0330
15	94	565	0.055	0.0531	89	295	0.027	0.0263	93	345	0.019	0.0321
20	100	596	0.032	0.0596	100	250	0.026	0.0250	100	345	0.034	0.0345
25	110	580	0.056	0.0638	100	277	0.031	0.0277	100	356	0.044	0.0356
30	420	555	0.180	0.2331	360	270	0.051	0.0972	260	350	0.022	0.0910
	specimen 451				specimen 452				specimen 453			
1	6500	0.1	0.008	0.0007	5600	0.01	0.002	0.0001	2200	0.92	0.006	0.0020
5	14000	0.0	0.000	0.0001	7800	0.10	0.001	0.0008	2600	0.45	0.001	0.0012
10	12000	-2.0	-0.090	-0.0240	11000	0.50	0.060	0.0055	3000	-2.20	-0.036	-0.0066
15	7900	-1.3	-0.028	-0.0103	9200	0.50	0.030	0.0046	2400	-2.40	-0.005	-0.0058
20	6700	0.3	0.016	0.0020	6500	1.19	0.015	0.0077	1900	0.23	0.004	0.0004
25	10000	5.0	0.013	0.0500	7100	1.12	0.016	0.0080	3100	-1.30	-0.169	-0.0040
30	15000	0.2	0.011	0.0033	29000	2.30	0.057	0.0667	5100	-3.20	-0.022	-0.0163

Appendix B

Monthly Reading	Half-cell Reading [volts]	Current [micro-amperes]	Half-cell Reading [volts]	Current [micro-amperes]	Half-cell Reading [volts]	Current [micro-amperes]
	specimen 100		specimen 101		specimen 102	
1	-0.304	30.0	-0.371	16.0	-0.211	43.0
2	-0.307	32.8	-	39.0	-	60.5
3	-0.326	45.0	-	17.5	-	43.0
4	-0.345	30.0	-0.313	37.0	-0.297	23.0
5	-0.312	10.0	-0.290	15.0	-0.318	19.0
6	-0.271	10.0	-0.264	5.0	-0.317	24.0
7	-0.280	8.0	-0.296	12.0	-0.331	25.0
8	-0.342	16.5	-0.344	34.0	-0.344	29.0
9	-0.396	90.0	-0.357	40.3	-0.364	23.0
	specimen 103		specimen 104		specimen 105	
1	-0.482	0.003	-0.262	0.002	-	-
2	-0.255	-	-0.267	0.002	-0.197	0.028
3	-0.375	0.008	-0.410	0.000	-0.504	0.040
4	-0.232	0.600	-0.485	0.190	-0.409	0.023
5	-0.189	0.010	-0.483	0.070	-0.441	0.004
6	-0.320	0.015	-0.581	3.700	-0.484	0.010
7	-0.294	0.030	-0.451	0.010	-0.430	0.120
8	-0.576	3.800	-0.580	0.120	-0.584	0.780
9	-0.528	-1.000	-0.554	-0.460	-0.570	-0.230
	specimen 106		specimen 107		specimen 108	
1	-0.009	0.001	-0.103	0.003	-0.053	0.009
2	-0.048	0.001	-0.053	0.002	-0.415	0.860
3	-0.149	0.002	-0.081	0.008	-0.353	5.400
4	-0.279	0.001	0.011	0.001	-0.126	0.002
5	-0.356	0.200	-0.313	0.080	-0.369	2.300
6	-0.042	0.055	-0.033	0.020	0.021	0.023
7	-0.332	19.000	-0.419	20.000	-0.462	25.600
8	-0.446	19.300	-0.530	5.400	-0.450	13.300
9	-0.497	0.230	-0.452	6.000	-0.457	0.550
	specimen 110		specimen 111		specimen 112	
1	-0.198	32.8	-0.417	64.0	-0.274	17.0
2	-0.170	8.0	-0.372	55.0	-0.251	10.0
3	-0.234	14.0	-0.360	40.0	-0.318	55.0
4	-0.269	12.0	-0.346	20.0	-0.370	31.6
5	-0.310	11.0	-0.270	-27.0	-0.365	27.0
6	-0.249	11.0	-0.316	-27.0	-0.321	27.0
7	-0.244	8.0	-0.327	10.0	-0.225	20.0
8	0.267	11.0	0.285	10.0	0.354	-2.0

Monthly Reading	Half-cell Reading [volts]	Current [micro-amperes]	Half-cell Reading [volts]	Current [micro-amperes]	Half-cell Reading [volts]	Current [micro-amperes]
	specimen 113		specimen 114		specimen 115	
1	-0.397	0.02	-0.229	0.01	-	-
2	-0.395	0.02	-0.370	0.20	0.430	0.00
3	-0.428	-0.09	-0.285	-0.01	-0.166	-1.00
4	-0.413	-0.03	-0.620	-1.30	-0.414	-2.50
5	-0.441	-0.05	-0.563	-0.10	-0.498	-0.08
6	-0.419	-0.33	-0.625	-0.04	-0.173	0.02
7	-0.370	0.40	-0.519	0.50	-0.350	0.10
8	-0.491	-3.10	-0.256	-0.06	-0.302	-3.10
9	-0.443	-3.30	-0.392	-0.69	-0.508	3.20
	specimen 116		specimen 117		specimen 118	
1	-0.526	400	-0.327	260	-0.297	255
2	-	240	-0.515	215	-	200
3	-	293	-0.518	210	-0.546	220
4	-0.501	300	-0.515	217	-	200
5	-0.554	180	-0.553	190	-0.558	205
6	-0.513	218	-0.529	205	-0.533	230
7	-0.478	132	-0.382	127	-0.387	90
8	-0.566	270	-0.528	235	-0.502	129
9	-0.547	68	-0.490	134	-0.476	65
	specimen 119		specimen 120		specimen 121	
1	-0.534	2.520	-0.491	8.900	-0.172	0.004
2	-0.606	-2.870	-0.499	-3.000	-0.404	-0.025
3	-0.431	3.290	-0.457	-1.500	-0.305	-0.000
4	-0.409	0.000	-0.467	-1.000	-0.152	-0.460
5	-0.453	0.000	-0.527	-1.400	-0.127	0.001
6	-0.378	0.010	-0.513	1.400	-0.197	0.100
7	-0.202	-17.000	-0.466	-34.000	-0.287	-4.500
8	-0.483	0.100	-0.548	42.000	-0.431	-15.000
9	-0.462	-3.200	-0.510	-15.000	-0.328	1.020
	specimen 122		specimen 123		specimen 124	
1	-0.275	0.004	-0.087	0.000	-0.087	0.001
2	-0.412	-2.700	-0.310	0.000	-0.069	-0.006
3	-0.509	-1.000	-0.023	0.000	-0.045	0.002
4	-0.474	-1.800	-0.234	0.000	-0.033	0.003
5	-0.401	-0.021	-0.065	0.048	-0.318	-1.400
6	-0.293	0.010	-0.322	0.001	-0.154	0.100
7	-0.295	-17.000	-0.215	-0.680	-0.271	-22.300
8	-0.478	-11.200	-0.460	1.300	-0.452	-9.700
9	-0.436	10.970	-0.324	-0.013	-0.415	-1.850

Monthly Reading	Half-cell Reading [volts]	Current [micro-amperes]	Half-cell Reading [volts]	Current [micro-amperes]	Half-cell Reading [volts]	Current [micro-amperes]
	specimen 125		specimen 126		specimen 127	
1	-0.406	0.005	-0.508	0.060	-0.450	0.020
2	-0.450	-0.200	-0.455	-0.080	-0.447	0.013
3	-0.442	-0.040	-0.501	0.050	-0.218	-0.180
4	-0.402	-0.010	-0.417	-0.050	-0.405	-0.010
5	-0.534	0.300	0.526	-0.050	0.422	-0.050
6	-0.339	-19.500	-0.250	-11.800	-0.390	-14.500
7	-0.532	-5.400	-0.483	-6.800	-0.572	-2.150
8	-0.530	-2.900	-0.535	-0.450	-0.529	-2.000
	specimen 128		specimen 129		specimen 130	
1	-0.531	320.0	-0.545	390.0	-0.518	330.0
2	-0.535	210.0	-0.558	260.0	-0.542	224.0
3	-0.535	205.0	-0.564	310.0	-0.552	233.0
4	-0.537	162.0	-0.575	254.0	-0.544	220.0
5	-0.738	124.0	-0.524	240.0	-0.500	175.0
6	-0.501	106.0	-0.271	185.0	-0.517	93.0
7	-0.395	32.0	-0.427	46.0	-0.426	-27.0
8	-0.488	33.0	-0.523	81.3	-0.497	-20.0
9	-0.467	-19.2	-0.515	42.0	-0.476	-49.0
	specimen 131		specimen 132		specimen 133	
1	-0.360	-0.0005	-0.430	0.0020	-0.374	0.0009
2	-0.334	0.0004	-0.444	-0.0009	-0.423	0.0009
3	-0.332	0.0003	-0.435	0.0030	-0.417	-0.0040
4	-0.383	-0.0065	-0.412	-0.0018	-0.403	-0.0022
5	-0.419	-0.0022	-0.415	-0.0005	-0.416	-0.0002
6	-0.423	-0.0010	-0.377	-0.0001	-0.416	-2.2000
7	-0.413	-0.0090	-0.392	-0.0018	-0.456	-0.0032
8	-0.542	0.0001	-0.383	0.0010	-0.399	0.0010
	specimen 201		specimen 202		specimen 203	
1	-0.232	2.20	-0.199	0.90	-0.244	3.40
2	-0.269	0.60	-0.211	0.19	0.000	0.70
3	-0.240	2.90	-0.214	1.00	-0.179	0.71
4	-0.281	2.35	-0.254	2.50	0.000	0.34
5	-0.215	1.70	-0.194	0.40	-0.241	0.25
6	-0.093	3.00	-0.120	6.40	0.296	6.00
7	-0.386	17.30	-0.404	19.70	-0.432	25.00
8	-0.418	-14.80	-0.444	5.60	-0.398	-6.00
9	-0.390	-11.20	-0.372	3.10	-0.421	0.25

Monthly Reading	Half-cell Reading [volts]	Current [micro-amperes]	Half-cell Reading [volts]	Current [micro-amperes]	Half-cell Reading [volts]	Current [micro-amperes]
	specimen 204		specimen 205		specimen 206	
1	-0.241	3.60	-0.206	1.50	-0.202	-0.17
2	-0.254	3.00	-0.255	-13.00	-0.226	1.00
3	-0.204	2.00	-0.302	13.00	-0.196	1.40
4	-0.288	6.00	-0.281	7.00	-0.263	1.30
5	-0.240	4.30	-0.296	4.30	-0.277	-1.60
6	-0.288	8.00	-0.040	32.00	-0.114	12.00
7	-0.207	7.10	-0.257	-30.00	-0.254	9.40
8	-0.338	-7.10	-0.448	6.20	-0.483	35.50
9	-0.413	-20.30	-0.442	6.40	-0.492	-0.07
	specimen 207		specimen 208		specimen 209	
1	-0.558	0.07	-0.576	0.06	-0.620	0.10
2	-0.452	0.01	-0.490	0.01	-0.629	0.07
3	-0.457	1.40	-0.439	0.06	-0.599	0.02
4	-0.455	0.03	-0.434	0.01	-0.393	0.01
5	-0.301	0.50	-0.441	0.30	-0.528	0.01
6	-0.508	-14.50	-0.365	-3.30	-0.410	-14.00
7	-0.530	-2.20	-0.313	-1.88	-0.522	-0.68
8	-0.517	-14.50	-0.507	-4.10	-0.513	-19.90
9	-0.488	3.37	-0.521	-2.80	-0.378	-30.00
	specimen 210		specimen 211		specimen 212	
1	-0.602	8.40	-0.614	7.30	-0.624	8.60
2	-0.585	4.10	-0.603	4.00	-0.593	8.50
3	-0.594	4.00	-0.570	2.60	-0.570	7.70
4	-0.569	2.40	-0.581	2.60	-0.545	2.30
5	-0.582	3.20	-0.561	3.60	-0.548	6.50
6	-0.411	-3.00	-0.443	-11.50	-0.454	-8.00
7	-0.488	6.20	-0.543	5.00	-0.526	2.05
8	-0.479	-2.75	-0.555	-8.00	-0.536	1.50
9	-0.437	3.25	-0.522	-1.75	-0.478	3.40
	specimen 216		specimen 217		specimen 218	
1	-0.513	-	-0.499	-	-0.488	-
2	-0.534	55.0	-	-	-0.486	36.0
3	-0.568	55.0	-0.611	77.0	-	32.0
4	-0.559	55.0	-0.587	78.0	-0.509	34.0
5	-0.577	46.0	-0.574	62.0	-0.471	25.0
6	-0.539	40.0	-0.590	55.0	-0.475	28.0
7	-0.516	39.0	-0.562	49.0	-0.472	17.0
8	-0.566	40.0	-0.593	56.0	-0.461	16.0

Monthly Reading	Half-cell Reading [volts]	Current [micro-amperes]	Half-cell Reading [volts]	Current [micro-amperes]	Half-cell Reading [volts]	Current [micro-amperes]
	specimen 219		specimen 220		specimen 221	
1	-0.498	-0.030	-0.552	0.007	-0.414	-0.001
2	-0.521	0.032	-0.508	0.003	-0.580	0.000
3	-0.514	-0.006	-0.414	-0.003	-0.493	-0.006
4	-0.271	0.022	-0.458	0.001	-0.515	0.001
5	-0.478	-0.002	-0.461	-0.002	-0.538	-0.002
6	-0.487	-0.010	-0.494	-0.005	-0.523	-0.010
7	-0.492	0.010	-0.532	-0.001	-0.532	-0.001
8	-0.526	0.020	-0.563	0.010	-0.549	0.010
	specimen 222		specimen 223		specimen 224	
1	-0.375	4.100	-	-	-	-
2	-0.490	2.150	-0.437	5.200	-0.587	4.440
3	-0.492	0.900	-0.549	4.100	-0.587	5.000
4	-0.503	-0.930	-0.512	1.600	-0.586	2.000
5	-0.492	0.800	-0.508	1.600	-0.583	2.900
6	-0.465	0.700	-0.494	1.800	-0.560	-0.060
7	-0.406	0.900	-0.537	0.250	-0.404	3.000
	specimen 301		specimen 302		specimen 303	
1	-0.236	1.00	-0.389	1.00	-0.247	1.10
2	-0.157	12.00	-0.323	5.10	-0.167	2.00
3	-0.202	16.00	-0.339	1.60	-0.219	3.50
4	-0.311	13.20	-0.358	2.00	-0.306	1.00
5	-0.344	7.80	-0.331	5.20	-0.235	4.00
6	-0.366	9.00	-0.194	7.20	-0.293	1.10
7	-0.323	11.00	-0.331	-22.00	-0.287	-12.00
8	-0.190	5.50	-0.345	3.10	-0.301	-16.20
9	-0.343	1.00	-0.356	-8.40	-0.302	-14.00
	specimen 304		specimen 305		specimen 306	
1	-0.517	42.0	-0.350	47.0	-0.418	53.0
2	-0.477	33.0	-0.442	34.0	-0.531	55.0
3	-0.459	34.0	-0.423	32.0	-0.487	32.0
4	-0.462	29.0	-0.432	28.0	-0.504	13.7
5	-0.480	48.0	-0.426	16.0	-0.502	18.4
6	-0.427	20.0	-0.400	25.0	-0.418	21.0
7	-0.465	21.0	-0.450	-12.0	-0.507	12.0
8	-0.512	23.0	-0.588	15.0	-0.548	23.0

Monthly Reading	Half-cell Reading [volts]	Current [micro-amperes]	Half-cell Reading [volts]	Current [micro-amperes]	Half-cell Reading [volts]	Current [micro-amperes]
	specimen 307		specimen 308		specimen 309	
1	-0.195	0.002	-0.360	-0.014	-0.257	-0.001
2	-0.297	0.007	-0.205	-0.025	-0.573	-0.038
3	-0.220	-0.020	-1.144	-0.300	-0.427	0.050
4	-0.011	-0.002	-	-	-0.415	-0.005
5	-0.285	0.004	0.058	-0.070	-0.070	-0.800
6	-0.180	0.010	-1.588	0.017	-0.590	-0.010
7	-0.502	-0.010	-0.209	0.004	-0.326	-1.300
8	-0.214	-0.013	-0.137	0.015	-0.266	-0.300
9	-0.236	0.010	-0.048	0.010	-0.008	5.000
	specimen 310		specimen 311		specimen 312	
1	-0.166	0.00	-0.160	0.67	-	-
2	-0.151	-1.70	-0.160	-0.70	-	1.00
3	-0.180	-2.00	-0.179	-0.03	-0.221	1.68
4	-0.199	-3.20	-0.219	-3.70	-0.242	0.25
5	-0.295	-2.50	-0.268	-6.00	-0.244	-1.60
6	-0.226	-3.30	-0.263	-2.80	-0.254	0.50
7	0.035	-5.00	0.158	0.20	0.380	10.00
	specimen 313		specimen 314		specimen 315	
1	-	72.0	-0.527	82.0	-0.399	90.0
2	-0.497	65.0	-0.535	74.0	-0.508	66.0
3	-0.493	70.0	-0.507	79.0	-0.465	66.0
4	-0.490	49.0	-0.536	65.0	-0.497	56.0
5	-0.492	52.0	-0.525	65.0	-0.288	56.0
6	-0.493	56.0	-0.577	70.0	-0.293	53.0
7	-0.204	47.0	-0.288	75.0	-0.488	48.0
	specimen 316		specimen 317		specimen 318	
1	-0.420	0.010	-0.495	0.006	-0.303	0.000
2	-0.413	-0.004	-0.396	-0.000	-0.518	-0.006
3	-0.411	-0.330	-0.510	0.001	-0.565	-0.150
4	-0.424	-0.690	-0.609	-0.002	-0.625	-0.003
5	-0.356	-0.007	-0.456	-0.003	-0.479	-0.001
6	-0.301	0.010	-0.530	0.010	-0.562	1.000
	specimen 401		specimen 402		specimen 403	
1	-	-	-0.415	217.0	-	-
2	-0.322	60.0	-0.357	114.0	-0.473	200.0
3	-0.287	68.0	-0.340	100.0	-0.431	156.0
4	-0.277	45.0	-0.281	96.0	-0.413	150.0
5	-0.414	190.0	-0.295	80.0	-0.521	230.0
6	-0.421	92.0	-0.290	41.0	-0.512	300.0

Monthly Reading	Half-cell Reading [volts]	Current [micro-amperes]	Half-cell Reading [volts]	Current [micro-amperes]	Half-cell Reading [volts]	Current [micro-amperes]
	specimen 411		specimen 412		specimen 413	
1	-	-	-0.516	-	-0.215	-
2	-0.389	0.820	-0.347	0.030	-0.242	-0.001
3	-0.306	0.460	-0.341	-0.120	-0.171	-0.001
4	-0.314	0.300	-0.594	-1.200	-0.234	-0.012
5	-0.375	0.650	-0.288	2.100	-0.080	0.350
	specimen 421		specimen 422		specimen 423	
1	-0.432	500	-0.392	644	-0.441	660
2	-0.422	340	-0.417	600	-	270
3	-0.420	607	-0.333	440	-0.110	310
4	-0.424	763	-0.314	515	-0.355	303
5	-0.536	1050	-0.432	940	-0.345	621
6	-0.510	900	-0.512	960	-0.556	946
	specimen 431		specimen 432		specimen 433	
1	-0.303	0.030	-0.491	0.040	-0.301	0.020
2	-0.403	0.220	-0.394	-	-0.599	0.040
3	-0.518	-0.440	-0.341	-0.280	-0.576	-0.310
4	-0.565	0.210	-0.333	0.330	-0.571	1.200
5	-0.625	-1.000	-0.368	-1.300	-0.590	1.760
6	-0.458	3.010	-0.326	-1.400	-	1.200
7	-0.479	2.100	-	6.200	-0.592	1.500
8	-0.106	2.800	-0.242	2.100	-	3.120
	specimen 441		specimen 442		specimen 443	
1	-0.419	680	-0.340	360	-0.346	360
2	-0.425	565	-0.299	250	-0.329	333
3	-0.419	550	-0.272	260	-0.295	340
4	-0.375	500	-0.275	246	-0.297	340
5	-0.473	545	-0.376	280	-0.330	295
	specimen 451		specimen 452		specimen 453	
1	-0.167	0.001	-0.642	0.060	-0.579	1.400
2	-0.529	0.000	-0.640	0.030	-0.391	0.460
3	-0.586	-0.009	-0.646	0.008	-0.439	-1.400
4	-0.613	-0.110	-0.640	0.026	-0.403	-2.000
5	-0.173	0.220	0.023	1.190	-0.063	1.700